สมดุลน้ำและปริมาณการใช้น้ำที่ปลอดภัย ในชั้นน้ำยุคควอเทอร์นารีของแอ่งแพร่

นายกรันต์ ตาระกา

วิทยานิพนธ์นี้เป็นส่วนหนึ่งของการศึกษาตามหลักสูตรปริญญาวิทยาศาสตรมหาบัณฑิต
สาขาวิชาโลกศาสตร์ ภาควิชาธรณีวิทยา
คณะวิทยาศาสตร์ จุฬาลงกรณ์มหาวิทยาลัย
ปีการศึกษา 2559

WATER BALANCE AND SAFE YIELD IN THE QUATERNARY AQUIFER OF PH RAE BASIN

Mr. Karun Taraka

A Thesis Submitted in Partial Fulfillment of the Requirements
for the Degree of Master of Science Program in Earth Sciences
Department of Geology
Faculty of Science
Chulalongkorn University
Academic Year 2016

Thesis Title	WATER BALANCE AND SAFE YIELD IN THE QUATERNARY AQUIFER OF PHRAE BASIN
By	Mr. Karun Taraka
Field of Study	Earth Sciences
Thesis Advisor	Associate Professor Srilert Chotpantarat, Ph.D.

Accepted by the Faculty of Science, Chulalongkorn University in Partial Fulfillment of the Requirements for the Master's Degree

.....Dean of the Faculty of Science
(Associate Professor Polkit Sangvanich, Ph.D.)

THESIS COMMITTEE

.....Chairman
(Assistant Professor Sombat Yumuang, Ph.D.)
.....Thesis Advisor
(Associate Professor Srilert Chotpantarat, Ph.D.)
.....Examiner
(Assistant Professor Thanop Thitimakorn, Ph.D.)
.....External Examiner
(Watchara Suiadee, Ph.D.)

กรันต์ ตาระกา : สมดุลน้ำและปริมาณการใช้น้ำที่ปลอดภัย ในชั้นน้ำยุคควอเทอร์นารีของแอ่งแพร่ (WATER BALANCE AND SAFE YIELD IN THE QUATERNARY AQUIFER OF PHRAE BASIN) อ.ที่ปรึกษาวิทยานิพนธ์หลัก: รศ. ดร. ศรีเลิศ โชติพันธรัตน์, 138 หน้า.

จังหวัดแพร่เป็นพื้นที่ที่ประสบปัญหาขาดแคลนน้ำ จุดมุ่งหมายของการศึกษานี้เพื่อประเมินการกระจายเชิงพื้นที่และเวลาของปริมาณการเติมน้ำลงสู่ชั้นหินอุ้มน้ำในหินตะกอนร่วนยุคควอเทอร์นารี ตลอดจนประเมินดุลของน้ำบาดาลและปริมาณการสูบน้ำปลอดภัยที่มีความเหมาะสมต่อชั้นหินอุ้มน้ำ โดยงานวิจัยนี้แบ่งเป็น 2 ส่วนหลัก ซึ่งประกอบด้วย

ส่วนแรก คือ ส่วนการจำลองน้ำผิวดินด้วยแบบจำลอง SWAT ผลการศึกษาพบว่าปริมาณน้ำท่าภายหลังการเปลี่ยนแปลงการใช้ประโยชน์ที่ดินมีปริมาณสูงขึ้นอย่างมีนัยสำคัญในทุกลุ่มน้ำสาขา โดยมีค่าอยู่ระหว่างร้อยละ 4.94 (สถานี Y.38) ถึงร้อยละ 77.64 (สถานี Y.24) การประเมินปริมาณการเติมน้ำลงสู่ชั้นหินอุ้มน้ำในแต่ละลุ่มน้ำย่อยอยู่ในช่วง 14.62 มิลลิเมตรต่อปี ถึง 433.86 มิลลิเมตรต่อปี ทั้งนี้จากการศึกษายังพบว่าผลกระทบจากการใช้ประโยชน์ที่ดินที่เปลี่ยนแปลงไปนั้น นอกจากจะมีผลต่อปริมาณน้ำท่าที่เพิ่มสูงขึ้นแล้ว ยังส่งผลต่ออัตราส่วนของการเติมน้ำลงสู่ชั้นหินอุ้มน้ำ (เมื่อเปรียบเทียบกับปริมาณฝนรายปี) ในแต่ละลุ่มน้ำย่อยที่ลดลงอีกด้วย โดยมีค่าอยู่ระหว่างร้อยละ 0.26 (สถานี Y.6) ถึงร้อยละ 5.12 (สถานี Y.36)

ส่วนที่สอง คือ ส่วนการจำลองน้ำบาดาลด้วยแบบจำลอง visual MODFLOW ผลการประเมินสมดุลน้ำบาดาลรวม มีค่าเท่ากับ +665.69 ลูกบาศก์เมตรต่อปี ทั้งนี้แสดงให้เห็นว่าพื้นที่ศึกษาสามารถเพิ่มอัตราการสูบได้สูงสุดไม่เกินร้อยละ 50 จากอัตราการสูบเดิม ซึ่งผลการศึกษาเหล่านี้จะเป็นประโยชน์ต่อการนำไปใช้พัฒนาและต่อยอดเพื่อบูรณาการการบริหารจัดการทรัพยากรน้ำผิวดินและทรัพยากรน้ำบาดาลที่เหมาะสมและยั่งยืนต่อไปในอนาคต

ภาควิชา ธรณีวิทยา ลายมือชื่อนิสิต .....

สาขาวิชา โลกศาสตร์ ลายมือชื่อ อ.ที่ปรึกษาหลัก .....

ปีการศึกษา 2559

5572218223 : MAJOR EARTH SCIENCES
KEYWORDS: SWAT MODEL / VISUAL MODFLOW / LAND USE CHANGE / GROUNDWATER RECHARGE / GROUNDWATER BALANCE / SAFE YIELD

KARUN TARAKA: WATER BALANCE AND SAFE YIELD IN THE QUATERNARY AQUIFER OF PHRAE BASIN. ADVISOR: ASSOC. PROF. SRILERT CHOTPANTARAT, Ph.D., 138 pp.

Phrae province has experienced a drought problem, especially in dry season. The aims of this research were to evaluate the spatio-temporal distribution of groundwater recharge into the Quaternary unconsolidated sedimentary aquifers as well as to assess groundwater balance and suitable safe yield of the aquifers. The research was divided into two main parts as follows: in the first part, surface water modeling, namely, SWAT. The results showed that runoff after land use changes from 2003 to 2009 appeared to be significantly increased in all sub-watersheds in a range from 4.94% (station Y.38) to 77.64% (station Y.24). The groundwater recharge of each sub-watershed was in a range from 14.62 mm/yr to 433.86 mm/yr. Interestingly, not only the impact of land use causes the increase of runoff hydrograph, but it also results in gradually decreasing in the percentage of groundwater recharge (as compared to total annual rainfall) of each sub-watershed, ranging from 0.26% (station Y.6) to 5.12% (station Y.36).

In the second part, after evaluating the amounts of monthly groundwater recharge from the previous part by SWAT model, the groundwater model, so-called, visual MODFLOW. We found that groundwater balance in the aquifers was approx. +665.69 m^3/yr and the suitable safe yield in the aquifers should not increase the pumping rate exceeding over 50%, as compared to the base case. The results of this research will benefit for implementing the sustainable water management plan, in terms of the integration of surface water and groundwater resources and can be further used as a database for government agency in the future.

Department:	Geology	Student's Signature	.....
Field of Study:	Earth Sciences	Advisor's Signature	.....
Academic Year:	2016		

ACKNOWLEDGEMENTS

I would like to express my sincere gratitude to my advisor Assoc. Prof. Srilert Chotpantarat for the continuous support of my study and related research, for his patience, motivation, and immense knowledge.

I really appreciated Mr. Patombong Polsanong, Water Resources and Environment Institute, Khon Kaen University for assistance with knowledge of technique and methodology to use SWAT model.

Also want to thankful for Mr. Narongsak Kaewdum for kindness with knowledge of technique and methodology to use MODFLOW model.

Be grateful Ms. Wanlapa Wisittammasri, Mr. Ms.Satika Boonkaewwan, Mr. Jaturon Kornkul and fellow researchers in the Earth Science and Geology programs, Chulalongkorn University for support my thesis and anything.

This research has been supported by the Graduate School of Chulalongkorn University and the Ratchadaphiseksomphot Endowment Fund and the Ratchadaphiseksomphot Endowment Fund of Chulalongkorn University (CU-57-061-CC).

Finally, I most gratefully my love Ms. Suponrat Wanichmaneebut and my family to supported anything to my life.

CONTENTS

Page

Page

LIST OF FIGURE

LIST OF TABLE

Chapter I
Introduction

1.1 Rationale

In recent years, Thailand has intensively used the groundwater together with surface water, so-called, conjunctive use, in various activities, for examples, for consumption, agriculture, industry and tourism. A large amount of groundwater demand has tended to increase, especially during the dry season and outside irrigation areas, because of the lack of rainfall and a proper assessment of groundwater usage. Therefore, research for evaluating the suitable groundwater yield of is particularly important issue. In order to obtain the more accurate and reliable estimation of the groundwater quantity, including water-balance components such as the amount of water flowing into reservoirs, groundwater recharge and groundwater pumping from the reservoir, etc., it is necessary to integrate the interaction between surface water and groundwater (Kim, Chung et al. 2008). The results obtained can be used to support a decision making on the proper management of surface water and groundwater resources. The model used in this study includes the surface water model called SWAT (Soil and Water Assessment Tool), which was developed by the Blackland Research Center, TAES and USDA-ARS (United States Department of Agriculture-Agricultural Research Service). For SWAT software, this study used ArcSWAT, an extension of ArcGIS software commercial by ESRI, to calibrate and verify with observed streamflow data of stations in the Yom river basin, and then assess the groundwater recharge. The second model is MODFLOW (Modular Three Dimensional Finite Difference Groundwater Flow Model), was developed by McDonald and Harbaugh, USGS (United-States Geological Survey). This research used the visual MODFLOW software to assess the groundwater balance and optimal safe yield of the Quaternary unconsolidated sedimentary aquifers in the study area. Both models composing of the corresponding variables includes surface water recharge to groundwater, evapotranspiration of groundwater to surface water, water exchange between aquifers of multi-layer and river-groundwater interaction with, etc. The study area is located in the Phrae Basin of the Central Part of Phrae Groundwater Basin, in the Northern Thailand (**Figure 1.1**). Boundary of the study area is scoped on

hydrogeological units, namely, Quaternary unconsolidated sedimentary aquifers. These aquifer consist of floodplain deposits aquifers (Qfd), younger terrace deposits aquifer (Qyt) and old terrace deposits aquifer (Qot), which interact with Yom river, the main perennial stream in this area.

As mentioned above, this study used SWAT model, can be used to spatially and temporally calibrate and verify with long-term observed streamflow data in the Yom river basin and then come up with the spatio-temporal groundwater recharge in the Quaternary unconsolidated sedimentary aquifers (i.e, Qfd, Qyt and Qot) and then incorporated with the groundwater model, Visual MODFLOW, to assess the safe yield and groundwater balance in the aquifers. These results presents the temporal and spatial distribution of recharge maps and get the information of suitable groundwater yield as can be used as a database for establishing the groundwater resource management plan.

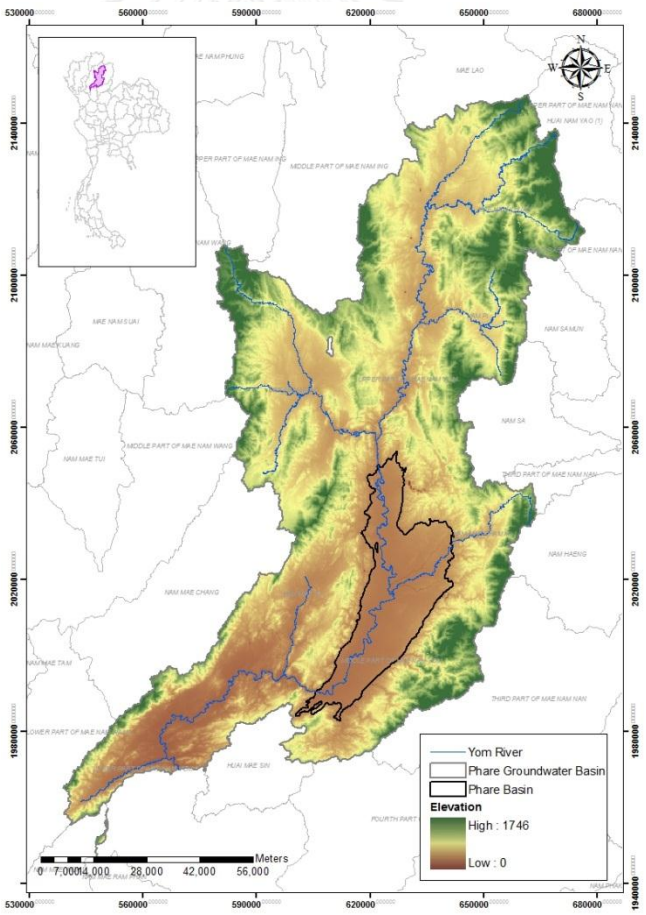

Figure 1.1 Map of the study area

1.2 Objectives

- To evaluate the spatial-temporal distribution of recharge groundwater into the Quaternary unconsolidated sedimentary aquifers of the Phrae Basin
- To assess water balance and suitable safe yield of groundwater in the aquifers.

1.3 Hypothesis

In general, the groundwater flow modeling uses groundwater recharge from lumped percolation estimated from a percentage of precipitation, not accounting for hydrological processes. However, hydrological modeling, SWAT, can simulate hydrological processes, especially the surface water runoff and infiltration process in root zones, and then calibrate and validate with streamflow hydrographs. So, the results can be used as real recharge, corresponding to several soils and land use types. Thus, assessing groundwater balance and safe yield in this area can be more accurate and reliable.

1.4 Conceptual framework

The application of SWAT model was used to estimate amount of additional recharge water into aquifers and MODFLOW model was used to assess the groundwater balance and safe yield of each aquifer in the Phrae Basin.

1.5 Scope of the study

1. Groundwater level measurement covered the area of Phrae Groundwater Basin, Phrae district.
2. Application of SWAT model using meteorology data such as the daily rainfall data, maximum and minimum daily temperature, average wind speed, relative humidity and runoff data.
3. Application of MODFLOW model using groundwater levels, which were measured in the area.

1.6 Expected outcomes

- Groundwater recharge maps in the Quaternary unconsolidated sedimentary aquifers of Phrae Basin
- Groundwater balance and safe yield the Quaternary unconsolidated sedimentary aquifers of the Phrae Basin.

1.7 Flow chart of the study

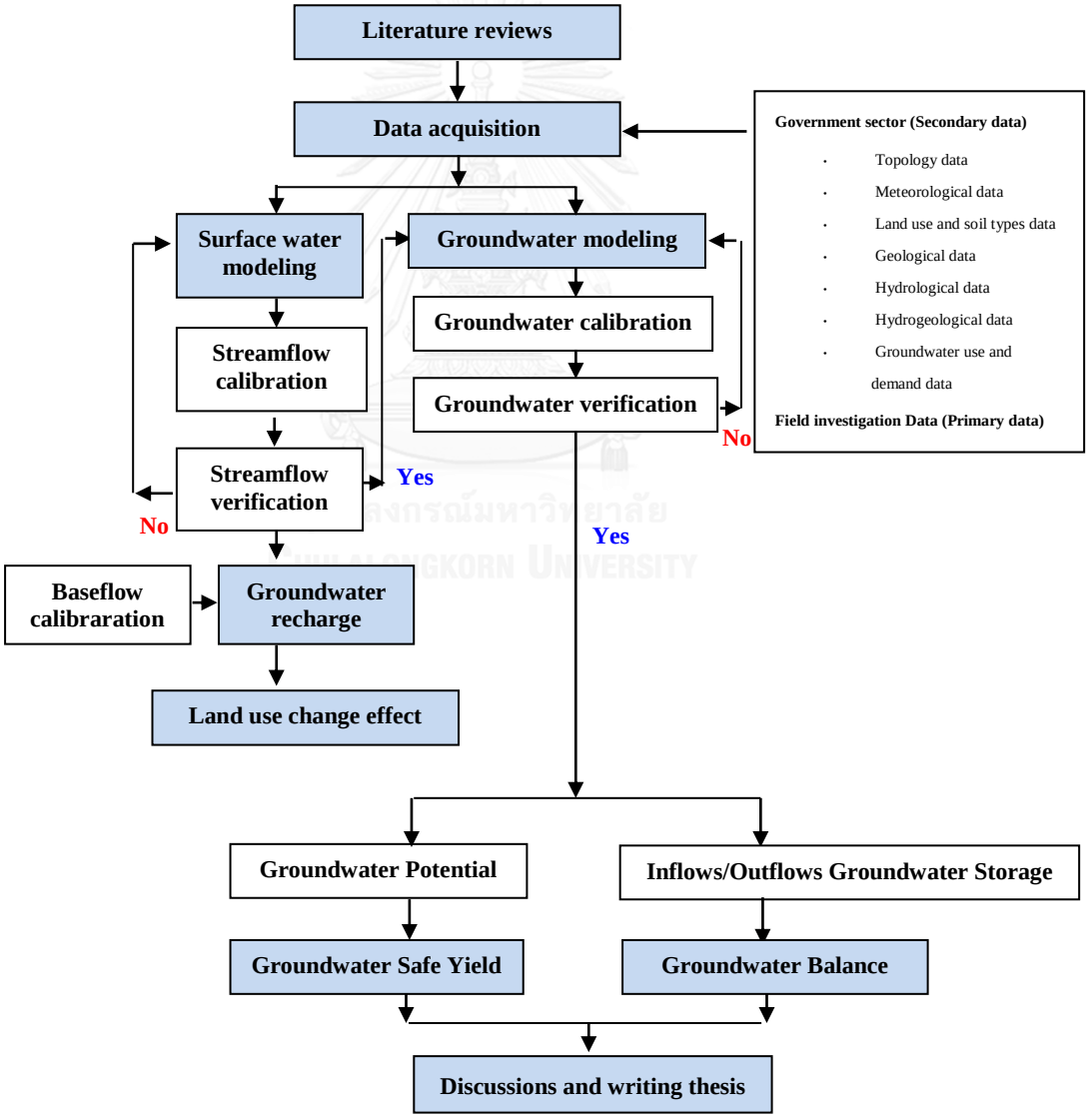

Figure 1.2 Flow chart of this study

Chapter II
Theoretical background and Literature Review

In the process of modeling for surface water and groundwater, it is necessary to understand the definition and meaning of various parameters used in the model, including theory and the equation of the model used for the analysis and computational simulation results. This will serve as a guide for adjusting the model to the accurate simulation results and as close as possible to the realities of the region.

2.1 Theoretical backgrounds of SWAT (Soil and Water Assessment Tool)

2.1.1 Surface Water Hydrology

Surface runoff occurs when the rate of water application to the ground surface exceeds the rate of infiltration. When water is applied to a dry soil, the infiltration rate is usually very high. However, it will decrease as the soil becomes wetter. When the application rate is higher than the infiltration rate, surface depressions begin to fill. If the application rate continues to be higher than the infiltration rate when all of surface depressions have filled, surface runoff will start. Theoretical from SWAT manual 2009 by S.L. Neitsch et al, 2009 and J.G. Arnold et al, 2009 are below.

SWAT provides two methods for estimating surface runoff, i.e. the SCS curve number procedure and the Green&Ampt infiltration method. This study used only the SCS curve number method.

The SCS runoff equation is an empirical model that was developed for more than 20 years from studying relationships of rainfall-runoff. The model provides a basis for estimating the amounts of runoff under vary land use and soil types. The SCS curve number equation is

$$Q_{surf} = \frac{(R_{day} - I_a)^2}{(R_{day} - I_a + S)} \quad (1)$$

Where Q_{surf} is the accumulated runoff or rainfall excess (mm H_2O), R_{day} is the rainfall depth for the day (mm H_2O), I_a is the initial abstractions which includes

surface storage, interception and infiltration prior to runoff (mm H_2O), and S is the retention parameter (mm H_2O). The retention parameter varies spatially due to changes in soils, land use, management and slope and temporally due to changes in soil water content. The retention parameter is defined as

$$S = 25.4\left(\frac{1000}{CN} - 10\right) \quad (2)$$

where CN is the curve number for the day. The initial abstractions, I_a, is commonly approximated as $0.2S$ and equation (1) becomes

$$Q_{surf} = \frac{(R_{day} - 0.2S)^2}{(R_{day} + 0.8S)} \quad (3)$$

Runoff will only occur when $R_{day} > I_a$. A graphical solution of equation (3) for different curve number values is presented as **Figure 2.1**.

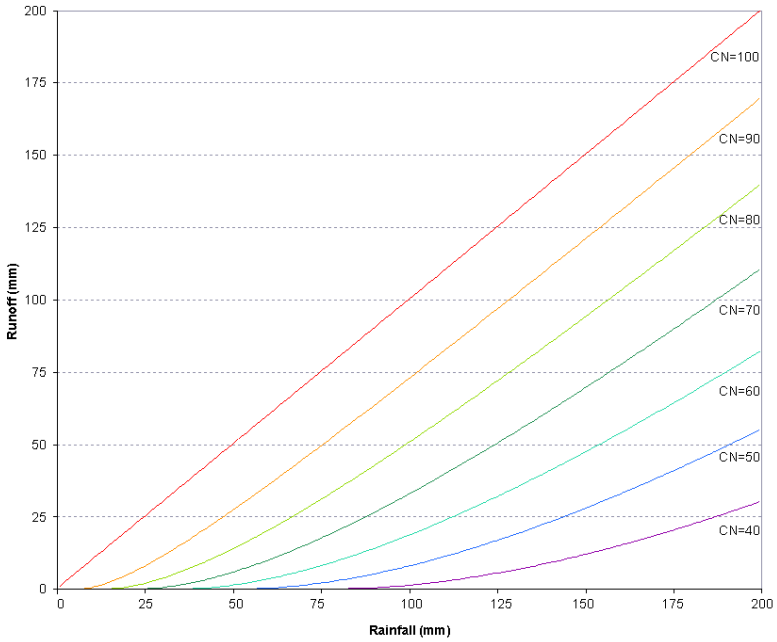

Figure 2.1 Relationship of runoff to rainfall in SCS curve number method.

2.1.1.1 SCS Curve Number

The SCS curve number is a function of the soil's permeability, land use and antecedent soil water conditions. Typical curve numbers for moisture condition II are listed in table2.1 for cultivated agricultural lands. These values are appropriate for a 5% slope.

Table 2.1 Runoff curve numbers for cultivated agricultural lands.

Cover			Hydrologic Soil Group			
Land Use	Treatment or practice	Hydrologic condition	A	B	C	D
Fallow	Bare soil	- - - -	77	86	91	94
	Crop residue cover*	Poor	76	85	90	93
		Good	74	83	88	90
Row crops	Straight row	Poor	72	81	88	91
		Good	67	78	85	89
	Straight roww/ residue	Poor	71	80	87	90
		Good	64	75	82	85
	Contoured	Poor	70	79	84	88
		Good	65	75	82	86
	Contoured w/ residue	Poor	69	78	83	87
		Good	64	74	81	85
	Contoured & terraced	Poor	66	74	80	82
		Good	62	71	78	81
	Contoured & terraced w/ residue	Poor	65	73	79	81
		Good	61	70	77	80
Small grains	Straight row	Poor	65	76	84	88
		Good	63	75	83	87
	Straight roww/ residue	Poor	64	75	83	86
		Good	60	72	80	84
	Contoured	Poor	63	74	82	85
		Good	61	73	81	84
	Contoured w/ residue	Poor	62	73	81	84
		Good	60	72	80	83
	Contoured & terraced	Poor	61	72	79	82
		Good	59	70	78	81
	Contoured & terraced w/ residue	Poor	60	71	78	81
		Good	58	69	77	80

Close-seeded or broadcast legumes or rotation	Straight row	Poor	66	77	85	89
		Good	58	72	81	85
	Contoured	Poor	64	75	83	85
		Good	55	69	78	83
	Contoured & terraced	Poor	63	73	80	83
		Good	51	67	76	80

* Crop residue cover applies only if residue is on at least 5% of the surface throughout the year.

2.1.1.2 Soil Hydrologic Groups

The U.S. Natural Resource Conservation Service (NRCS) classifies soils into four hydrologic groups based on infiltration characteristics of the soils. NRCS Soil Survey Staff (1996) defined a hydrologic group as a group of soils having similar runoff potential under similar storm and cover conditions. Properties of soil that influence runoff potential are those that impact the minimum rate of infiltration for a bare soil after prolonged wetting and when not frozen. These properties are depth to seasonally high water table, saturated hydraulic conductivity, and a very slowly permeable layer. Soil may be placed in one of four groups, A, B, C, and D, or three dual classes, A/D, B/D, and C/D. Definitions of the classes are

A: (Low runoff potential). The soils have a high infiltration rate even they are wetted. They have a high rate of water transmission.

B: The soils have a moderate infiltration rate when thoroughly wetted. They have a moderate rate of water transmission.

C: The soils have a slow infiltration rate when thoroughly wetted. They have a slow rate of water transmission.

D: (High runoff potential). The soils have a very slow infiltration rate when thoroughly wetted. They have a very slow rate of water transmission.

Dual hydrologic groups are given for certain wet soils that can be adequately drained. The first letter means to the drained condition, the second is the undrained. Only rated D soil in their natural condition are assigned to dual classes.

2.1.1.3 Antecedent Soil Moisture Condition

SCS defines three antecedent moisture conditions: I is dry (wilting point), II is average moisture, and III is wet (field capacity). The moisture condition I curve number is the lowest value of the daily curve number can assume in dry conditions. The curve numbers for moisture conditions I and III are calculated from the equations below.

$$CN_1 = CN_2 - \frac{20 \cdot (100 - CN_2)}{(100 - CN_2 + exp[2.533 - 0.0636 \cdot (1000 CN_2)])} \quad (4)$$

$$CN_3 = CN_2 \cdot exp[0.00673 \cdot (1000 CN_2)] \quad (5)$$

where CN_1 is the moisture condition I curve number, CN_2 is the moisture condition II curve number, and CN_3 is the moisture condition III curve number.

The daily curve number value adjusted for moisture content is calculated by rearranging equation (2) and inserting the retention parameter calculated for that moisture content.

$$CN = \frac{25400}{(S + 254)} \quad (6)$$

where CN is the curve number on a given day and S is the retention parameter calculated for the moisture content of the soil on that day.

2.1.1.4 Slope Adjustments

The moisture condition II curve numbers provided in the tables are assumed to be appropriate for 5% slopes. Williams (1995) developed an equation to adjust the curve number to a different slope.

$$CN_{2s} = \frac{(CN_3 - CN_2)}{3} \cdot [1 - 2 \cdot exp(-13.86 \cdot slp)] + CN_2 \quad (7)$$

where CN_{2s} is the moisture condition II curve number adjusted for slope, CN_3 is the moisture condition III curve number for the default 5% slope, CN_2 is the moisture condition II curve number for the default 5% slope, and slp is the average fraction slope of the subbasin. SWAT does not adjust curve numbers for slope. If the user wishes to adjust the curve numbers for slope effects, the adjustment must be done before enter the curve numbers in the management input file.

Table 2.2 SWAT input variables for surface runoff calculated with the SCS curve number method.

Variable Name	Definition	Input File
IEVENT	Rainfall, runoff, routing option.	.bsn
ICN	Daily curve number calculation method: 0 calculate daily CN value as a function of soil moisture; 1 calculate daily CN value as a function of plant evapotranspiration	.bsn
CNCOEF	$cncoef$: Weighting coefficient used to calculate the retention coefficient for daily curve number calculations dependent on plant evapotranspiration	.bsn
PRECIPITATION	R_{day}: Daily precipitation (mm H_2O)	.pcp
CN2	CN_2: Moisture condition II curve number	.mgt
CNOP	$CNOP$: Moisture condition II curve number	.mgt

2.1.2 Groundwater Hydrology

Groundwater is the water in the saturated zone of geological materials under pressure greater than atmospheric, i.e. positive pressure. Water enters groundwater storage primarily by infiltration, percolation, or recharge by seepage from surface water bodies. Water leaves groundwater storage primarily by discharge into rivers or lakes. But it is possible for water to move upward from the water table into the capillary fringe, i.e. a saturated zone above the groundwater table.

2.1.2.1 Groundwater Systems

Within the saturated zone of groundwater, regions of high and low conductivity will be found. The regions of high conductivity are made up from coarse-grained particles with a large percentage of macropores that allow waterto move easily. The regions of low conductivity are made up from fine-grained particles with a large percentage of mesopores and micropores that restrict the rate of water movement.

An aquifer is a geologic unit that can store enough water and transmit it at a rate fast enough to be hydrologically significant. An unconfined aquifer is an aquifer whose upper boundary is the water table. A confined aquifer is an aquifer bounded above and below by geologic formations whose hydraulic conductivity is lower than that of the aquifer. **Figure 2.2** illustrates the two types of aquifers.

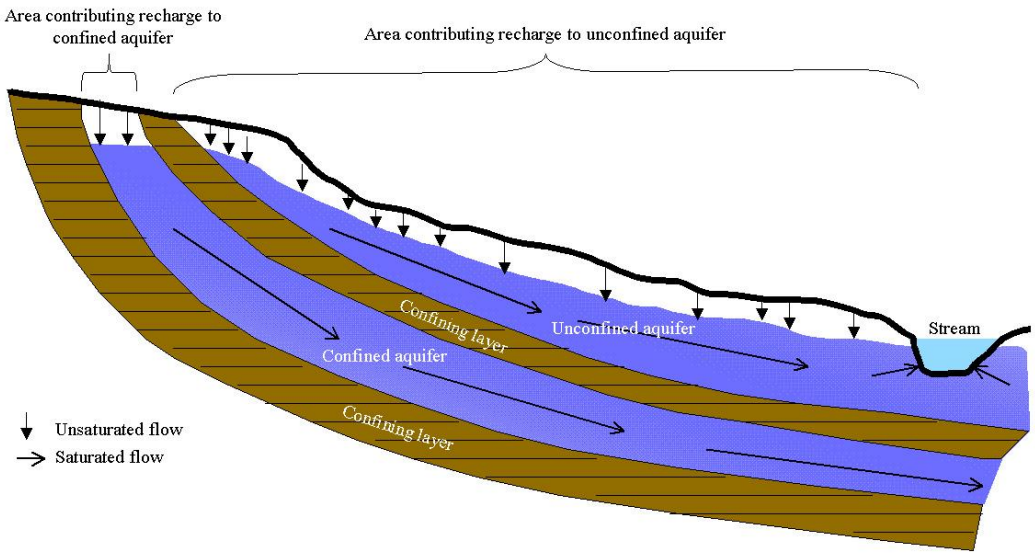

Figure 2.2 Unconfined and confined aquifers (Modified from Dingman, 1994).

Unconfined aquifers recharging occurs via percolation to the water table from a significant portion of the land surface. In contrast, confined aquifers recharging by percolation from the surface occurs only at the upstream end of the confined aquifer, where the geologic formation containing the aquifer is exposed at the earth's surface.Flow is not confined, and a water table is present.

Topography has an important influence on groundwater flow. The flow of groundwater in an idealized hilly upland area is illustrated as **Figure 2.3**. The landscape can be divided into areas of recharge and areas of discharge. A recharge area is defined as a portion of a drainage basin where ground water flow directs away from the water table. A discharge area is defined as a portion of the drainage basin where ground water flow directs toward the water table. The water table is at or near the surface in discharge areas and surface water bodies are normally located in discharge areas.

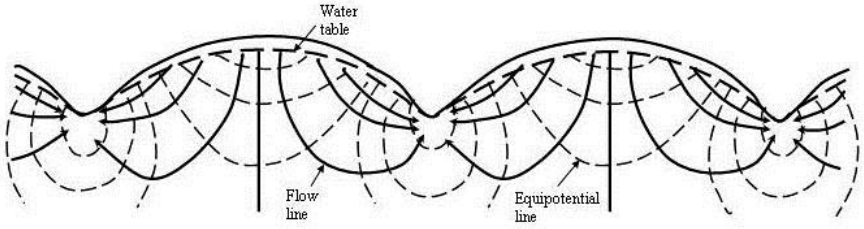

Figure 2.3 Groundwater flow net in an idealized hilly region with homogenous permeable material resting on an impermeable base (Modified from Hubbert, 1940).

Streams may be categorized by their relationship to the groundwater system. A stream located in a discharge area that receives groundwater flow is a gaining or effluent stream (**Figure 2.4(a)**). These types of stream are characterized by an increase of discharge downstream. A stream located in a recharge area is a losing or influent stream. These types of stream are characterized by a decrease of discharge downstream. A losing stream may be connected to (**Figure 2.4(b)**) or perched above (**Figure 2.4(c)**) the groundwater flow area. A stream that simultaneously receives and loses groundwater is a flow-through stream (**Figure 2.4(d)**).

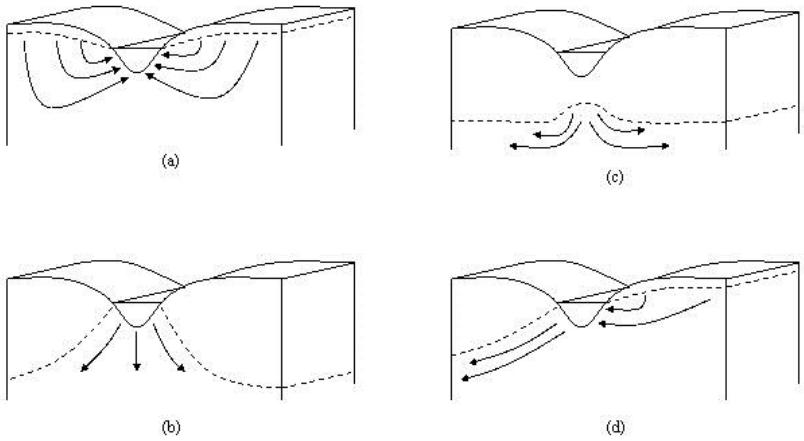

Figure 2.4 Stream-groundwater relationships: **(a)** gaining stream receiving water from groundwater flow, **(b)** losing stream connected to groundwater system, **(c)** losing stream perched above groundwater system and **(d)** flow-through stream (Modified from Dingman, 1994).

SWAT simulates two aquifers in each subbasin. The shallow aquifer is an unconfined aquifer that flow in the main channel or reach of the subbasin. The deep aquifer is a confined aquifer. Water that enters the deep aquifer is assumed to contribute to streamflow somewhere outside of the watershed (Arnold et al., 1993).

2.1.2.2 Shallow Aquifer

The water balance for the shallow aquifer is

$$aq_{sh,i} = aq_{sh,i-1} + w_{rechrg,sh} - Q_{gw} - w_{revap} - w_{pump,sh} \quad (8)$$

where $aq_{sh,i}$ is the amount of water stored in the shallow aquifer on day i (mm H_2O), $aq_{sh,i-1}$ is the amount of water stored in the shallow aquifer on day $i-1$ (mm H_2O), $w_{rechrg,sh}$ is the amount of recharge entering the shallow aquifer on day i (mm H_2O), Q_{gw} is the groundwater flow or base flow into the main channel on day i (mm H_2O), w_{revap} is the amount of water moving into the soil zone response to water deficiencies on day i (mm H_2O), and $w_{pump,sh}$ is the amount of water removed from the shallow aquifer by pumping on day i (mm H_2O).

Recharge

Water that moves through the lowest depth of the soil by percolation or bypass flow enters and flows through the vadose zone before becoming a shallow and/or deep aquifer recharge. The lag time between the water exits the soil profile and enters the shallow aquifer depends on the depth to the water table and the hydraulic properties of the geologic in the vadose and groundwater zones.

An exponential decay weighting function proposed by Venetis (1969) and used by Sangrey et al. (1984) in a precipitation or groundwater response model is utilized in SWAT to estimate the time delay in aquifer recharge once the water exits the soil profile. The delay function is used when the recharge from the soil zone to the aquifer is not instantaneous, i.e. 1 day or less. The recharge to both aquifers on a given day is calculated by

$$w_{rechrg,i} = \left(1 - \exp\left[-1/\delta_{gw}\right]\right) \cdot w_{seep} + \exp\left[-1/\delta_{gw}\right] \cdot w_{rechrg,i-1} \qquad (9)$$

where $w_{rechrg,i}$ is the amount of recharge entering the aquifers on day i (mm H_2O), δ_{gw} is the delay time or drainage time of the overlying geologic formations (days), w_{seep} is the total amount of water exiting the bottom of the soil profile on day i (mm H_2O), and $w_{rechrg,i-1}$ is the amount of recharge entering the aquifers on day $i-1$ (mm H_2O). The total amount of water exiting the bottom of the soil profile on day i is calculated by

$$w_{seep} = w_{perc,ly=n} + w_{crk,btm} \qquad (10)$$

where w_{seep} is the total amount of water exiting the bottom of the soil profile on day i (mm H_2O), $w_{perc,ly=n}$ is the amount of water percolating out of the lowest layer,n, in the soil profile on day i (mm H_2O), and $w_{crk,btm}$ is the amount of water flow past the lower boundary of the soil profile due to bypass flow on day i (mm H_2O).

The delay time, δ_{gw}, cannot be directly measured. It can be estimated by simulating aquifer recharge using different values of $\delta_{gw}$and comparing the simulated variations in water table level with observed values. Johnson (1977) developed a program to iteratively test and statistically evaluate different delay times for a watershed. Sangrey et al. (1984) noted that monitoring wells in the same area had similar values for δ_{gw}. So once a delay time value for a geomorphic area is defined, similar delay times can be used in adjacent watersheds within the same geomorphic.

Partitioning of Recharge between Shallow and Deep Aquifer

A fraction of the total daily recharge can pass through the deep aquifer. The amount of water that will be diverted from the shallow aquifer due to percolation to the deep aquifer on a given day is

$$w_{deep} = \beta_{deep} \cdot w_{rchrg} \qquad (11)$$

where w_{deep} is the amount of water moving into the deep aquifer on day i (mm H_2O), β_{deep} is the aquifer percolation coefficient, and w_{rchrg} is the amount of recharge entering both aquifers on day i (mm H_2O). The amount of recharge to the shallow aquifer is

$$w_{rchrg,sh} = w_{rchrg} - w_{deep} \tag{12}$$

where $w_{rchrg,sh}$ is the amount of recharge entering the shallow aquifer on day i (mm H_2O).

Groundwater/Base Flow

The shallow aquifer contributes base flow to the main channel or reaches within the subbasin. Base flow is allowed to enter the reach only if the amount of water stored in the shallow aquifer exceeds a threshold value specified by the user, $aq_{shthr,q}$. The steady-state response of groundwater flow to recharge is (Hooghoudt, 1940)

$$Q_{gw} = \frac{8000 \cdot K_{sat}}{{L_{gw}}^2} \cdot h_{wtbl} \tag{13}$$

where Q_{gw} is the groundwater flow, or base flow, into the main channel on day i (mm H2O), K_{sat} is the hydraulic conductivity of the aquifer (mm/day), L_{gw} is the distance from the ridge or subbasin divided for the groundwater system to the main channel (m), and h_{wtbl} is the water table height (m).

Water table fluctuations due to non-steady-state response of groundwater flow to periodic recharge are calculated by (Smedema and Rycroft, 1983)

$$\frac{dh_{wtbl}}{dt} = \frac{w_{rchrg,sh} - Q_{gw}}{800 \cdot \mu} \tag{14}$$

where $\frac{dh_{wtbl}}{dt}$ is the change in water table height with time (mm/day), $w_{rchrg,sh}$ is the amount of recharge entering the shallow aquifer on day i (mm H_2O), Q_{gw} is the groundwater flow into the main channel on day i (mm H_2O), and μ is the specific yield of the shallow aquifer (m/m).

Assuming that variation in groundwater flow is linearly related to the rate of change in water table height, equations (13) and (14) can be combined to obtain

$$\frac{dQ_{gw}}{dt} = 10 \cdot \frac{K_{sat}}{\mu \cdot {L_{gw}}^2} \cdot \left(w_{rchrg,sh} - Q_{gw}\right) = \alpha_{gw} \cdot \left(w_{rchrg,sh} - Q_{gw}\right) \quad (15)$$

where Q_{gw} is the groundwater flow into the main channel on day i (mm H_2O), K_{sat} is the hydraulic conductivity of the aquifer (mm/day), μ is the specific yield of the shallow aquifer (m/m), L_{gw} is the distance from the ridge or subbasin divide for the groundwater system to the main channel (m), $w_{rchrg,sh}$ is the amount of recharge entering the shallow aquifer on day i (mm H_2O) and α_{gw} is the baseflow recession constant or constant of proportionality. Integration of equation (15) and rearranging to solve for Q_{gw} yields

$$Q_{gw,i} = Q_{gw,i-1} \cdot \exp\left[-\alpha_{gw} \cdot \Delta t\right] + w_{rchrg,sh} \cdot \left(1 - \exp\left[-\alpha_{gw} \cdot \Delta t\right]\right)$$

$$\text{If } aq_{sh} > aq_{shthr,q}$$

$$Q_{gw,i} = 0 \qquad \text{if } aq_{sh} \leq aq_{shthr,q} \quad (16)$$

where $Q_{gw,i}$ is the groundwater flow into the main channel on day i (mm H_2O), $Q_{gw,i-1}$ is the groundwater flow into the main channel on day $i-1$ (mm H_2O), α_{gw} is the baseflow recession constant, Δt is the time step (1 day), $w_{rchrg,sh}$ is the amount of recharge entering the shallow aquifer on day i (mm H_2O), aq_{sh} is the amount of water stored in the shallow aquifer at the beginning of day i (mm H_2O) and $aq_{shthr,q}$ is the threshold water level in the shallow aquifer for groundwater contribution to the main channel to occur (mm H_2O).

The baseflow recession constant, α_{gw}, is a direct index of groundwater flow response to changes in recharge (Smedema and Rycroft, 1983). Values vary from 0.1 to 0.3 for land with slow response to recharge and from 0.9 to 1.0 for land with a rapid response. Although the baseflow recession constant may be calculated, the best estimates are obtained by analyzing measured streamflow during periods of no

recharge in the watershed. When the shallow aquifer receives no recharge, equation (16) simplifies to:

$$Q_{gw} = Q_{gw,0} \cdot \exp\left[-\alpha_{gw} \cdot t\right] \qquad \text{if } aq_{sh} > aq_{shthr,q}$$

$$Q_{gw,i} = 0 \qquad \text{if } aq_{sh} \leq aq_{shthr,q} \tag{17}$$

where Q_{gw} is the groundwater flow into the main channel at time t (mm H_2O), $Q_{gw,0}$ is the groundwater flow into the main channel at the beginning of the recession (time , $t = 0$) (mm H_2O). The baseflow recession constant is measured by rearranging equation (17).

$$\alpha_{gw} = \frac{1}{N} \cdot \ln\left[\frac{Q_{gw,N}}{Q_{gw,0}}\right] \tag{18}$$

where α_{gw} is the baseflow recession constant, N is the time lapsed since the start of the recession (days), $Q_{gw,N}$ is the groundwater flow on day N (mm H_2O), $Q_{gw,0}$ is the groundwater flow at the start of the recession (mm H_2O).

It is common to find the baseflow days reported for a stream gage or watershed. This is the number of days for base flow recession to decline through one log cycle. When baseflow days are used, equation 18 can be simplified to

$$\alpha_{gw} = \frac{1}{N} \cdot \ln\left[\frac{Q_{gw,N}}{Q_{gw,0}}\right] = \frac{1}{BFD} \cdot \ln[10] = \frac{2.3}{BFD} \tag{19}$$

where BFD is the number of baseflow days for the watershed.

Revap

Water may move from the shallow aquifer into the overlying unsaturated zone. When the material overlying the aquifer is dry, water in the capillary fringe that separates the saturated and unsaturated zones will evaporate and diffuse upward. As water is removed from the capillary fringe by evaporation, water from the underlying aquifer will replace. Water may also be removed from the aquifer by deep-rooted plants which are able to pull water directly from the aquifer.

SWAT creates a model of the movement of water into overlying unsaturated layers as a function of water demand for evapotranspiration. To avoid confusion between soil evaporation and transpiration, this process has been called “revap”. This process is significant in watersheds where the saturated zone is not very far below the surface or where deep-rooted plants are growing. Because the type of plant cover will affect revap in the water balance. The parameters governing revap are usually varied by land use. Revap is allowed to occur only if the amount of water stored in the shallow aquifer exceeds a threshold value specified by the user, $aq_{shthr,rvp}$. The maximum amount of water that will be removed from the aquifer via revap on a given day is

$$w_{revap,mx} = \beta_{revap} \cdot E_0 \tag{20}$$

where $w_{revap,mx}$ is the maximum amount of water moving into the soil zone in response to water deficiencies (mm H_2O), β_{revap} is the revap coefficient, and E_0 is the potential evapotranspiration for the day (mm H_2O). The actual amount of revap that will occur on a given day is calculated by

$$w_{revap} = 0 \qquad \text{if } aq_{sh} \leq aq_{shthr,rvp}$$

$$w_{revap} = w_{revap,mx} - aq_{shthr,rvp} \qquad \text{if } aq_{shthr,rvp} < aq_{sh} < \left(aq_{shthr,rvp} + w_{revap,mx}\right)$$

$$w_{revap} = w_{revap,mx} \qquad \text{if } aq_{sh} \geq \left(aq_{shthr,rvp} + w_{revap,mx}\right) \tag{21}$$

where w_{revap} is the actual amount of water moving into the soil zone in response to water deficiencies (mm H_2O), $w_{revap,mx}$ is the maximum amount of water moving into the soil zone in response to water deficiencies (mm H_2O), aq_{sh} is the amount of water stored in the shallow aquifer at the beginning of day i (mm H_2O) and $aq_{shthr,rvp}$ is the threshold water level in the shallow aquifer for revap to occur (mm H_2O).

Pumping

If the shallow aquifer is specified as the source of irrigation water or water removed for using outside the watershed, the model will allow an amount of water up to the total volume of the shallow aquifer to be removed on any given day.

Groundwater Height

Although SWAT does not currently print groundwater height in the output files, the water table height is updated daily by the model. Groundwater height is related to groundwater flow by equation (22).

$$Q_{gw} = \frac{8000 \cdot K_{sat}}{{L_{gw}}^2} \cdot h_{wtbl} = \frac{800 \cdot \mu}{10} \cdot \frac{10 \cdot K_{sat}}{\mu \cdot {L_{gw}}^2} \cdot h_{wtbl} = 800 \cdot \mu \cdot \alpha_{gw} \cdot h_{wtbl} \qquad (22)$$

where Q_{gw} is the groundwater flow into the main channel on day i (mm H_2O), K_{sat} is the hydraulic conductivity of the aquifer (mm/day), L_{gw} is the distance from the ridge or subbasin divide for the groundwater system to the main channel (m), h_{wtbl} is the water table height (m), μ is the specific yield of the shallow aquifer (m/m), and α_{gw} is the baseflow recession constant. Substituting this definition for Q_{gw} into equation (22) gives

$$h_{wtbl,i} = h_{wtbl,i-1} \cdot \exp\left[-\alpha_{gw} \cdot \Delta t\right] + \frac{w_{rchrg,sh} \cdot (1 - \exp[-\alpha_{gw} \cdot \Delta t])}{800 \cdot \mu \cdot \alpha_{gw}} \qquad (23)$$

where $h_{wtbl,i}$ is the water table height on day i (m), $h_{wtbl,i-1}$ is the water table height on day $i-1$ (m), α_{gw} is the baseflow recession constant, Δt is the time step (1 day), w_{rchrg} is the amount of recharge entering the aquifer on day i (mm H_2O), and μ is the specific yield of the shallow aquifer (m/m).

Table 2.3 SWAT input variables used in shallow aquifer calculations.

Variable Name	Definition	File Name
GW_DELAY	δ_{gw}: Delay time for aquifer recharge (days)	.gw
GWQMN	$aq_{shthr,q}$: Threshold water level in shallow aquifer for base flow (mm H_2O)	.gw
ALPHA_BF	α_{gw}: Baseflow recession constant	.gw
REVAPMN	$aq_{shthr,rvp}$: Threshold water level in shallow aquifer for revap (mm H_2O)	.gw
GW_REVAP	β_{revap}: Revap coefficient	.gw
RCHRG_DP	β_{deep}: Aquifer percolation coefficient	.gw
GW_SPYLD	μ: Specific yield of the shallow aquifer (m/m)	.gw

2.1.2.3 Deep Aquifer

The water balance for the deep aquifer is

$$aq_{dp,i} = aq_{dp,i-1} + w_{deep} - w_{pump,dp} \quad (24)$$

where $aq_{dp,i}$ is the amount of water stored in the deep aquifer on day i (mm H_2O), $aq_{dp,i-1}$ is the amount of water stored in the deep aquifer on day $i-1$ (mm H_2O), w_{deep} is the amount of water percolating from the shallow aquifer into the deep aquifer on day i (mm H_2O), and $w_{pump,dp}$ is the amount of water removed from the deep aquifer by pumping on day i (mm H_2O). If the deep aquifer is specified as the source of irrigation water or water removed for using outside the watershed, the model will allow an amount of water up to the total volume of the deep aquifer to be removed on any given day.

Water entering the deep aquifer is not considered in future water budget calculations and can be considered to be lost from the system.

2.2 Theoretical and Calculation of MODLOW (Modular Three Dimensional Finite Difference Groundwater Flow Model)

2.2.1 Mathematical Model

The three-dimensional movement of ground water of constant density through porous earth material may be described by the partial-differential equation below.

$$\frac{\partial}{\partial x}\left(K_{xx}\frac{dh}{dx}\right)+\frac{\partial}{\partial x}\left(K_{yy}\frac{dh}{dy}\right)+\frac{\partial}{\partial z}\left(K_{zz}\frac{dh}{dz}\right)+W=S_s\frac{dh}{dt} \quad (25)$$

where K_{xx}, K_{yy}, and $K_{zz}$are values of hydraulic conductivity along the x, y, and z coordinate axes, which are assumed to be parallel to the major axes of hydraulic conductivity (L/T).h is the potentiometric head (L).W is a volumetric flux per unit volume representing sources and/or sinks of water, with $W < 0.0$ for flow out of the ground-water system, and $W > 0.0$ for flow into the system (T^{-1}).$S_s$is the specific storage of the porous material (L^{-1}). And t is time (T).

The finite-difference analog of equation (25) may be derived by applying the rules of difference calculus. However, an alternative approach is used with the aim of simplifying the mathematical treatment and explaining the computational procedure in terms of familiar physical concepts regarding the flow system. Theoretical from MODFLOW manual by USGS, 2005 and Waterloo Hydrogeologic, 2011 are below.

2.2.2 Finite-Difference Equation

Development of the ground-water flow equation in finite-difference form follows from the application of the continuity equation that is the sum of all flows into and out of the cell must be equal to the rate of change in storage within the cell. Under the assumption that the density of ground water is constant, the continuity equation expressing the balance of flow for a cell is

$$\sum Q_i = SS\frac{\Delta h}{\Delta t}\Delta V \quad (26)$$

where Q_i is a flow rate into the cell (L^3T^{-1}), SS is the notation for specific storage in the finite-difference formulation. Its definition is equivalent to that of S_s in

equation (25). So, SS is the volume of water that can be injected per unit volume of aquifer material per unit change in head (L^{-1}), ΔV is the volume of the cell (L^3), and Δh is the change in head over a time interval of length Δt.

The term on the right-hand side is equivalent to the volume of water taken into storage over a time interval Δt given a change in head of Δh. Equation (26) is stated in terms of inflow and storage gain. Outflow and loss are represented by defining outflow as negative inflow and loss as negative gain.

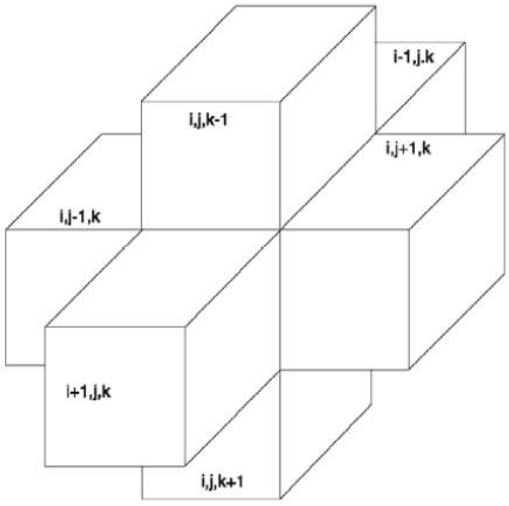

Figure 2.5 Indices for the six adjacent cells surrounding cell i, j, k (hidden) (Modified from McDonald and Harbaugh, 1988).

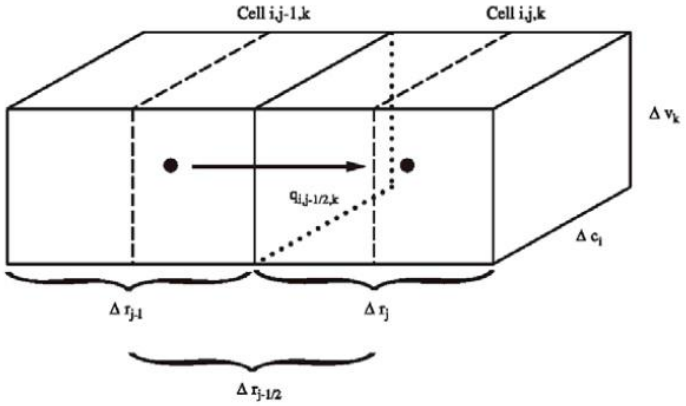

Figure 2.6 Flow into cell $i, j, k$from cell $i, j-1, k$ (Modified from McDonald and Harbaugh, 1988).

Figure 2.5 depicts six aquifer cells adjacent to cell i,j,k; $i-1,j,k$; $i+1,j,k$; $i,j-1,k$; $i,j+1,k$; $i,j,k-1$; and $i,j,k+1$. To simplify the following development, flows are considered positive if they are entering cell *i,j,k*. The negative sign usually incorporated in Darcy's law has been dropped from all terms. Following these conventions, flow into cell i,j,kin the row direction from cell $i,j-1,k$ (**Figure 2.6**) is given by Darcy's law as

$$q_{i,j-1/2,k} = KR_{i,j-1/2,k}\Delta c_i \Delta v_k \frac{(h_{i,j-1,k}-h_{i,j,k})}{\Delta r_{j-1/2}} \quad (27)$$

where $h_{i,j,k}$ is the head at node i,j,k, and $h_{i,j-1,k}$ is the head at node $i,j-1,k$, $q_{i,j-1/2,k}$ is the volumetric flow rate through the face between cells i,j,k and $i,j-1,k$ (L^3T^{-1}), $KR_{i,j-1/2,k}$ is the hydraulic conductivity along the row between nodes i,j,k and $i,j-1,k$(LT^{-1}), $\Delta c_i \Delta v_k$ is the area of the cell faces normal to the row direction, and$\Delta r_{j-1/2}$ is the distance between nodes i,j,k and $i,j-1,k$ (L).

Conceptual Aspects of Vertical Discretization

MODFLOW handles discretization of space in the horizontal direction by reading the number of rows, the number of columns, and the width of each row and column (that is, the width of the cells in the direction transverse to the row or column). Discretization of space in the vertical direction is handled in the model by specifying the number of layers to be used, and by specifying the top and bottom elevations of every cell in each layer.

At one extreme, vertical discretization can be visualized simply as an extension of a real discretization, a more or less arbitrary process of dividing the flow system into segments in the vertical dimension, governed in part by the vertical resolution desired in the results. At the opposite extreme, vertical discretization can be viewed as an effort to represent individual aquifers or permeable zones by individual layers of the model. **Figure 2.7(a)** shows a typical geohydrologic sequence that has been discretized in **Figure 2.7(b)** and **2.7(c)** according to both interpretations. The first viewpoint (**Figure 2.7(b)**) leads to rigid superposition of an orthogonal three-dimensional grid on the geohydrologic system. While there may be a general

correspondence between geohydrologic layers and model layers. No attempt is made to make the grid conform to stratigraphic irregulaties. Under the second viewpoint (**Figure 2.7(c)**), model layer thickness is considered variable to simulate the varying thickness of geohydrologic units. This leads, in effect, to a deformed grid.

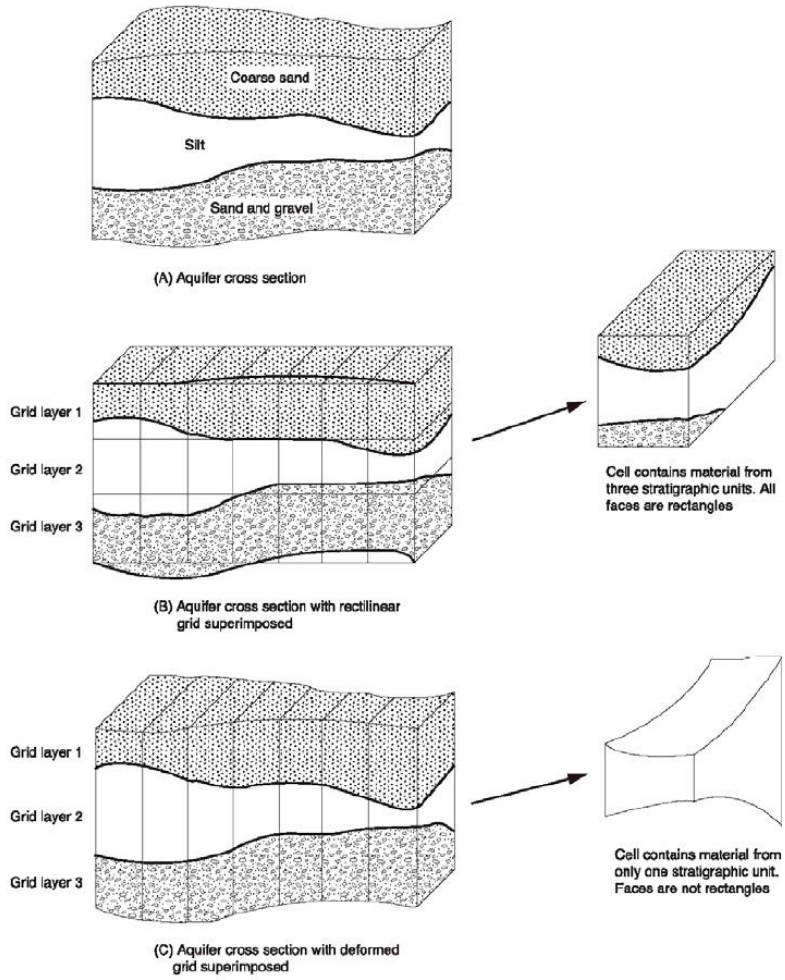

Figure 2.7 Schemes of vertical discretization (Modified from McDonald and Harbaugh, 1988).

Each of these methods of viewing the vertical discretization process has advantages and each presents difficulties. The model equations are based on the assumption that hydraulic properties are uniform within individual cells or at least that meaningful average or integrated properties can be specified for each cell. These conditions are more likely to be met when model layers conform to geohydrologic units as in **Figure 2.7(c)**. Moreover, greater accuracy can be expected if model layers

correspond to intervals within which vertical head loss is negligible, and this is also more likely under the configuration of **2.7(c)**. On the other hand, the deformed grid of **2.4(c)** fails to conform to many of the assumptions upon which the model equations are based; for example, individual cells no longer have rectangular faces, and the major axes of hydraulic conductivity may not be aligned with the model grid. Some error is always introduced by these departures from assumed conditions.

2.3 Theoretical and Calculation of BFLOW (Baseflow Filter Program)

From research of arnold (Arnold and Allen 1999), (Arnold, Allen et al. 1995) and (Arnold, Muttiah et al. 2000) baseflow theoretical by Recharge to an aquifer was estimated from its relation to other measured components of the hydrologic budget. Part of precipitation on the basins infiltrates through the soil zone to the water table and becomes groundwater. Some of this groundwater is subsequently discharged to the streams as baseflow and some is lost to the atmosphere by evapotranspiration. In a given period of time, precipitation recharged to the water table is balanced by baseflow (ground water discharge to the stream), seepage to deeper aquifer units and evapotranspiration.

$$R = BF + ET + S + St \tag{28}$$

where R is groundwater recharge, BF is groundwater discharge (baseflow), ET is evapotranspiration, S is subsurface seepage out of the basin, and St is change in groundwater storage.

Ground water runoff, or baseflow, and groundwater evapotranspiration were determined from the mean groundwater stage-runoff rating curves. These were prepared by plotting mean weekly groundwater stages from monitored wells in the basin against streamflow on corresponding dates when streamflow consisted entirely of groundwater runoff. Separate rating curves were prepared for late fall through early spring, and late spring through early fall. The difference in the groundwater runoff between the two curves was taken as the approximate groundwater evapotranspiration. The curves were also used to evaluate the separation of the total

flow hydrographs into direct runoff and ground water runoff. Subsurface seepage was estimated for the three Illinois basins from the Darcy equation below

$$Q = TIL \tag{29}$$

where Q is the underflow, T is the coefficient of transmissivity, I is the hydraulic gradient of the water table, and L is the width of the cross section of the deposits. Seepage was considered negligible in calculations for all the basins studied and deleted from the equation. The change in groundwater storage was estimated from the change in mean groundwater stage from observation wells and the estimated gravity yield of the wells.

$$St = H \cdot (S_y) \tag{30}$$

where H is mean change in ground water stage, and S_y, is specific yield of the deposits. Specific yield was estimated from the ratio of the annual integration of the winter baseflow recession curve to the average water table response inferred from laboratory tests on grain size and porosity, or a similar indirect method. This is similar to methods used by Fairchild et al. (1990) in their assessment.

SWAT Bflow is a baseflow filter program that offers a Web Interface to determine runoff/baseflow fraction in streamflow and the baseflow alpha factor required in SWAT .gw files. Its search algorithm is adopted from Arnold and Allen (1999). SWAT Bflow offers a Google Map interface with one-click query to access USGS gages.

2.4 Literature Review

2.4.1 Related Research in the Area of Yom River Basin and Phare Groundwater Basin

Bureau of Groundwater Conservation and Restoration, Department of Groundwater Resources of Thailand, 2013, summarized results of monitoring of groundwater levels of Phrae groundwater Basin. The direction of the groundwater flow was the same direction as the Yom River Basin, from the north to the south. Both of groundwater flow from the east and west converged to the main as well as the tributaries of the river. Older terrace deposits were aquifer that is the most water application efficiency. Younger terrace deposits remained moderate and Carbonate Metasediment and Metamorphic groundwater that is the least water application efficiency, except in case of cracks, faults and joints between the stones. Information of groundwater monitoring wells in the area showed groundwater levels and water quality in unconsolidated sediments with depth of groundwater about 20 to 30 and 60 to 100 m. Groundwater level data from monitoring had changed during 10 years since 2004 to 2013. Observation wells from all 3 stations with a total of 4 wells in sedimentary area showed that groundwater levels fluctuate with seasonal averages about 1 to 3 m from surface at the area of underground water springs in Thung Nao subdistrict, Sung Men district, with water level of 0.6 m and in area of Ban Don Mun subdistrict, Song district. From 2009 to the present, level of groundwater has decreased steadily. Groundwater levels were very low from the surface at 40 to 60 m. Pumping of groundwater in the drought and scarce of rain area was more used. As a result, groundwater levels dropped from normal level and when it rains, groundwater level rises to the normal.

Kasetsart University, 2012, evaluated the quantity of groundwater from rate of change in the groundwater level, aquifer areas and storage coefficient of groundwater basins in Thailand. The review reported the groundwater resources which has an estimated volume of water in unconsolidated sediments in mainly groundwater basins in each region of Thailand. Using value of groundwater levels fluctuation, the aquifers had average level at 5 m. Storage coefficient of unconfined aquifer was 0.16, confined

aquifer was 2×10^{-4} and semi-confined aquifer was 0.085. The amount of groundwater that can be developed without impact (safe yield) was naturally balanced with the amount of groundwater recharge. This value was used for recovery the water when the level drops to 5 m. The conclusion was that the area of Phrae Basin has groundwater storage about 180 mcm/yr. And the amount of water that can be developed without impact (safe yield) was 32 mcm/yr or 0.087 mcm/day.

(Sawatpru and Konyai), estimated storage efficiency of catchment area and groundwater inflow to a particular river by using Base Flow Index (BFI) to analyze the streamflow daily data. Analysis process was written by M-file function on MATLAB program. Total 8 streamflow gauge stations in the study area covered Yom basin in Phrae, Sukhothai, Phichit province including Y.20, Y.1C, Y.14, Y.6, Y.3A, Y.4, Y.17 and Y.5 these follow to river flow direction. The results of the analysis showed the maximum BFI about 0.33 was at station Y.6 in Sukhothai and storage volume was 28,835.83 cms day.The minimum BFI about 0.15 was at station Y.17 and storage volume was 52,342.91 cmsday. The trend of the amount of groundwater had the highest increase at station Y.6 in Sukhothai and the lowest decrease at station Y.5 in Phichit.

Department of Groundwater Resources of Thailand, 2011, concluded all consumptive usage of groundwater in Phrae Groundwater Basin. They found that the amount of water used for consumption was19 mcm/yr. The highest water usage was from the municipal water system and supply for the village with the rate of 14 mcm/yr. The second was from the provincial waterworks authority regional supply system about 3 mcm/yr. Private groundwater wells was 2 mcm/yr, and the minimum was from shallow wells totally 0.28 mcm/yr. The groundwater usage in the future may be more likely to increase. The most of water used from groundwater resources accounted for approximately 80 percent of water consumption that is equal to 315.16mcm/yr. And the water used from surface water accounted for approximately 20 percent of water consumption that is equal to 3.83 mcm/yr. They also found that the current groundwater used for agriculture is totally 8.36 mcm/yr. The amount of groundwater was mainly used in shallow aquifers and deep aquifers in some areas.

Pitaksaithong (2004), used the model to find simple surface water balance in Yom watershed. To calculate the amount of groundwater storage in basin, many data such as weather, rainfall and runoff was collected for using in statistical analysis according to the hydrological principle, and for determining the evapotranspiration, plant water usage and storage volume in watershed. The study area was 23,616 km^2. Yom River flew through the center of the study area and had many tributaries flowing lines converge to Yom River. The reference evapotranspiration was calculated by the Modified Penman method with the average value about 1,588 mm/yr. While the average annual rainfall was 1,119 mm/yr, the average crop water requirement was about 5,440 mcm/yr, and the water consumption was about 5,478 mcm/yr. The water balance conditions were made in 3 scenarios in 2001 to 2002 from dry and wet year. It was found that the proportion of the amount of water distributed in the system could be classified to evapotranspiration from 41.5 to 45.6 percent, consumptive use from 16.6 to 18.2 percent, infiltration and groundwater recharge from 5.5 to 20.2 percent, and the runoff from 16.7 to 35.0 percent, approximately. Furthermore, the results showed that the most of watershed areas were shortage of water in the dry season and the beginning of wet season because the water requirement was higher than the available rainfall, especially in the middle and the lower watershed areas. Because of that, this period was a period of cultivation that the demand of water for planting preparation was more than rain but considering to the average runoff during the rainy season, the amount of excess water was at all areas of the watershed.

Amares Boksuwan, 2003, studied the drought of Yom watershed caused by rain in some years less than normal rate and the population increase that results to increase of water usage. Severe drought was more in year from 1992 to 1993 and 1997 to 1998 that was usually occurrence in a period of 5 to 6 years. Therefore, to understand the problems of drought, the study aimed to analyze the drought of Yom watershed. The study began by examining the drought conditions of the past to find the cause and severity of drought conditions in each area. Based on the amount of natural water in the area, e.g. rainfall and runoff, to compare with water activities in each area and then set the drought index in the Yom River Basin. Lower Yom River Basin in main channel often suffered from lack of water every year in the past 5 to 6

years and would be a very serious one. The areas far from the rivers were affected by drought during the rainy season and the dry season due to very less of rainfall in the dry season. Upper Yom River Basin experienced drought less than the lower basin because the total rainfall is higher than other areas and water usage was low. Water for consumption was scarce during the dry seasons almost all areas of the Yom River, especially in Sukhothai and Phrae province. It was also found that around 40 years ago, trend of annual rainfall had decreased by 1 to 14 mm/yr and runoff decreased in dry seasons because the water demand had increased continuously.

Seree Supharatid and Chalongrat Sakornrat, 2000, analyzed the frequency and severity of drought that occurred in the area of Phrae and Sukhothai provinces. The definition of drought is the average rainfall in one month less than precipitation threshold, calculated by Truncation Level. The results showed that the distribution of information during times of extreme drought had spread geometrically and the average time for lack of water in Phraewas more than Sukhothai. Phrae and Sukhothaihadprobability of drought for one month period in 2.5 years and 1.6 years, respectively.

2.4.2 Related Research in SWAT Hydrological Model

(Boonkaewwan 2013), studied to evaluate the surface water quality data, nitrate-N concentrations (NO_3-N) and phosphate (PO_4^{3-}) discharging along the Lower Yom River and to assess the relative impact of point source and non-point sources. In sensitivity analysis process affecting runoff, 9 parameters was adjusted including CN2 (curve number), SOL_AWC (available soil water capacity), GWQMN (threshold depth of water in the shallow aquifer required for return flow), GW_DELAY (groundwater delay time), ESCO (soil evaporation compensation factor), RECHRG_DP (deep aquifer percolation fraction), ALPHA_BF (baseflow alpha factor), GW_REVAP (revap coefficient) and REVAPMN (threshold depth of water in the shallow aquifer for re-evaporation or percolation to the deep aquifer). It was found that the significant parameters to simulate runoff were CN2, SOL_AWC, GWQMN, and GW_DELAY.

(Petchprayoon, Blanken et al. 2010), determined the hydrological impacts of land use/land cover (LULC) change in the Yom watershed in central–northern Thailand over a 15-year period using an integration of remote sensing, Geographic Information System, statistical methods and hydrological modeling. The LULC changes showed an expansion of urban areas by 132% (from 210 km^2 in 1990 to 488 km^2 in 2006). The Yom River's daily discharge long-term trend significantly increased at the most of the measurement stations (p value <0.05). And the rate of increase in discharge at areas downstream of the rapid urbanization was significantly greater than that at areas upstream. There were no significant long-term trends in precipitation characteristics in the basin, except for one station. The rate of change in discharge after changes in LULC showed a systematic increase over a range from 0.0039 to 0.0180 $m^3s^{-1}day^{-1}$ over a 15-year period, with the increase in urbanized area spanning a range from 81 to 149% in two flood-prone provinces. A rainfall-runoff model simulated a small increase (~10%) in peak flows. The coupling of surface observations, remote sensing, and rainfall-runoff modeling demonstrated the impacts of changes in LULC on peak river discharge, hence flooding behavior, of a major river in central–northern Thailand.

(Vesurai 2005), studied the distributed parameter model SWAT which was tested on monthly basis for estimating surface runoff from the Upper Nan River Basin, to determine the impacts of land use changes. The network of streams in the basin was delineated from the DEM data. Land uses data for the year 1977, 1994 and 2001 which shown significant land use changes in the watershed were utilized to classify the basin hydrologic response units (HRUs) for each case study. The period of 5 to 10 years for continuous observed monthly runoff of each land use data was used to calibrate the model. The analyses showed the similarities between the generated stream network and the actual basin network. The calibrations were also acceptable for all cases. Sensitivity analysis was performed by varying range of model parameters recommended by the models developer. The significant sensitive parameters were the physical properties such as the available water capacity and the Curve Number (CN). The year 1977, 1994 and 2001 calibrated models were then used to estimate runoffs from the observed daily rainfalls during 1998 to 2002. The

comparison of each runoff series showed the impact of land use changes. Besides, three scenarios postulating changes in land uses, reforestation, agricultural and the urban expansions, were modeled and then used to assess the consequences on surface runoff. The results demonstrated that impacts on runoff can be clearly detected, and hence verify the applicability of using SWAT model in the planning and management of water resource of the river basin.

(Abbaspour, Rouholahnejad et al. 2015), studied a subbasin-scale hydrologic model of Europe using the well-established SWAT program. The model was calibrated for a large number of river discharge stations, nitrate loads of rivers, and yields of wheat, maize, and barley. The program SUFI-2 in SWAT-CUP package was used for calibration or uncertainty analysis, validation, and sensitivity analysis. Only readily available data were used for model setup as well as calibration and validation. In the part of calibration protocol for large-scale distributed base on models parameterized using the guidelines summarized in table.

2.4.3 Related research in MODFLOW Hydrogeological Model

(Kornkul 2013), estimated groundwater recharge to aquifers include evaluated groundwater flow and groundwater balance. The result of creating a conceptual framework model of hydrogeology found in three aquifers categories such as floodplain deposited aquifers (Qfd), terraces deposited aquifers (Qyt and Qot) and the consolidated aquifers (TRjik and PCms). The main groundwater direction of the unconsolidated and consolidated aquifers flew from the northern to the southern area with a mean hydraulic gradient approximately 0.0013, which is corresponding to the groundwater flow simulated by MODFLOW. The central part of the region and the Yom river were found as discharge areas. The groundwater recharge rates were spatially determined by WetSpass module for estimating seasonal variability patterns of groundwater recharge which were vary between 0 to 320 mm/year. In addition, the results showed that the potentiality of recharge area corresponds to the topography and hydrologic characteristics. Groundwater recharge derived from WetSpass was then imported into MODFLOW for calibration and verification of groundwater modeling. The results revealed that the variations of groundwater balance are seasonal

dependent, which found relatively high recharge rates and groundwater inflow during the rainy season. According to groundwater modeling, the groundwater inflow is relatively higher than the groundwater outflow approximately 111,320 m^3/year. Finally, in order to determine groundwater safe yield and propose the sustainable groundwater management, the groundwater model was simulated by increasing the pumping rates under three situations: 25, 50 and 100%. The results showed that the availability of the pumping rate is not higher than 50% relatively compared to the base condition. These contributions would be further applied as the fundamental data for appropriately sustainable groundwater management.

(Chaisayun and Kwanyuen 2004), studied to simulate groundwater movement using MODFLOW program for Sukhothai Groundwater Project. In the model calibration, comparison of the levels of simulated and observed well water was made and found that the fluctuations and trends of both water levels are similar. It should be noted that pumping rate and amount of rainfall were two factors affecting water level fluctuations, particularly, the water levels in TW4, OW4 and OW7 wells around the middle studied area where high pumping rates were operated. Estimation of annual safe yield was calculated basing on the data obtained from continuous operations for altogether 10 years of varied pumping rates of 35 to 55 mcm/yr. It was found that the suitable pumping rates enabling the stabilization of the water level should be between 35 to 40 mcm/yr. Comparing the present simulation to two previously made simulations using MIKE SHE and SGDP models, the results indicated that MODFLOW model was more accurate. It is a public software so it is economical and appropriate for ground water modeling in the other areas.

2.4.4 Related Research of the Interoperability Operation of SWAT and MODFLOW Models

(Kim, Chung et al. 2008), developed an HRU–cell conversion interface which exchanges flow data between the cells in MODFLOW and the HRUs (hydrologic response units) of SWAT. HRUs were defined by overlaying soil and land use and lumping similar soil/land use combinations. On the basis of these modifications, the groundwater model in SWAT was successfully replaced with MODFLOW. Therefore, it was possible to establish a fully integrated modeling program, which was able to form a linkage in each time step. Therefore, the distributed groundwater recharge rate and the groundwater evapotranspiration could be effectively simulated. Considering the interaction between the stream network and the aquifer to reflect boundary flow completes the linkage. For this purpose, the RIVER package in MODFLOW was used for river–aquifer interaction. The water transfer method in SWAT was enhanced in order to use daily/monthly/yearly water transfer options as well as either a constant amount, a constant rate, or a minimum value from the water source. The application demonstrated that an integrated SWAT–MODFLOW is capable of simulating the spatio-temporal distribution of groundwater recharge rates, aquifer evapotranspiration and groundwater levels. And it was enables for an interaction between the saturated aquifer and channel reaches. This interaction played an important role in the generation of groundwater discharge in the Musimcheon Basin, especially during the low flow period.

(Chung, Kim et al. 2010), used the SWAT-MODFLOW model to research a multi-reservoir storage routing module instead of a single storage routing module in SWAT. This represented a more realistic delay in the travel of water through the vadose zone. By using this module, the parameter related to the delay time could be optimized by checking the correlation between simulated recharge and observed groundwater levels. The final step of this procedure was to compare simulated groundwater levels as well as the simulated watershed stream flow with the observed groundwater levels and watershed stream flow. This method was applied to the Mihocheon watershed in South Korea to estimate spatio-temporal groundwater recharge distribution. The computed annual recharge rate was compared with the

independently estimated recharge rate using BFLOW. The hydrologic modeling results showed that the annual average recharge rate should be estimated by a long-term continuous simulation with a distributed hydrologic modeling technique.

(Bejranonda 2006), studied to develop the integrated SWAT–MODFLOW model. This study used 2 partition of coupling parameters that is water entering groundwater storage by infiltration/percolation and interconnection between seepage and surface water bodies based on models theoretical of river-gw interaction in MODFLOW and percolation in SWAT. The simulation of SWAT was considered for exchanging water in a format of the groundwater recharge (baseflow) from groundwater head (h) obtained by assuming constant of groundwater head in basin, boundary length of groundwater basin (L_{gw}), and hydraulic conductivity of the groundwater layer (K_{sat}). The simulation of MODFLOW was considered for exchanging water (river-gw interaction) from the difference of the water level in the river (H_{riv}) and groundwater table (H_{aq}) derived from the calculation and calibration by groundwater flow equations. Beside, SWAT model did not focus on the groundwater parameters to calculate directly in grid cells, but calculated the average groundwater level in the subbasin. In addition, river-aquifer interconnection was only from seepage to surface water bodies in one-way direction and cannot be accurately calculated groundwater levels. The river-aquifer interconnection theory was chosen from MODFLOW partition of coupling models. In conclusion, the parameters that can be used to interface between surface water and groundwater were percolation, recharge, spring, streamflow, baseflow and streams (gw).

(Wang, Luo et al. 2013), developed hydrologic modeling of surface water and groundwater interaction by coupling SWAT (for surface water simulation) and MODFLOW (for groundwater simulation). The newly developed modeling framework reasonably captured the spatiotemporal variability of the hydrological processes of the surface water and groundwater in the Haihe River Basin, China. The modeling results showed a good agreement with the measurements of surface water and groundwater during 1996 to 2006. Results of model evaluation indicated that the developed model could be a promising tool in watershed management planning under

the context of global climate change and the “South-North Water Transfer Project”. In the Haihe River Basin, climate change had significant effects on surface hydrology as indicated by the predicted increases on actual evapotranspiration and precipitation during 2041 to 2050 relative to those during 1991 to 2000. Changes of groundwater storage were mainly contributed by water diversion which would reduce the requirement of water pumping from groundwater especially for domestic and industrial uses. By the middle of the 21st century, increased water supply by projected precipitation and water diversion would result in annual increases of 3.9~9.9 billion m^3 for river discharge and 1.7~2.9 billion m^3 for groundwater storage as annual averages.

Chapter III
Methodology

3.1 Description of the Study Area

This research aims for assessing the water balance and safe yield of water consumption of each layer in Quaternary unconsolidated sedimentary aquifers of Phrae basin. It is necessary to separate bisect process of data analysis in the study area. SWAT was used to simulate the divided data for hydrological characteristics and surface water modeling. Another data was used for simulating the same by MODFLOW.

Scope of workspace to simulate surface water is a boundary of Phare groundwater basin (GW) or upper and central part of Yom river basin (SF) based on the location of the meteorological and hydrological gauging stations distributed in each sub-watershed. They are suitable for model calibration and validation, and many output results is in units of subbasin. The results of the simulations will be used as baseline data for groundwater recharge using in further groundwater modeling.

Similarly, scope of workspace to simulate groundwater is a boundary of Phare Basin (GW) based on the interaction between rivers and aquifers. The interaction between the rivers and Quaternary unconsolidated sedimentary aquifers is focused because the water fluctuation in a short time period is significantly more than the semi-consolidated and consolidated aquifers.

Thus, data was set together by inserting layers of data requirement and attach boundary of two models. This chapter describes in detail of data requirement in the study area.

3.1.1 Boundary and Location

Phare groundwater basin is located at the north of Thailand. An area is approximately 10,711 km^2 representing 44.73% of the total area of Yom watershed. Phare basin has an area approximately 992 km^2 representing 9.26% of the total area of the Phare groundwater basin. Administrative province of Phare Groundwater Basin is consisting of some part of Phayao, Nan, Lampang, and entire of Phare and Phare Basin is in the center of Phare province.

In hydrological situation (surface water consider), north side of the boundary is adjacent to Mekong river watershed, south side of boundary is adjacent to Ping river basin, east side of boundary is adjacent to Nan river basin, and west side of boundary is adjacent to Wang and Ping river basin.

In hydrogeological situation (groundwater consider), north side of boundary is adjacent to Chiang Rai - Phayao groundwater basin in Phayao province, south side of boundary is adjacent to Upper Chao Phraya groundwater basin in Sukhothai and Uttaradit province, east side of boundary is adjacent to Nan groundwater basin in Nan province, and west side of boundary is adjacent to Lampang groundwater basin in Lampang province (**Figure 3.1**).

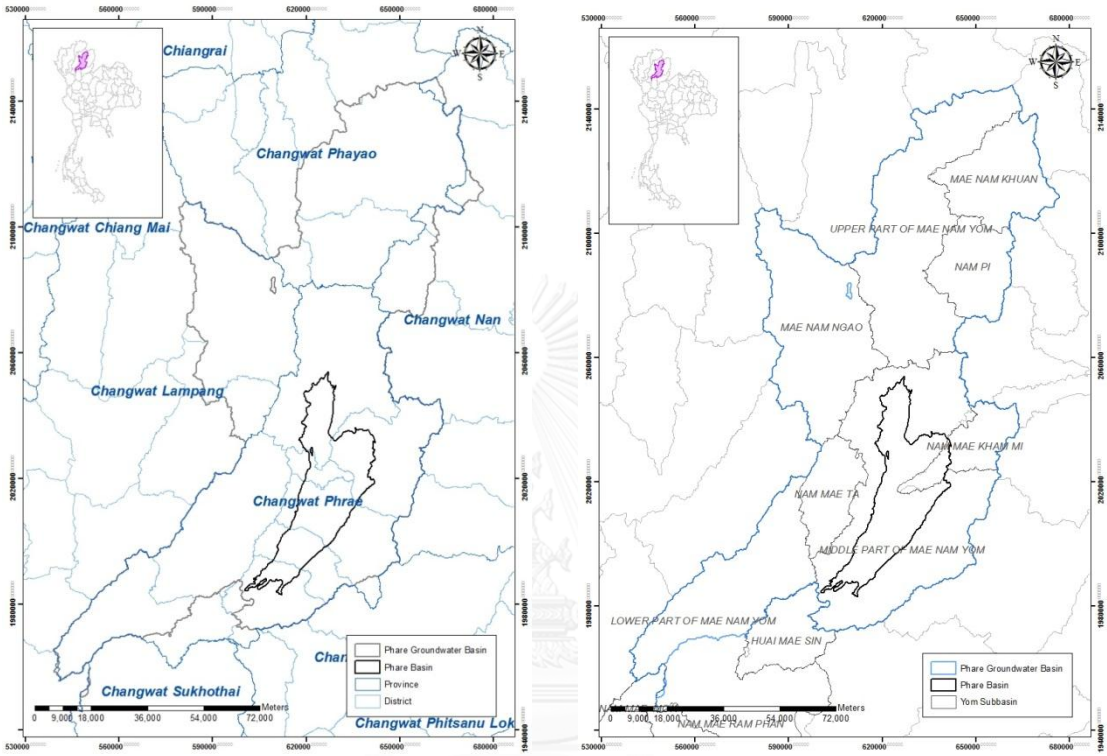

(a) **(b)**

Figure 3.1 (a) Phare Groundwater Basin and Phare Basin compared with administrative provinces. **(b)** Phare Groundwater Basin and Phare Basin compared with Yom River Subbasin.

3.1.2 Topography

Phare groundwater basin has characteristics of the watershed along the north-south and the Yom River flows through the center of the area. Topography in the upper part is mountains and plains of the valley along the river. The central part is large plains in area of Song, Muang, and Den Chai district, caused by the deposits of Quaternary era sediments, i.e. Phare Basin. The lower part is highland and mountain range.

Yom River originated from the Phi Pan Nam Mountains in Pong and Chiang Muan district of Phayao province runs through a very steep slope valley with stream gradient approximately 1:310 and has an elevation of 280 to 360 m (msl). Then it flows through narrow range of plain near the canals before flows into Phare province. It flows out into a large plain in Song, Sung Men, and Den Chai district of Phare province with stream gradient approximately 1:1180 and has an elevation of 180 to 280 m (msl). After that, it flows into the west side valley in Long and Wang Chin district, and then flows down into the Si Satchanalai floodplains, Sukhothai province. During Yom River flew parallel to the Nan River, it begins a steep decline with stream gradient approximately 1:2300 and has an elevation of 50 to 180 m (msl). Total length of Yom River in the boundary is approximately 366.2 km (figure 3.2a).

Phare Groundwater Basin boundary has cover 7 subbasins of upper and middle part of Yom River basin and some area of lower part subbasin. In addition, the Phare Basin as a part of the Phare Groundwater basin locates in the center of Phare province (**Figure 3.2b**), and descriptions are below.

Upper part of Mae Nam Yom subbasin locates in the upper basin, which is the source of the Yom River. The catchment area has approximately 1,978 km^2 equivalent to 18.47% of the Phare Groundwater Basin. It covers over the area of Pong, Chiang Muan, Dok Kham Tai district of Phayao province, Ngao district of Lampang province, and Song district of Phare province. Topography is high and there are steep mountain and narrow range of plain near the canals.

Mae Nam Khuan subbasin locates in the northeast of boundary. The catchment area has approximately 858 km^2 equivalent to 8.01% of the Phare Groundwater Basin. It covers the area of Pong, Chiang Muan district of Phayao province and Tha Wangpha, Ban Luang district of Nan province. Topography is high and there are steep mountain and narrow range of plain near the canals.

Nam Pi subbasin locates below Mae Nam Khuan subbasin. The catchment area has approximately 636 km^2 equivalent to 5.94% of the Phare Groundwater Basin. It covers the area of Chiang Muan district of Phayao province and Ban Luang district of Nan province. Topography is high and there are steep mountain and narrow range of plain near the canals,

Mae Nam Ngao subbasin locates in the northwest of boundary against the upper part of Mae Nam Yom subbasin. The catchment area has approximately 1,644 km^2 equivalent to 15.35% of the Phare groundwater Basin. It covers the area of Ngao, Mae Mo district of Lampang province and Song district of Phare province. Topography is high and there are steep mountain and narrow range of plain near the canals.

Middle part of Mae Nam Yom subbasin locates in the middle to lower of boundary. The catchment area has approximately 2,884 km^2 equivalent to 26.93% of the Phare groundwater basin. It covers the area of Song, Nong Muang Khai, Rong Kwang, Den Chai, Muang, Long, Sungmen, and Wang Chin district of Phare province. Topography is flanked by mountain range which slope is down to the Yom River in the central area with a large flat plain area along the Yom River.

Nam Mae Kham Mi subbasin locates in the middle part slightly east of boundary. The catchment area has approximately 444 km^2 equivalent to 4.15% of the Phare Groundwater Basin. It covers the area of Muang, Rong Kwang, and Nong Muang Khai district of Phare province. Topography is high hill at the east and slope is down to the southwest, and there is a narrow range of plain near the canals.

Nam Mae Ta subbasin locates in the middle part slightly west of boundary. The catchment area has approximately 518 km^2 equivalent to 4.84% of the Phare

Groundwater Basin, covering area of Muang, Long, Song, Sungmen, and Nong Muang Khai district of Phare province. Topography is a high hill slope along the north-south and there is a narrow range of plain near the canals, and then flat plain extends at the end of subwatershed.

Some area of lower part of Mae Nam Yom subbasin locates at the lower part to the end of boundary, covering area of Long and Wang Chin district of Phare province. Topography is flanked by mountain range which slope is down to the Yom River in the end of boundary and there is a narrow range of plain near the canals.

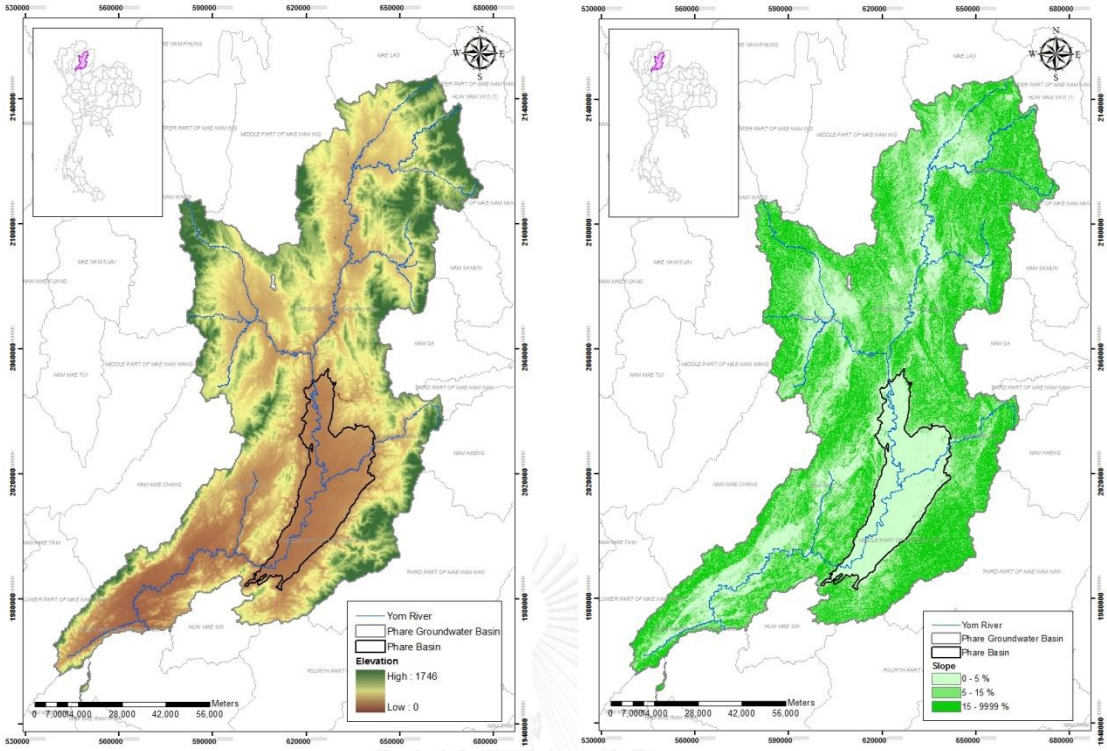

(a) **(b)**

Figure 3.2 (a) Topographic map in the study area and **(b)** Slope classification for SWAT HRUs setting up in the study area.

3.1.3 Meteorology

The climate of the study area is under the influence of the southwest monsoon and northeast monsoon, and also depression and typhoon which blew into the South China Sea from time to time. Thus it results to seasons such as rainy season from May to October, winter from October to February, and summer from February and May.

Meteorological data of The Meteorological Department recorded from the year 1988 to 2013 at 5 weather stations in the study area was used. The average annual values of meteorological parameters are shown in **Table 3.1** and the details are summarized below. (Chotpantarat, Chuangcham et al. 2011)

Temperature

The monthly average temperature ranges from 19.8 to 31.5°C. The lowest temperature is in December, while the maximum temperature is in April. The annual average temperature is between 25.1 and 28.2°C.

Relative Humidity

The monthly average relative humidity is between 57 and 85%. The lowest humidity is in February, March and April, and the highest is in September. The change of relative humidity is directly influenced by the monsoon. Moisture content is brought by southwest monsoon but the northeast monsoon brings dry air. The annual average relative humidity is between 71 and 77%.

Cloudiness

The monthly average of cloudiness is between 2.0 and 8.0 out of 10 parts of the sky. The lowest cloudiness is in January and February but the highest is in July and August. A yearly average of cloudiness is 5.0 out of 10 parts of the sky.

Wind Speed

The wind speed ranges from 0.2 to 5.0 knots. The minimum wind speed is in October and January, and the maximum wind speed is in July, June, April and March. The annual average of wind speed is between 0.4 and 2.7 knots.

Evaporation

Generally, evaporation is lower in rainy season and higher in summer. The monthly average evaporation varies from 79.0 to 234.0 mm. The highest average evaporation is in April, while the lowest is in November, December and January. Full year evaporation by Class A pan is from 1,251 to 1,947 mm.

Reference crop evapotranspiration (ETo)

The monthly data is shown in **Table 3.1.**

Table 3.1 Monthly reference crop evapotranspiration (ETo) in the boundary

Stations	Reference Crop Evapotranspiration (mm)												
	Jan	Feb	Mar	Apr	May	Jun	Jul	Aug	Sep	Oct	Nov	Dec	Annual
Phayao	73.80	85.19	116.68	127.47	120.12	102.33	96.27	92.23	89.77	88.31	72.60	64.48	1129.23
Lampang	77.89	89.39	119.08	130.83	123.70	104.29	98.41	94.64	92.11	91.15	76.03	68.24	1165.76
Phare	78.39	89.03	120.27	135.64	125.09	104.32	97.82	95.95	92.75	90.80	77.15	69.67	1176.89
Nan	75.26	84.45	113.64	127.87	125.26	107.09	102.01	97.99	91.47	92.72	77.99	69.66	1165.42
Uttaradit	81.42	90.44	118.24	133.52	129.10	108.29	103.57	99.62	93.58	97.45	84.63	77.52	1217.38

Monthly reservoir evaporation

The monthly data is shown in **Table 3.2.**

Table 3.2 Monthly reservoir evaporation in the boundary.

Stations	Monthly Reservoir Evaporation (mm)												
	Jan	Feb	Mar	Apr	May	Jun	Jul	Aug	Sep	Oct	Nov	Dec	Annual
Phayao	66.50	79.10	111.30	122.50	107.10	93.80	85.40	79.10	72.10	70.00	60.90	59.50	1007.30
Lampang	63.00	79.10	111.30	125.30	113.40	95.20	88.20	82.60	74.90	71.40	62.30	57.40	1024.10
Phare	72.10	83.30	121.80	137.20	126.00	102.90	97.30	91.00	84.70	82.60	71.40	67.90	1138.20
Nan	56.70	63.70	86.10	100.10	97.30	79.10	72.10	67.20	69.30	69.30	59.50	55.30	875.70
Uttaradit	77.70	84.00	112.00	126.70	117.60	94.50	85.40	83.30	83.30	87.50	81.20	79.10	1112.30

Precipitation Rainfall data from 29 weather stations and 8 hydrological gauging stations covered the boundary in upper Yom River Basin has annual average rainfall about 1700 mm.

Table 3.3 Range of meteorological parameters in 30 years period (1977 to 2006) of weather stations located in the study area and vicinage

Weather Stations	Meteorological Parameters	Units	Range of Average Monthly Data	Average Annual Data
Phayao Province	Temperature	˚C	19.8 (Dec) - 28.6 (Apr)	25.1
Capital District	Relative Humidity	%	62 (Apr) - 85 (Sep)	75
	Cloudiness	0-10	2.0 (Jan, Feb) - 8.0 (Jun-Jul)	5
	Wind Speed	knot	0.4 (Oct) - 1.4 (Jun)	0.9
	Class A pan Evaporation	mm.	85.0 (Dec) - 175.0 (Apr)	1,439
Lampang	Temperature	˚C	21.4 (Dec) - 29.9 (Apr)	26.2
Province	Relative Humidity	%	57 (Mar) - 83 (Sep)	73
Capital District	Cloudiness	0-10	2.0 (Jan-Mar) - 8.0 (Jun-Aug)	5
	Wind Speed	knot	0.4 (Oct-Dec) - 1.4 (Jun)	0.9
	Class A pan Evaporation	mm.	82.0 (Dec) - 179.0 (Apr)	1,463
Phare Province	Temperature	˚C	21.8 (Dec) - 29.9 (Apr)	26.3
Capital District	Relative Humidity	%	61 (Mar) - 84 (Sep)	75
	Cloudiness	0-10	3.0 (Dec-Mar) - 8.0 (Jun-Sep)	5
	Wind Speed	knot	0.7 (Jan, Oct) - 2.1 (Apr)	1.3
	Class A pan Evaporation	mm.	97.0 (Dec) - 196.0 (Apr)	1,626
Nan Province	Temperature	˚C	20.8 (Dec) - 28.9 (Apr)	25.8
Capital District	Relative Humidity	%	66 (Mar) - 85 (Aug, Sep)	11
	Cloudiness	0-10	2.0 (Feb, Mar) - 8.0 (Jun-Aug)	5
	Wind Speed	knot	0.2 (Oct-Dec) - 0.6 (Mar, Apr, Jun, Jul)	0.4
	Class A pan Evaporation	mm.	79.0 (Dec) - 143.0 (Apr)	1,251
Sukhothai	Temperature	˚C	24.2 (Dec) – 30.6 (Apr)	27.6
Province	Relative Humidity	%	68 (Apr) – 84 (Sep)	77.2
Capital District	Cloudiness	0-10	3.0 (Jan) - 8.0 (Jun)	6
	Wind Speed	knot	1.6 (Jan) – 3.8 (Jul)	2.6
	Class A pan Evaporation	mm.	106.0 (Dec) - 194.0 (Apr)	1,662
Uttaradit	Temperature	˚C	23.7 (Dec) - 30.8 (Apr)	27.50
Province	Relative Humidity	%	62 (Mar) - 83 (Aug, Sep)	73
Capital District	Cloudiness	0-10	2.0 (Jan, Feb) - 8.0 (Jun-Aug)	5
	Wind Speed	knot	0.6 (Jan) - 1.0 (Apr)	0.8
	Class A pan Evaporation	mm.	111.0 (Jan) - 181.0 (Apr)	1,589

3.1.4 Hydrology

North side of boundary is adjacent to the Mekong river watershed, south side of boundary is adjacent to Ping river basin, east side of boundary is adjacent to Nan river basin, and west side of boundary is adjacent to Wang and Ping river basin. The details are at subsections 3.1.1 and 3.1.2.

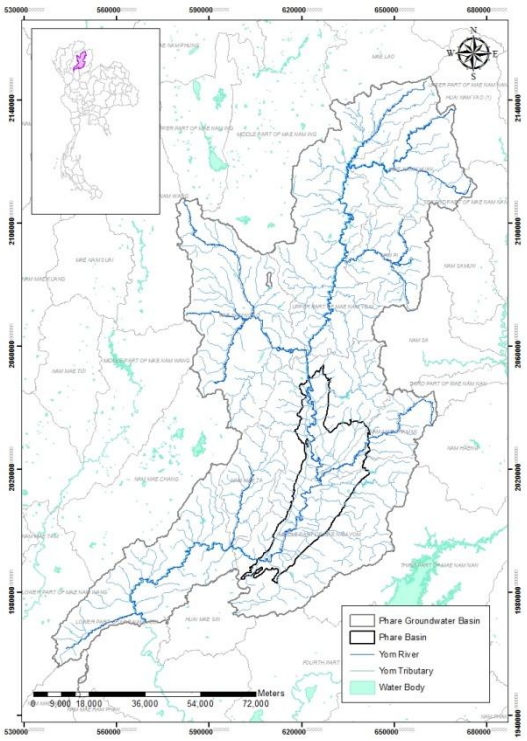

Figure 3.3 Hydrological map of the study area modified data from the Department of Groundwater Resource (DGR) in 2011.

3.1.5 Hydrogeology

Hydrogeological classifications of aquifers are divided to 2 major types; unconsolidated rocks and consolidated rocks, and sub-divided in hydrogeological units as well as geological units. Classification of hydrogeological units may be consistent or inconsistent with the classification of geological units depending on hydrogeological properties. (Chotpantarat, Chuangcham et al. 2011)

Hydrogeological characteristic of Phare groundwater basin is shown in **Figure 3.4** and the summary table of aquifer potential yield ranges is shown in **Table 3.4**.

Unconsolidated Aquifers

The Quaternary floodplain deposited (Qa/Qfd)

It composes of clay, sand, gravel and debris deposits from the Yom River and tributaries caused by sediment in narrow plain nearly canal. The environment of sedimentation and deposit age has 2 generation layers; sand and gravel layers in the present and along the river deposit in the central basin of the larger South-old Prime scene.

The youngest units, found in the depth of 0 to 15 m, occur along the Yom River by fluvial process in the central part of Phrae province. The yield of the aquifer was 3-8 m^3/hr. It composes of gravel layers, sand or silt layers overlay with clay layers found in Muang, Sung Men, Nong Muang Kai, Song and Long district.

The Quaternary younger terrace deposited or Chiang Rai aquifers (Qyt/Qcr)

It is found in the depth of 25 to 40 m, and the average thickness is 25 m. It occurs along the foothills by weathering and erosion process. The younger terrace deposited mostly composes of gravel mixing with clay layers, which lap over clay or sandy clay layers, i.e. called multi-aquifers. The groundwater is stored in the gravel beds. The yield of the aquifer is 2 to 5 m^3/hr. It is found in Amphoe Muang, Amphoe Sung Men, Amphoe Nong Muang Kai, Amphoe Song and Amphoe Long.

The Quaternary old terrace deposited or Chiang Mai aquifers (Qot/Qcm)

The composition of the aquifer is gravel mixing with clay layers. The uppermost of the aquifer, which the depth is not higher than 100 m, is a poor source of groundwater because of large size of the gravel beds and coarse grains of sand and clay. The yield of the layer is 5 to 10 m^3/hr. Meanwhile, the Quaternary terrace sub-layers found in the depth of 100 to 300 m are a good source of groundwater. Three sand layers mixing with gravel have the thicknesses about 10 to 15 m, and have the yield of layers about 10 to 50 m^3/hr.

The Quaternary Old Terrace aquifer is found in Amphoe Muang, Amphoe Sung Men, Amphoe Nong Muang Kai, Amphoe Song, Amphoe Long and Amphoe Wang Chin.

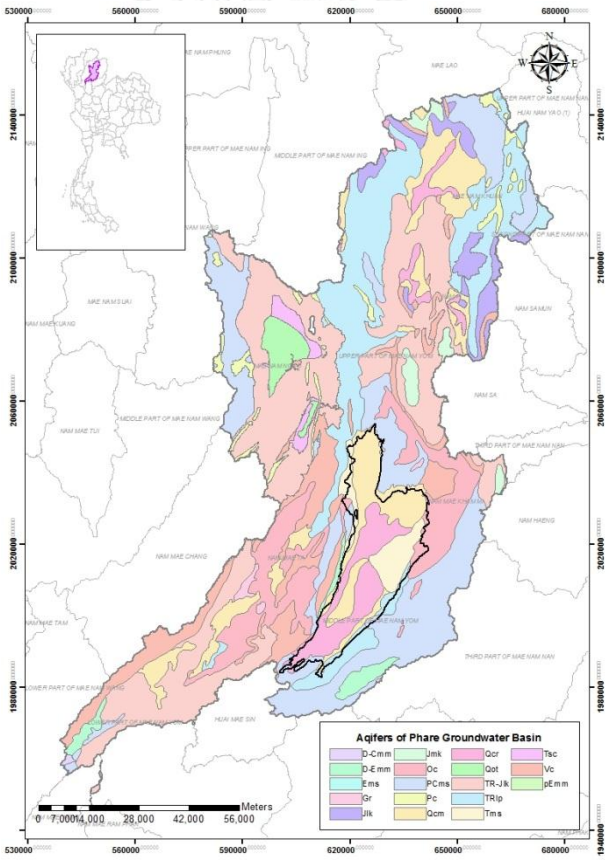

Figure 3.4 Hydrogeological map of the study area modified data from the Department of Groundwater Resource (DGR) in 2011

Table 3.4 Aquifer potential yield ranges in the study area

No	Symbol	Period	Description	Groundwater Depth (m)	Aquifer Potential Yield (m^3/hr)	Area (km^2)	Percentage
1	Qa/Qfd	Quaternary	Alluvial complex / Floodplain deposites	0-15	3-8	840.278	7.73%
2	Qcl	Quaternary	Colluvial deposits	-	-	45.274	0.42%
3	Qyt/Qcr	Quaternary	Younger Terrace deposited / Chiang Rai aquifers	25-40	2-5	517.046	4.75%
4	Qot/Qcm	Quaternary	Old Terrace deposited / Chiang Mai aquifers	40-100, 100-300	5-10, 10-50	170.771	1.57%
5	Tms	Tertiary	Mae Sot aquifers	-	-	200.572	1.84%
6	Tsc/T	Tertiary	Semiconsolidated aquifer	-	-	98.870	0.91%
7	Jlk	Jurassic	Lower Korat group aquifers	-	-	326.377	3.00%
8	Jmk	Jurassic	Middle Korat group aquifers	30-100	-	132.819	1.22%
9	TRJlk	Triassic-Jurassic	Lower Korat group aquifers	-	-	2592.491	23.84%
10	TRlp	Triassic	Lampang group aquifers	30-40	-	1582.866	14.55%
11	Pc	Permian	Carbonates aquifers	30-150	-	422.421	3.88%
12	PCms	Permian-Carboniferous	Metasediments aquifers	30-150, 50-100	10-20, 5	1922.136	17.67%
13	Oc	Ordovinian	Carbonates aquifers	-	-	927.892	8.53%
14	Ems	Cambrian	Metasediments aquifer	-	-	0.170	0.00%
15	pEmm	Pre-Cambrian	Metamorphic aquifers	-	-	0.009	0.00%
16	DCmm	Devonian-Carboniferous	Metamorphic aquifers	-	-	6.855	0.06%
17	DEmm	Cambrian-Devonian	Metamorphic aquifers	-	-	140.775	1.29%
18	Vc	Triassic- Cretaceous	Volcanic aquifers	20-60	-	912.454	8.39%
19	Gr	Triassic- Cretaceous	Granite aquifers	20-30	-	35.813	0.33%

Phare Groundwater Basin is a feature of 3 layers of unconsolidated rock such as alluvial complex or floodplain deposited (Qa/Qfd) posing from surface levels to depth of 1.5 m, Quaternary younger terrace deposited or Chiang Rai aquifers (Qyt/Qcr) posing depth approximately 25 to 40 m with an average thickness of 25 m, and old terrace deposited or Chiang Mai aquifers (Qot/Qcm) posing depth more than 40 m and maximum thickness more over 100 m. Mainly unconsolidated groundwater layer expand in plain of groundwater subbasin. Major consolidated aquifers are feature of Permian-Carboniferous metasediments aquifers (PCms), Permian carbonates aquifers (Pc), Triassic carbonates aquifers (TRc), Triassic Lampang group aquifers (TRlp), and Triassic-Jurassic lower Korat group aquifers (TRJlk). However, these mainly aquifers important to groundwater developing are old terrace deposited or Chiang Mai aquifers (Qot/Qcm) and Triassic-Jurassic lower Korat group aquifers (TRJlk).

Groundwater levels data of observation wells of the Department of Groundwater Resources (DGR) installed in both the unconsolidated and consolidated rocks are different, but the change of groundwater is not much from the past, except for seasonal change only.

Table 3.5 Groundwater storage volume and groundwater development potential without consequences (safe yield).

Subbasin	Groundwater storage volume (mcm)	Yearly Groundwater available (mcm)	Daily Groundwater available (m^3)
Upper Part of Mae Nam Yom	93.50	19.00	52,000
Mae Nam Khuan	38.00	8.00	21,000
Nam Pi	30.50	6.00	16,000
Mae Nam Ngao	62.00	12.00	32,000
Middle Part of Mae Nam Yom	158.00	32.00	87,000
Nam Mae Kham Mi	20.00	4.00	11,000
Nam Mae Ta	15.00	3.00	8,000

3.1.6 Soil Types

From the Geo-Informatics database of the Land Development Department in 2005, soil group units of the area are classified into 34 groups of soil properties according to the origin and landforms. The most soil group is unit 62, which covers 58.18% of total area, located on mountainous area. This group of soils includes all steep lands with more than 35% slopes. Soil properties vary as geological setting of the areas, which are the most of parent material. This group of soils should restrict their uses to woodland, watershed protection and wildlife conservation.

Soil group unit 47 covers 14.96% of total area. This group of soils is well-drained, shallowly deep coarse-textured that developed from weathered rocks in dry areas. It is low fertility. Soil pH of this group unit varies from 6.0 to 7.5. Soil series in this unit consist of Li series (Li), Muak Lek Series (Ml), Nakhon Sawan series (Ns), Pong Nam Ron series (Pon), Sop Prap series (So) and Tha Li series (Tl).

Soil group unit 15 covers 4.77% of total area, located on alluvial floodplain. This group of soils, which is low fertility, is coarse-drained, highly deep sandy silt-textured that developed from stream sediment. Soil pH of this group unit varies from 5.0 to 8.0. Soil series in this unit composes of Lom Sak series (La), Mae Sai series (Ms) and Mae Tha series (Mta).

The other soil group units are represented as map as shown in Figure 3.5, and the summary data in Table 3.6. In addition, the summary of soil texture, soil permeability and soil properties are related to the land use in the study area, slope complex, low fertility, and may have a problem of the soil erosion.

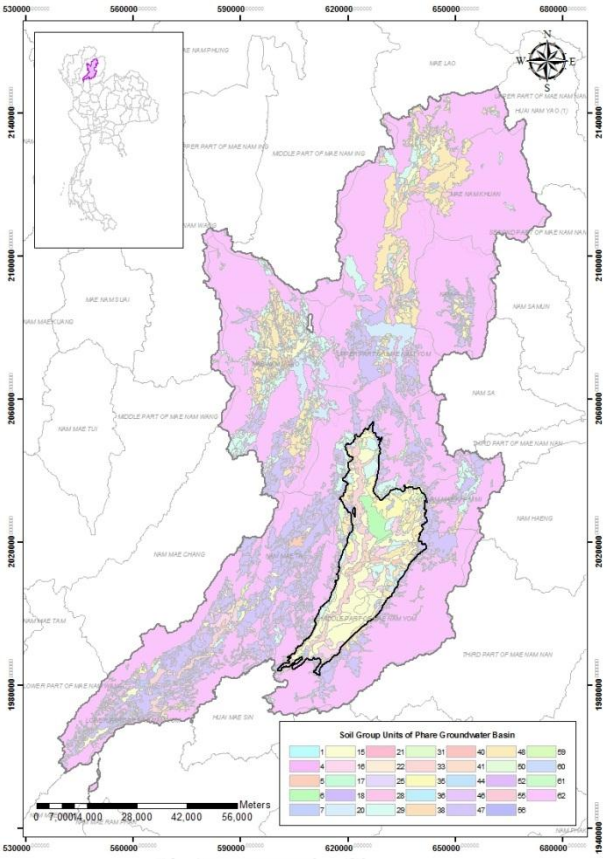

Figure 3.5 Soil group unit map of the study area data derived from the Land Development Department (LDD) (2011).

Table 3.6 Soil group units detail in the Phare Groundwater Basin

No	Soil Group Units	Area (km^2)	Percentage	No	Soil Group Units	Area (km^2)	Percentage
1	Soil-1	0.1714	0.0016	33	Soil-33	224.3360	2.0734
2	Soil-2			34	Soil-34		
3	Soil-3			35	Soil-35	147.0420	1.3590
4	Soil-4	0.3167	0.0029	36	Soil-36	8.6056	0.0795
5	Soil-5	52.6079	0.4862	37	Soil-37		
6	Soil-6	67.0467	0.6197	38	Soil-38	54.3802	0.5026
7	Soil-7	49.8079	0.4603	39	Soil-39		
8	Soil-8			40	Soil-40	3.3092	0.0306
9	Soil-9			41	Soil-41	3.8192	0.0353
10	Soil-10			42	Soil-42		
11	Soil-11			43	Soil-43		
12	Soil-12			44	Soil-44	1.6622	0.0154
13	Soil-13			45	Soil-45		
14	Soil-14			46	Soil-46	64.4852	0.5960
15	Soil-15	516.2936	4.7717	47	Soil-47	1614.3542	14.9202
16	Soil-16	88.8279	0.8210	48	Soil-48	768.6134	7.1037
17	Soil-17	2.4187	0.0224	49	Soil-49		
18	Soil-18	27.2450	0.2518	50	Soil-50	0.9592	0.0089
19	Soil-19			51	Soil-51		
20	Soil-20	204.1113	1.8864	52	Soil-52	0.1438	0.0013
21	Soil-21	2.2302	0.0206	53	Soil-53		
22	Soil-22	0.1643	0.0015	54	Soil-54		
23	Soil-23			55	Soil-55	8.6839	0.0803
24	Soil-24			56	Soil-56	6.7415	0.0623
25	Soil-25	3.6052	0.0333	57	Soil-57		
26	Soil-26			58	Soil-58		
27	Soil-27			59	Soil-59	54.8752	0.5072
28	Soil-28	3.0618	0.0283	60	Soil-60	11.5349	0.1066
29	Soil-29	486.1203	4.4928	61	Soil-61	13.6517	0.1262
30	Soil-30			62	Soil-62	6295.3656	58.1833
31	Soil-31	33.2963	0.3077	63	WATER		
32	Soil-32				**Total**	10819.8881	100.0000

3.1.7 Land Use

Land use and land cover (LULC) classification of Phare Groundwater Basin for the Geo-Informatics database of the Land Development Department in 2003 and 2009 are 6 types of forests, paddy field, field crop, perennial area, urban area, and water body as shown in **Figure 3.7**. It can be summarized as **Table 3.6**. Moreover, comparisons of landuse classification in 29 and 6 types in the Phare Groundwater Basin was shown in **Table 3.8** and **Figure 3.7**.

Forest area The forest area (FRST) was the highest land cover type of total area consisted of deciduous forest (FRSL) and the evergreen forest (FRSE) in the mountainous landforms.

Urban area The urban area (URBN) consisted of commercial area (UCOM), residential area (URBN), institutional area (UINS), airport and transportation (UTRN), industrial area (UIDU), and recreation area and others (URLD).

Agriculture area The agriculture area was the second largest area of forest land. Commonly this area was paddy field (PDDY), field crop (FCRP), and perennial area (PRNL).

Water body The water body (WATR) was minimal land cover type of total area because this study area did not have a large reservoir. The mainly land covers were Yom River, tributary, and aquaculture and (AQUA).

Table 3.7 The proportion of landuse in the Phare GWBSN in 2003 and 2009.

LU Code	Description	2003		2009	
		sq.km	%	sq.km	%
FCRP	Field crop	1323.00	12.23	1299.00	12.01
FRST	Forest area	7450.00	68.86	7450.00	68.86
PDDY	Paddy field	814.40	7.53	828.80	7.66
PRNL	Perennial land	1017.00	9.40	1020.00	9.43
URBN	Urban area	174.10	1.61	180.10	1.66
WATR	Water body	41.08	0.38	41.06	0.38
	Total	10819.58	100.00	10818.96	100.00

Table 3.8 Comparisons of landuse classification in 29 and 6 types in the Phare Groundwater Basin.

GLU_Code	Description	Landuse (29 Classes)	Landuse (6 Classes)
A1	Paddy field	PDDY	PDDY
IA1	Paddy field-Irrigation	PDDI	PDDY
A2	Cassava	CSSV	FCRP
A2	Corn	CORN	FCRP
A2	Sugarcane	SUGC	FCRP
A2	Peanut	PNUT	FCRP
A2	Green bean	GRBN	FCRP
A2	Tobacco	TOBC	FCRP
A2	Watermelon	WMEL	FCRP
A3	Perennial land	PRNL	PRNL
A4	Orchard	ORCD	FCRP
A6	Field crop	FCRP	FCRP
A6	Miscellaneous land	MISC	FCRP
A6	Swidden cultivation	SWID	FCRP
A7	Meadow/Pasture	MEAD	FCRP
A7	Residential-Medium Density	URMD	FCRP
A9	Aquaculture land	AQUA	WATR
M1	Disturbed forest land	DTFR	FCRP
M2	Wasteland	MISC	FCRP
M3	Mineral field	MISC	FCRP
M4	Garbage dump	SPAS	FCRP
F1	Forest-Evergreen	FRSE	FRST
F2	Forest land	FRSL	FRST
F3	Perennial land	PRNL	PRNL
F3	Forest/Misc. land	FRMC	PRNL
U1	Commercial	UCOM	URBN
U2	Residential	URBN	URBN
U3	Institutional	UINS	URBN
U4	Airport/Transportation	UTRN	URBN
U5	Industrial	UIDU	URBN
U6	Recreation area/Others	URLD	URBN
W1	River/Canal	WATR	WATR
W2	Reservoir/Human	WATR	WATR

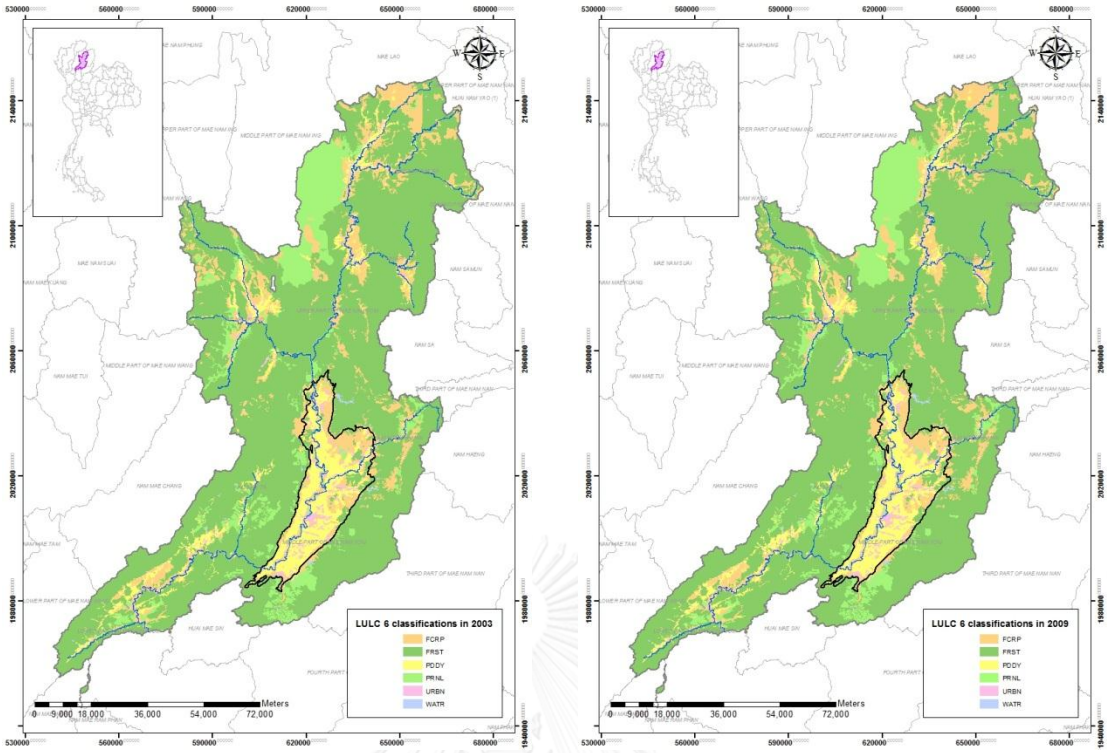

(a) **(b)**

Figure 3.6 Map of classification of 6 land use categories of year **(a)** 2003 and **(b)** 2009 modified data derived from the Land Development Department (LDD) (2011).

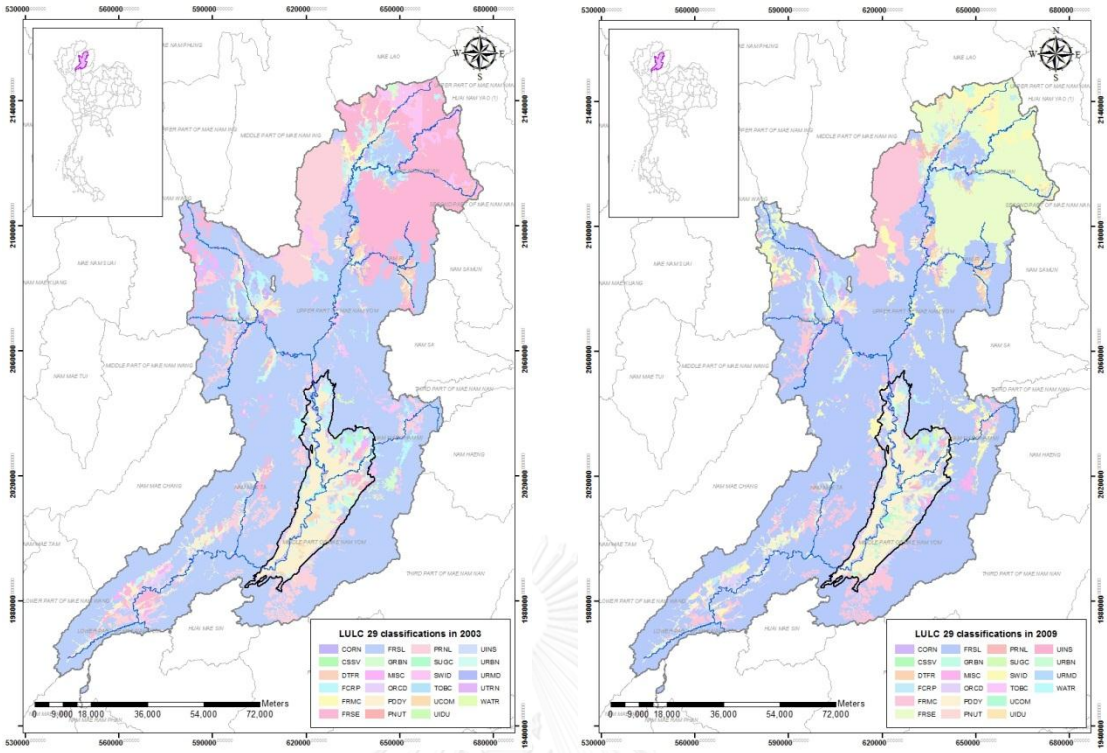

(a) **(b)**

Figure 3.7 Map of classification of 29 land use categories of year **(a)** 2003 and **(b)** 2009 data derived from the Land Development Dpartment (LDD) (2011).

3.2 Materials and Devices

3.2.1 Modeling Equipment

1) Personal computer
2) ArcGIS 9.3
3) SWAT 2009 model extensions
4) Baseflow Filter Program (online)
5) Surfer 10 (32 bit)
6) Visual MODFLOW 2010.1

3.2.2 Field Investigation Equipment

1) Water level meters
2) Hammer, wrench, spanner
3) Jack
4) Flashlights

3.3 Input Data Preparation

3.3.1 Field Investigation

Field investigation for groundwater head measuring and pumping rate checking was performed in two periods; dry season (June 2012) and rainy season (October 2012). After wells data filtering which made incomplete information in both seasons, number of groundwater wells remained 169 (all aquifers types) in the Phare province.

Table 3.9 A list of government agencies supporting the data used in this research.

Acronym	Government Sector
TMD	Thai Meteorological Department
RID	Royal Irrigation Department
LDD	Land Development Department
DGR	Department of Groundwater Resources
DWR	Department of Water Resources
DMR	Department of Mineral Resources
MOI	Ministry of Interior
MOAC	Ministry of Agriculture and Cooperatives
KKU	Water Resources and Environment Institute, Khon Kaen University
FI	Field investigation

3.3.2 Data Collection for SWAT

This research used SWAT model extensions of ArcGIS to estimate the streamflow and baseflow. Preparation of input data required comprehensive Yom watershed for the most effective evaluating results. The data used to imported SWAT model are shown in Table 3.10.

Table 3.10 Lists of data collection for use in surface water modeling.

	Data type	Source	Year	Remark
1	**General data**			
	Boundary of Phare Groundwater Basin	DGR	2011	Shape file (.shp)
	Administrative province/district	LDD	2011	Shape file (.shp)
	Basin/Subbasin	LDD	2011	Shape file (.shp)
2	**Topography and landscape data**			
	Digital elevation model data	LDD	2011	Grid file (.ras)
	Land use and land cover pattern	LDD	2003/2009	Shape file (.shp)
	Soil group properties	LDD	2011	Shape file (.shp)
3	**Meteorology data**			
	Weather stations	TMD	2011	Shape file (.shp)
	Daily/Monthly precipitation	TMD	1981-2013	Statistical (.xls)
	Daily/Monthly humidity	TMD	1981-2013	Statistical (.xls)
	Daily/Monthly temperature	TMD	1981-2013	Statistical (.xls)
	Daily/Monthly potential evaporation	TMD	1981-2013	Statistical (.xls)
4	**Hydrology data**			
	Hydrological gauging stations	DWR	2011	Shape file (.shp)
	Stream line	DWR	2011	Shape file (.shp)
	Daily/Monthly Runoff data	RID	1981-2013	Statistical (.xls)
	SWAT Thailand database	KKU	2016	Statistical (.mdb)
5	**Geology data**			
	Lithology	DMR	2011	Shape file (.shp)

3.3.3 Data Collection for MODFLOW

After calibration and validation processes of SWAT model, the boundary of MODFLOW model would be crated. Scope of the study area will focus on the Quaternary unconsolidated sedimentary aquifers of Phrae Basin. Visual MODFLOW were estimated groundwater balance and safe yield. The data used to import MODFLOW model is shown in Table 3.11.

Table 3.11 Lists of data collection for using in groundwater modeling.

No.	Data type	Source	Year	Remark
1	**General data**			
	Boundary of Phare Basin	DGR	2011	Shape file (.shp)
2	**Topology data**			
	Digital elevation model data	LDD	2011	Grid file (.ras)
3	**Hydrology data**			
	Stream line	DWR	2011	Shape file (.shp)
	River stage	RID	2012	Statistical (.xls)
	River bed/thickness	RID	2012	Statistical (.xls)
	River width	RID	2012	Statistical (.xls)
4	**Geology data**			
	Lithology	DMR	2011	Shape file (.shp)
5	**Hydrogeology data**			
	Groundwater wells (Pasutara)	DGR	2011	Shape file (.shp)
	Depth of groundwater table	DGR, FI	2012 - 2013	Statistical (.xls)
	Aquifer unit	DGR	2011	Shape file (.shp)
	Aquifer properties	DGR	2011	Statistical (.xls)
	Groundwater usages	DGR, MOI, MOAC	2011	Statistical (.xls)

3.4 Model setting up

3.4.1 SWAT

1. Watershed Delineation

Process of sub watersheds delineation is based on an automatic procedure using Digital Elevation Model (DEM) data of boundary (without government data).

Basin generated by SWAT will need to locate the outlet. The location is usually determined at the outlet and junction of each subbasin for an accuracy of calibration and validation of outlets positioning as well as the hydrological gauging stations.

In this research, watershed delineation generated 15 sub watersheds. Calculated output from DEM data has numerical resolution size of 60 m × 60 m.

2. Hydrologic Response Unit (HRUs) Analysis

HRUs analysis defines land use, soil types, and slope characterization and determines the landuse/soil/slope classify combinations and distributions for the delineated watersheds and each respective subwatershed.

In process of land use and soil layer reclassify with SWAT land cover classes, the databases of the SWAT model use USGS LULC and NLCD 1992 in landuse classification and U.S.STATSGO in soil type classification. Dataset of Thailand databases is needed for the model to classify and apply in the calculation. After that, creating a slope classification based on the DEM was used during watershed delineation. This case designed 5 categories such as 0-3, 3-8, 8-20, 20-45 and 45 upward.

3. Importing hydro-meteorological gauging stations

Meteorological data in 1981-2013 of precipitation, temperature, humidity, wind speed, and solar radiation in Yom River Basin was imported to the boundary (figure 3.8).

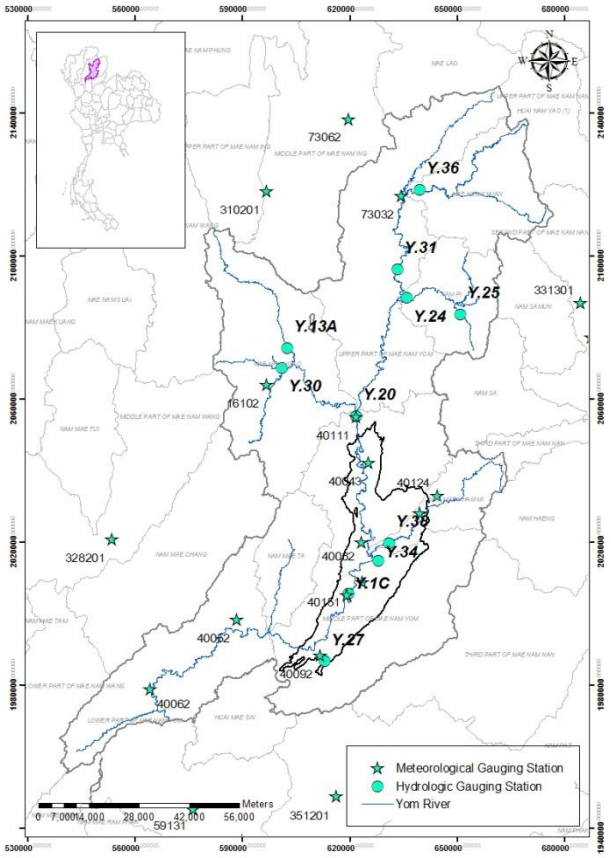

Figure 3.8 Hydro-meteorological gauging station map in the study area data derived from the Royal Irrigation Department (RID) and Thai Meteorological Department (TMD) in 2011.

4. Calibration and validation

The differences between river discharge response before and after land use changes were examined under similar precipitation conditions by using the SWAT model, spatial-temporal mathematical model, which operated on a monthly time step. SWAT projects was designed to calibrate (2006 to 2009) and validate (2000 to 2004 and 2010 to 2013) runoff data in the Y.36, Y.24, Y.20, Y.38, Y.1C, Y.14, and Y.6 station for 13 years during 2 periods. Data was obtained from hydrological guaging stations of the Royal Irrigation Department (RID) and outputs of Baseflow Filter Program (BFLOW) used in beseflow calibration in same period.

Chapter IV
Result

4.1 Surface water modeling

SWAT hydrological model was used to calibrate and verify observed streamflow with the 7 hydroligical stations in study area, derived from the Royal Irrigation Depertment (RID). The calibration and verification processes in this part can be used to explain effects of land use change onto streamflow and assess spatio-temporal monthly groundwater recharge, finally. The framework of calibration and verification of SWAT model is shown in **Table 4.1**. The calibration and verification processes were divided into three periods, consisting of one calibration period during 2006-2009 with land use in 2009, as well as 2 verification periods during 2000-2004 and 2010-2013, which used land use data in 2003 and 2009, respectively (Boonkaewwan 2013). In this part, the outcomes from the SWAT model were the spatio-temporal distribution of groundwater recharge into the Quaternary unconsolidated sedimentary aquifers, which would be used to assess groundwater balance and suitable safe yield of the aquifers in the next section.

Table 4.1 Framework of the calibration and verification processes of SWAT and MODFLOW models and land use in 2003 and 2009

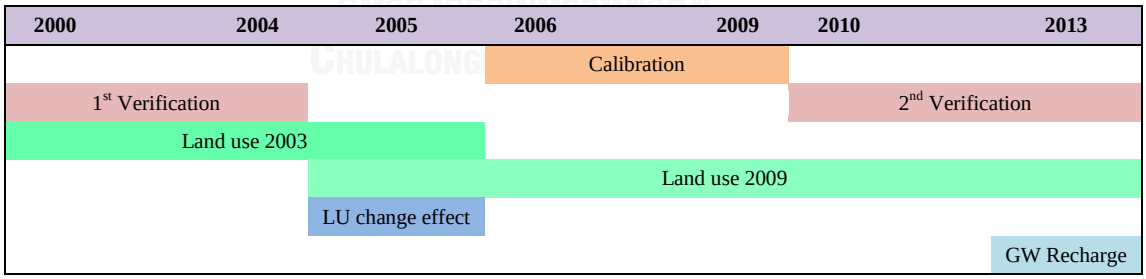

The predicted discharge, sediment, nitrate and phosphate levels were graphically evaluated statistically using the coefficient of determination (R^2), which was used as an indicator of model performance for calibration and validation periods. Models with higher R^2 coefficients are presumed to perform better than models with lower coefficients. The coefficient of determination is calculated using the following equation Gikas et al. (2006), (Abraham, Roehrig et al. 2007), (Silva, Souza et al. 2015) and (Guzman, Moriasi et al. 2012):

$$R^2 = \left(\frac{\sum_{i=1}^{n}(O_i - \bar{O})(P_i - \bar{P})}{\sqrt{\sum_{i=1}^{n}(O_i - \bar{O})^2}\sqrt{\sum_{i=1}^{n}(P_i - \bar{P})^2}} \right)^2$$

Where P_i is the predicted value, O_i is the observed value at time i, $\bar{O}$ is the mean observed value and $\bar{P}$ is the mean predicted value for the entire time period i. Furthermore, additional parameters were adjusted during flow calibration and validation procedures as presented in **Table 4.2**.

Table 4.2 Description, optimal values used in the SWAT model calibration and validation.

Parameter	File name	Description	Unit	Limitation		Optimal value						
				Min	Max	Subbasin 2	Subbasin 3	Subbasin 5	Subbasin 7	Subbasin 8	Subbasin 14	Subbasin 15
SOL_Z	.sol	Depth form soil surface to bottom of layer	mm	0	3500	72 - 360	56 - 266	60 - 300	40 - 170	48 - 120	40 - 100	50 - 120
SOL_BD	.sol	Moist bulk density	g/cm3	0.9	2.5	1.4 - 1.6	1.4 - 1.6	1.4 - 1.6	1.4 - 1.7	1.4 - 1.6	1.4 - 1.6	1.4 - 1.6
SOL_AWC	.sol	Available water capacity of the soil layer	mm H2O/mm soil	0	1	0.121 - 0.220	0.124 - 0.252	0.144 - 0.168	0.198 - 0.342	0.168 - 0.3	0.11 - 0.14	0.14 - 0.16
SOL_K	.sol	Saturated hydraulic conductivity	mm/hr	0	2000	0.48 - 5.44	0.88 - 9.978	0.40 - 11.64	0.48 - 20.8	0.132 - 13	0.6 - 26	0.84 - 14.56
CH_K1	.sub	Effective hydraulic conductivity in tributary channel alluvium	mm/hr	0	300	0.5	0.4	0.5	0.5	0.5	0.5	0.5
CH_N1	.sub	Manning's n value for tributary channels		0.01	30	0.14	0.12	0.14	0.14	0.14	0.14	0.14
CH_K2	.rte	Effective hydraulic conductivity in main channel alluvium	mm/hr	-0.01	500	0	0	0	0	0	0	0
CH_N2	.rte	Manning's n value for main channels		-0.01	0.3	0.14	0.12	0.14	0.14	0.14	0.14	0.14
SLSUBBSN	.hru	Average slope length	m	10	150	9.15 - 91.46	18.29 - 91.46	7.32 - 48.78	9.14 - 60.98	9.15 - 60.98	9.15 - 60.98	9.15 - 91.46
HRU_SLP	.hru	Average slope steepness	m/m	0	0.6	0.02 - 2.96	0.02 - 0.19	0.08 - 0.3	0.02 - 0.35	0.07 - 0.36	0.09 - 0.39	0.02 - 0.39
OV_N	.hru	Manning's n value for overland flow		0.01	30	0.1 - 0.14	0.1 - 0.14	0.01 - 0.1	0.1 - 0.14	0.1 - 0.14	0.1 - 0.14	0.1 - 0.14
ESCO	.hru	Soil evaporation compensation factor		0	1	0.8	1.44	0.8	0.8	0.8	0.8	0.8
GW_DELAY	.gw	Groundwater deley	days	0	500	31	31	31	31	31	31	31
ALPHA_BF	.gw	Baseflow alpha factor	days	0	1	0.48	0.48	0.48	0.48	0.48	0.48	0.48
GWQMIN	.gw	Threshold depth of water in shallow aquifer required for return flow to occur	mm	0	5000	500	500	500	500	500	500	500
GW_REVAP	.gw	Groundwater revap coefficient		0.02	0.2	0.02	0.02	0.02	0.02	0.02	0.02	0.02
REVAPMN	.gw	Threshold depth of water in shallow aquifer for revap to occur	mm	0	500	1	1	1	1	1	1	1
RECHRG_DP	.gw	Deep aquifer percolation fraction		0	1	0.05	0.05	0.05	0.05	0.05	0.05	0.05

4.1.1 Streamflow calibration and verification

Output in monthly simulation results was calibrated with observed streamflow data with land use in 2009 and 4-year period of meteorological data during from 2006 to 2009. Then, simulation was validated with observed streamflow data in 2 phases as follows: the 1st phase was used land use data in 2003 and 5-year period of meteorological data from 2000 to 2004 and the 2nd phase was used land use data in 2009 and 4-year period of meteorological data from 2010 to 2013.

In calibration and validation processes, subbasin outlets were chosen by the same or most nearly position of hydrological gauging stations. Total 7 observed locations selected, covered the area of the Phare groundwater basin as follows (see **Table 4.3** and **Figure 4.1**):

1. Y.36 station at Khuan River located in Ban Pa Kha, Pong, Phayao
2. Y.24 station at Pi River located in Ban Mang, Chiang Muan, Phayao,
3. Y.20 station at Yom River located in Ban Huai Sak, Song, Phrae,
4. Y.38 station at Mae Kham Mi River located in Ban Mae Kham Mi Tamnak Tham, Nong Muang Kai, Phrae,
5. Y.1C station at Yom River located in Ban Nam Khong, Muang, Phrae,
6. Y.14 station at Yom River located in Ban Don Rabiang, Si Satchanalai, Sukhothai, and
7. Y.6 station at Yom River located in Ban Kaeng Luang, Si Satchanalai, Sukhothai.

Table 4.3 Description of delineate subwatershed by SWAT model with difference of land use between 2003 and 2009 and representative subbasin.

Station	Location	Delineate subwatershed		Representative subbasin
		LU 2003	LU 2009	
Y.36	Ban Pa Kha, Pong, Phayao	2	1	Mae Nam Khuan
Y.24	Ban Mang, Chiang Muan, Phayao	3	4	Nam Pi
Y.20	Ban Huai Sak, Song, Phrae	5	11	Upper Part of Mae Nam Yom
Y.38	Ban Mae Kham Mi Tamnak Tham, Nong Muang Kai, Phrae	7	17	Nam Mae Kham Mi
Y.1C	Ban Nam Khong, Muang, Phrae	8	22	Middle Part of Mae Nam Yom
Y.14	Ban Don Rabiang, Si Satchanalai, Sukhothai	14	35	Lower Part of Mae Nam Yom
Y.6	Ban Kaeng Luang, Si Satchanalai, Sukhothai	15	39	Lower Part of Mae Nam Yom

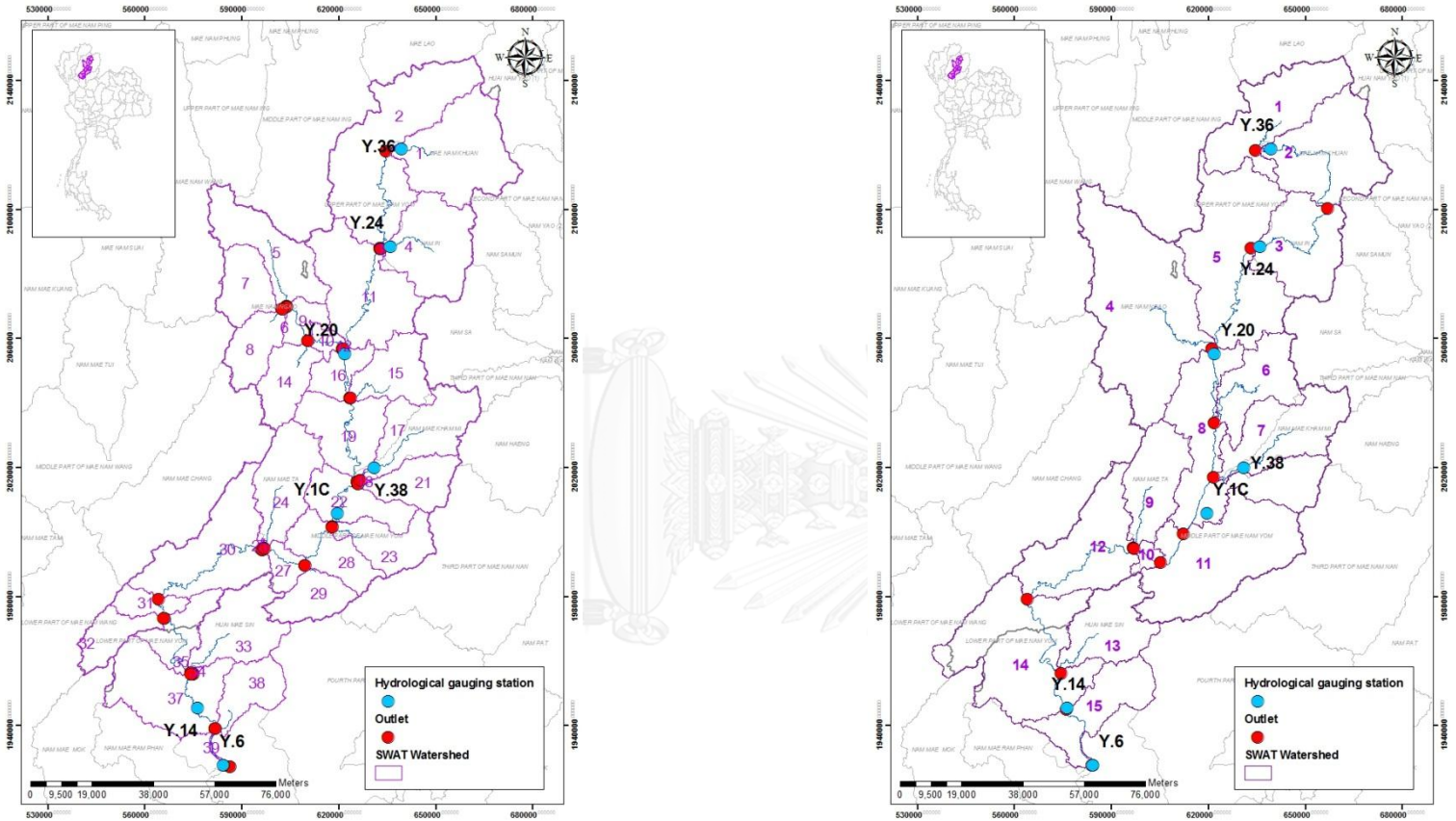

(a) **(b)**

Figure 4.1 Delineate subwatershed generated by SWAT model with **(a)** land use 2003 and **(b)** with land use 2009.

1) *Y.36 station*

The Y.36 station is located in Ban Pa Kha, Pong, Phayao, covering the area of delineate sub-watersheds no.2. Monthly streamflow calibration with observed streamflow data showed good agreement between simulation and observation with R^2 of 0.833, which is more than 0.60 for acceptable correlation in case of monthly streamflow (Abraham, Roehrig et al. 2007)

The validation results were divided into 2 phases. The 1st validation has a same pattern but peak of streamflow simulation is less than observation. The 2nd validation is quite well but simulation in April to October 2011 has abnormally streamflow peak because of the error precipitation measurement data. Therefore, the 1st validation has R^2 about 0.563, but 2nd validation has R^2 about 0.594 as shown in **Figure 4.2**.

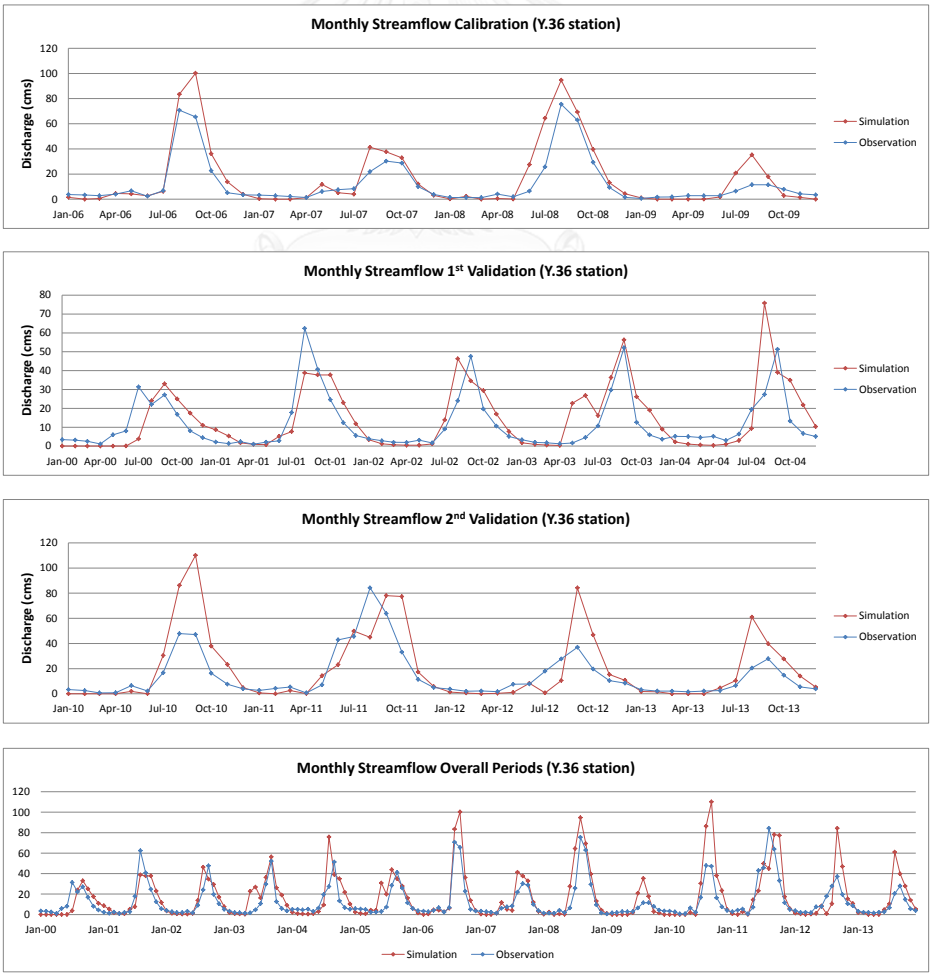

Figure 4.2 Calibration and validation results represented comparison of gauging data and simulate streamflow from SWAT at station Y.36 during 2000-2013

2) *Y.24 station*

The Y.24 station located in Ban Mang, Chiang Muan, Phayao covering area of delineate sub-watersheds no.3. Monthly streamflow calibration with observed streamflow data did not show a good agreement with R^2 about 0.726 because the abnormally of total flow of simulation is more than observation but looks like same pattern. But R^2 is more than 0.60 for acceptable correlation in case of monthly streamflow (Abraham, Roehrig et al. 2007).

The validation results were divided into 2 phases. The 1st validation has loops shifting between observation and simulation. For the 2nd validation, at the same calibration part, total flow are over but it appears to be similar pattern. The 1st validation has R^2 about 0.433, which may be error from the rainfall data, but the 2nd validation has R^2 about 0.660, R^2 is more than 0.60 for acceptable correlation as shown in **Figure 4.3**.

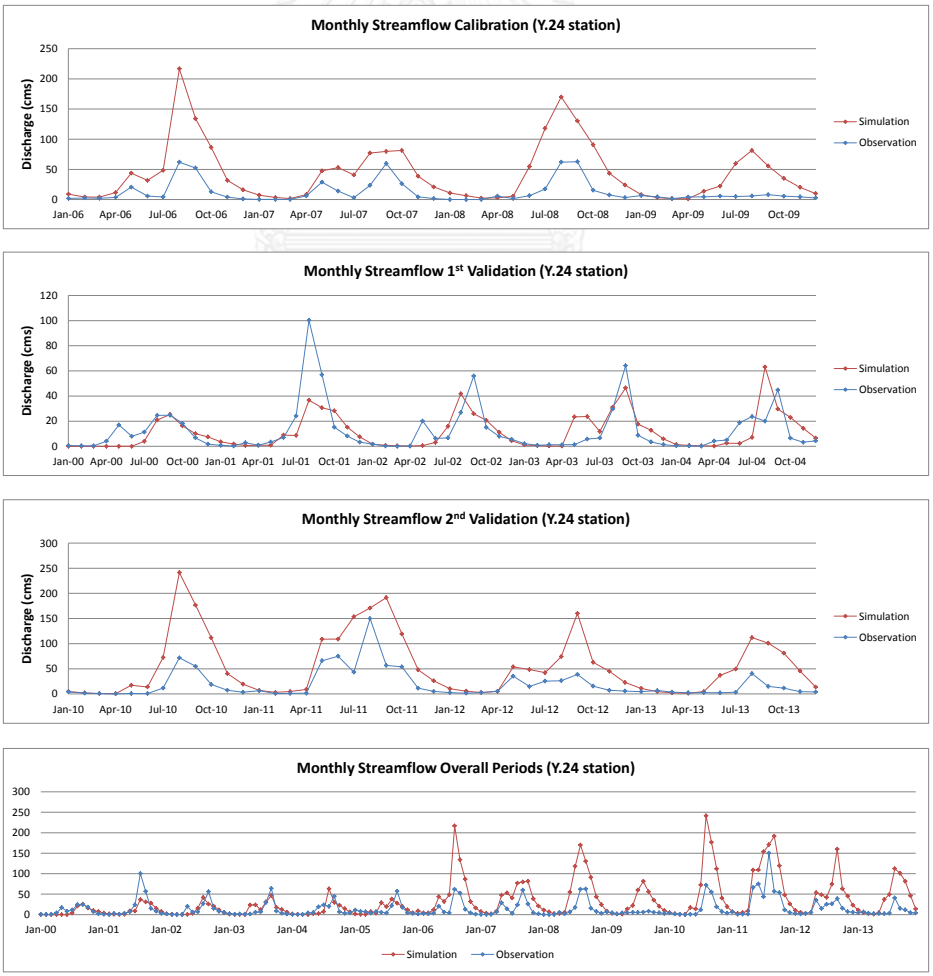

Figure 4.3 Calibration and validation results represented comparison of gauging data and simulate streamflow from SWAT at station Y.24 during 2000-2013

3) *Y.20 station*

The Y.20 station is located in Ban Huai Sak, Song, Phrae covering area of delineate subwatersheds no.5. Monthly streamflow calibration with streamflow data showed a good agreement although the peak of observation is more than simulation with R^2 about 0.899, which is more than 0.65 for acceptable correlation in case of monthly streamflow (Abraham, Roehrig et al. 2007).

The validation results were divided into 2 phases. The 1st and 2nd validation showed the same situation that peak of observation is more than simulation with a same pattern. The 1st validation has R^2 about 0.533, which may be error from the rainfall data, but the 2nd validation has R^2 about 0.813, which is more than 0.60 for acceptable correlation in case of monthly streamflow as shown in **Figure 4.4**.

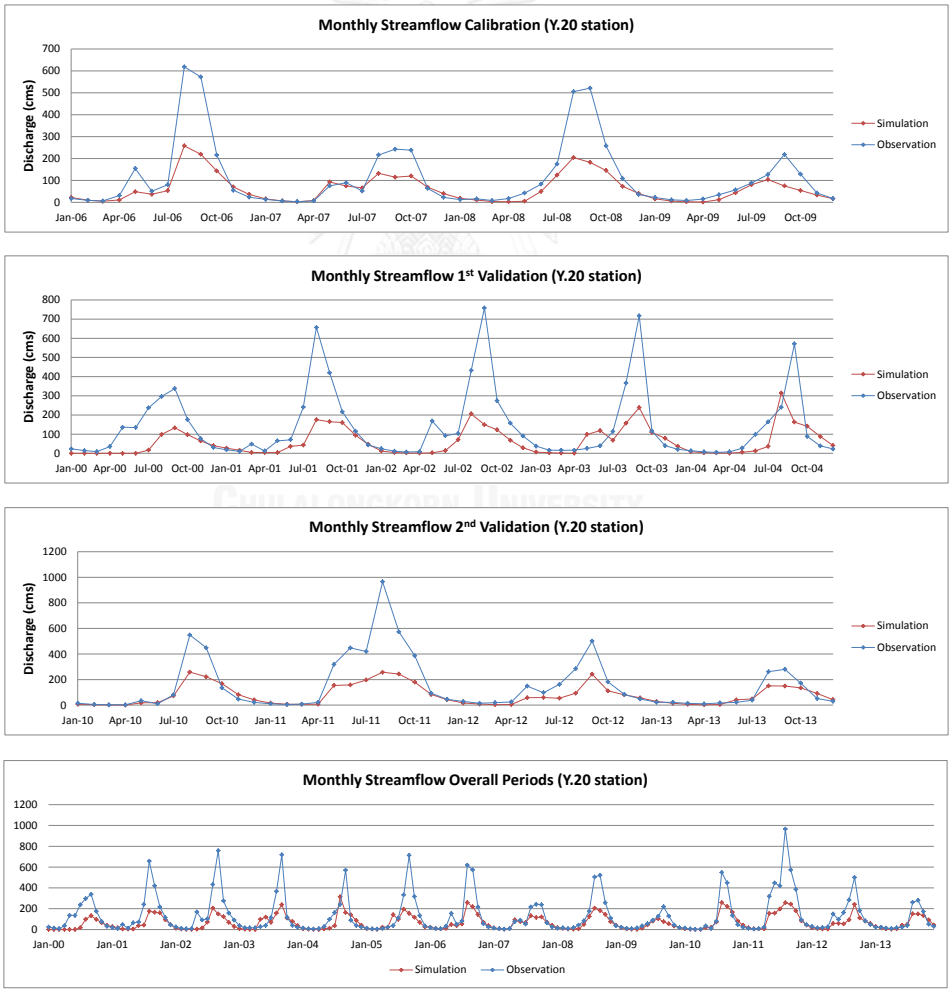

Figure 4.4 Calibration and validation results represented comparison of gauging data and streamflow simulation of station Y.20 during 2000-2013

4) *Y.38 station*

The Y.38 station is located in Ban Mae Kham Mi Tamnak Tham, Nong Muang Kai, Phrae covering area of delineate subwatersheds no. 7. Monthly streamflow calibration with streamflow data showed a good agreement between simulation and observation with R^2 about 0.745, which is more than 0.60 for acceptable correlation in case of monthly streamflow (Abraham, Roehrig et al. 2007).

Validation results were divided into 2 phases. The 1st validation has a same pattern, but peak of streamflow simulation is less than observed streamflow. The 2nd validation has similar graphs, but peak of streamflow simulation is less than observed streamflow. However, the 1st validation has R^2 about 0.703, and 2nd validation has R^2 about 0.686, which is more than 0.60 for acceptable correlation in case of monthly streamflow, as shown in **Figure 4.5**.

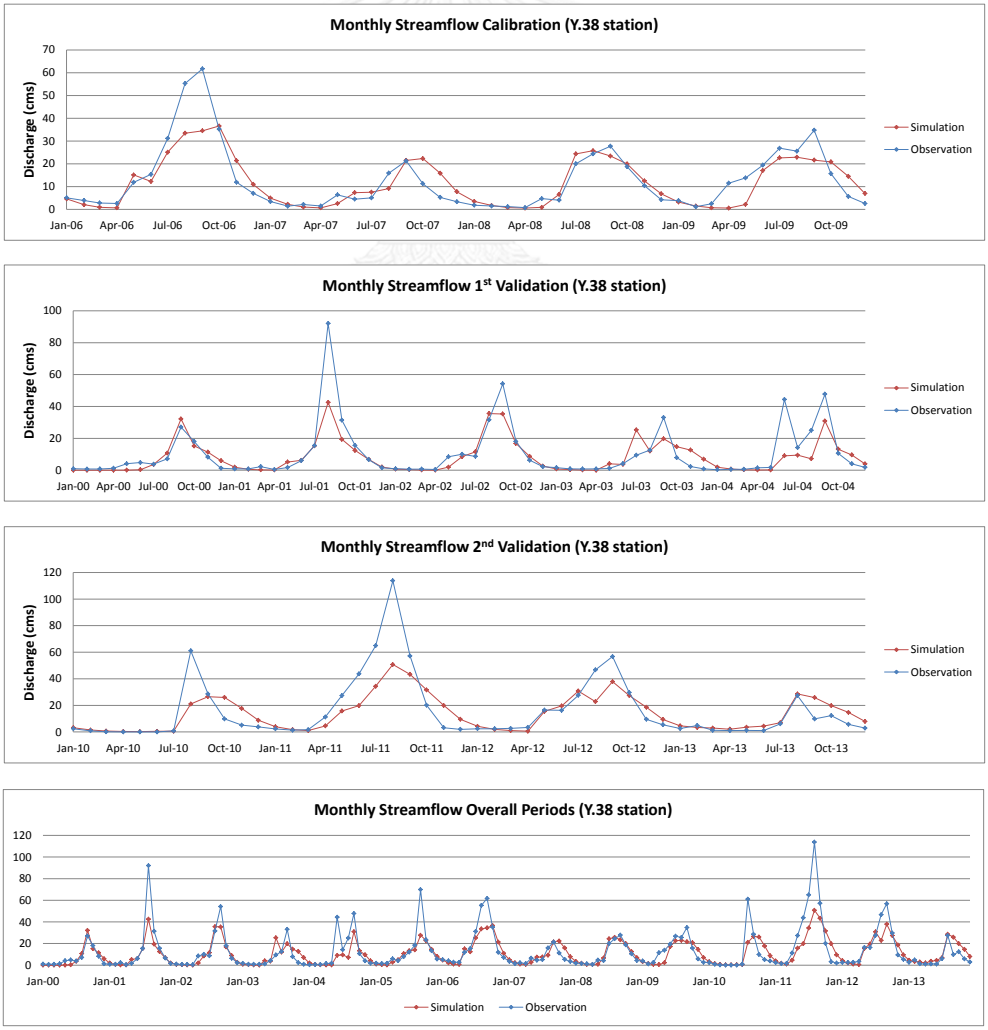

Figure 4.5 Calibration and validation results represented comparison of gauging data and streamflow simulation of station Y.38 during 2000-2013

5) *Y.1C station*

The Y.1C station is located in Ban Nam Khong, Muang, Phrae covered area of delineate subwatersheds no.8. Monthly streamflow calibration with streamflow data showed a good agreement between simulation and observation with R^2 of 0.849, which is more than 0.60 for acceptable correlation in case of monthly streamflow (Abraham, Roehrig et al. 2007).

The validation results were divided into 2 phases. The 1st validation has same pattern but peak of streamflow simulation is less than observation. The 2nd validation has similar graph, but peak of streamflow simulation is less than that of observed streamflow. The 1st validation has R^2 about 0.678, and the 2nd validation has R^2 at 0.772, which is more than 0.60 for acceptable correlation in case of monthly streamflow as shown in **Figure 4.6**.

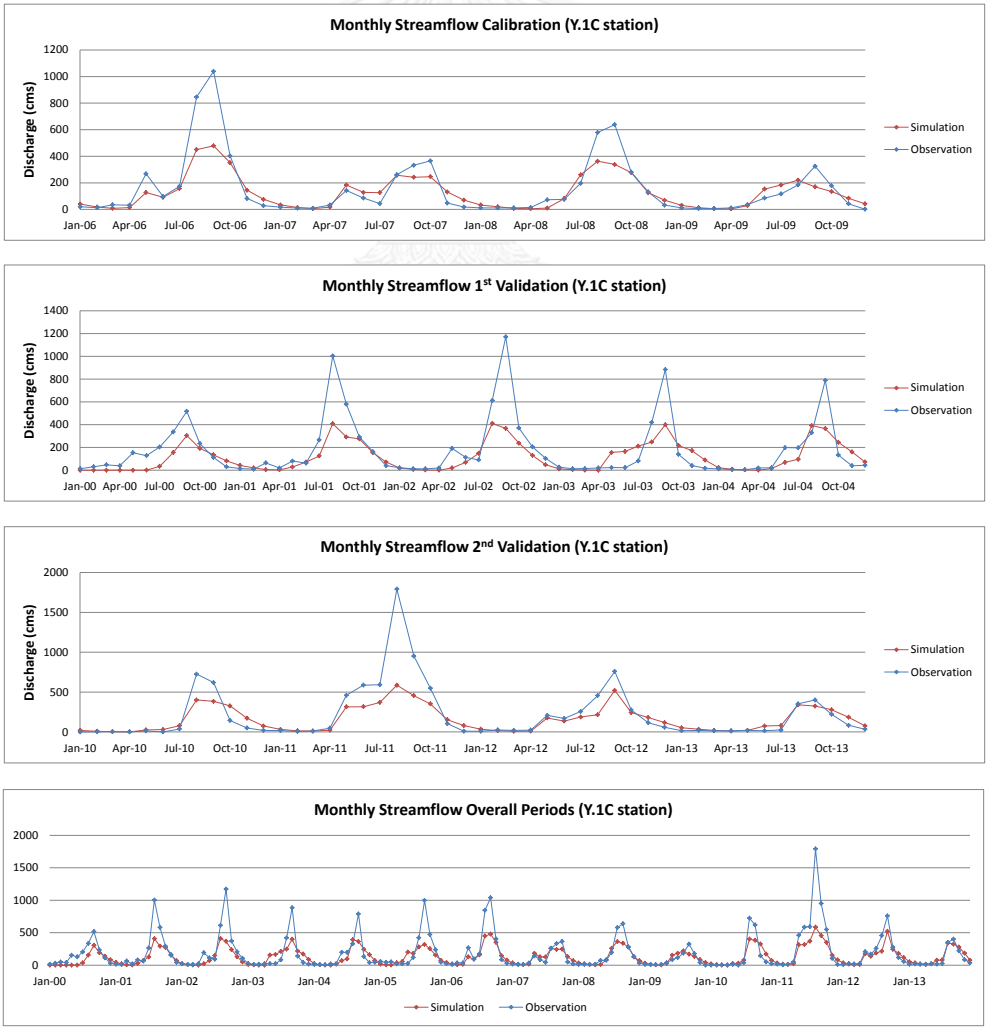

Figure 4.6 Calibration and validation results represented comparison of gauging data and streamflow simulation of station Y.1C during 2000-2013

6) *Y.14 station*

The Y.14 station is located in Ban Don Rabiang, Si Satchanalai, Sukhothai covering area of delineate subwatersheds no.14. Monthly streamflow calibration with streamflow data showed good agreement between simulation and observation with R^2 about 0.852, which is more than 0.65 for acceptable correlation in case of monthly streamflow (Abraham, Roehrig et al. 2007).

Validation results were divided into 2 phases. The 1st validation has a same pattern, but peak of streamflow simulation is less than observation. The 2nd validation has similar graph but but peak of streamflow simulation is less than observation. The 1st validation has R^2 about 0.674, and the 2nd validation has R^2 about 0.893, which are higher than 0.65 for acceptable correlation in case of monthly streamflow as shown in **Figure 4.7**.

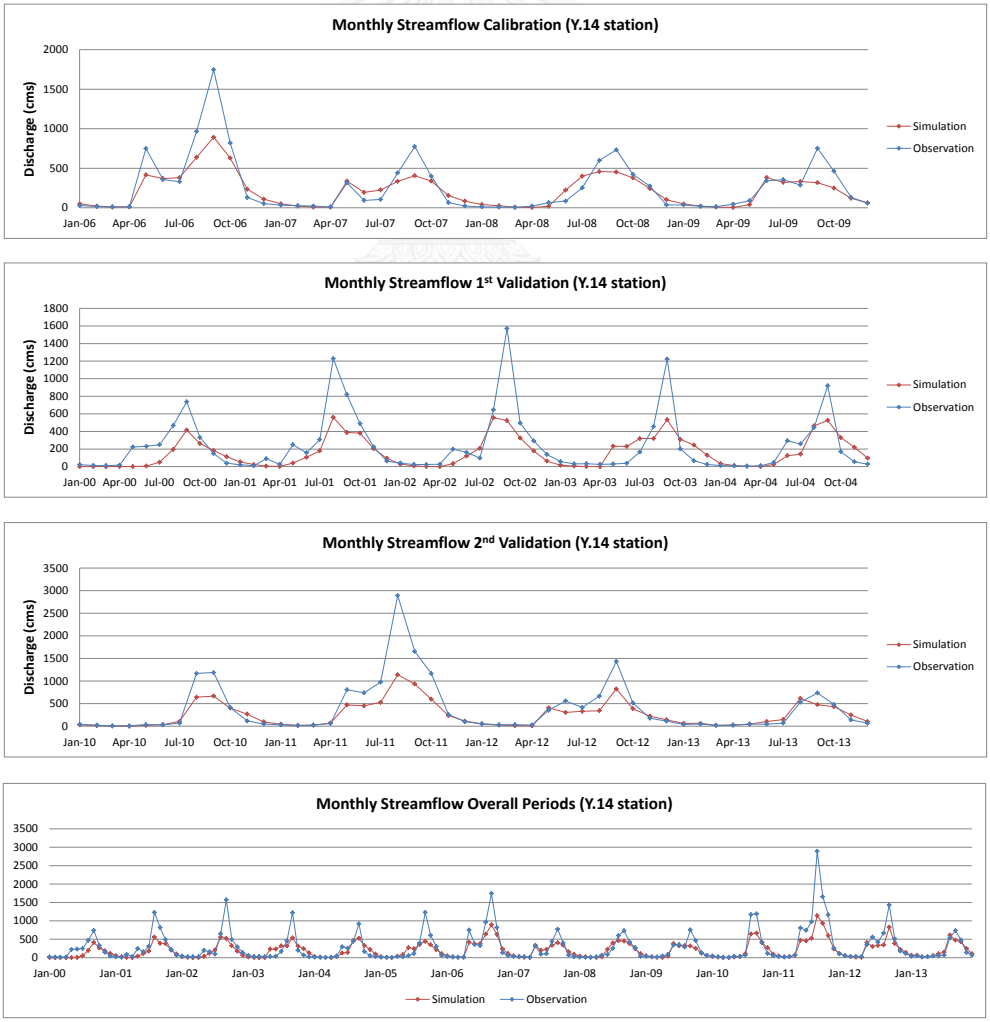

Figure 4.7 Calibration and validation results represented comparison of gauging data and streamflow simulation of station Y.14 during 2000-2013

7) *Y.6 station*

The Y.6 station is located in Ban Kaeng Luang, Si Satchanalai, Sukhothai covered area of delineate subwatersheds no.15. Monthly streamflow calibration with streamflow data showed a good agreement between simulation and observation with R^2 about 0.794, which is more than 0.60 for acceptable correlation in case of monthly streamflow (Abraham, Roehrig et al. 2007).

The validation results were divided into 2 phases. The 1st validation has a same pattern but peak of streamflow simulation is less than observed streamflow data. The 2nd validation has similar graph but peak of streamflow simulation is less than observation. The 1st validation has R^2 about 0.643, and the 2nd validation has R^2 about 0.883, which both were more than 0.60 for acceptable correlation in case of monthly streamflow as shown in **Figure 4.8**.

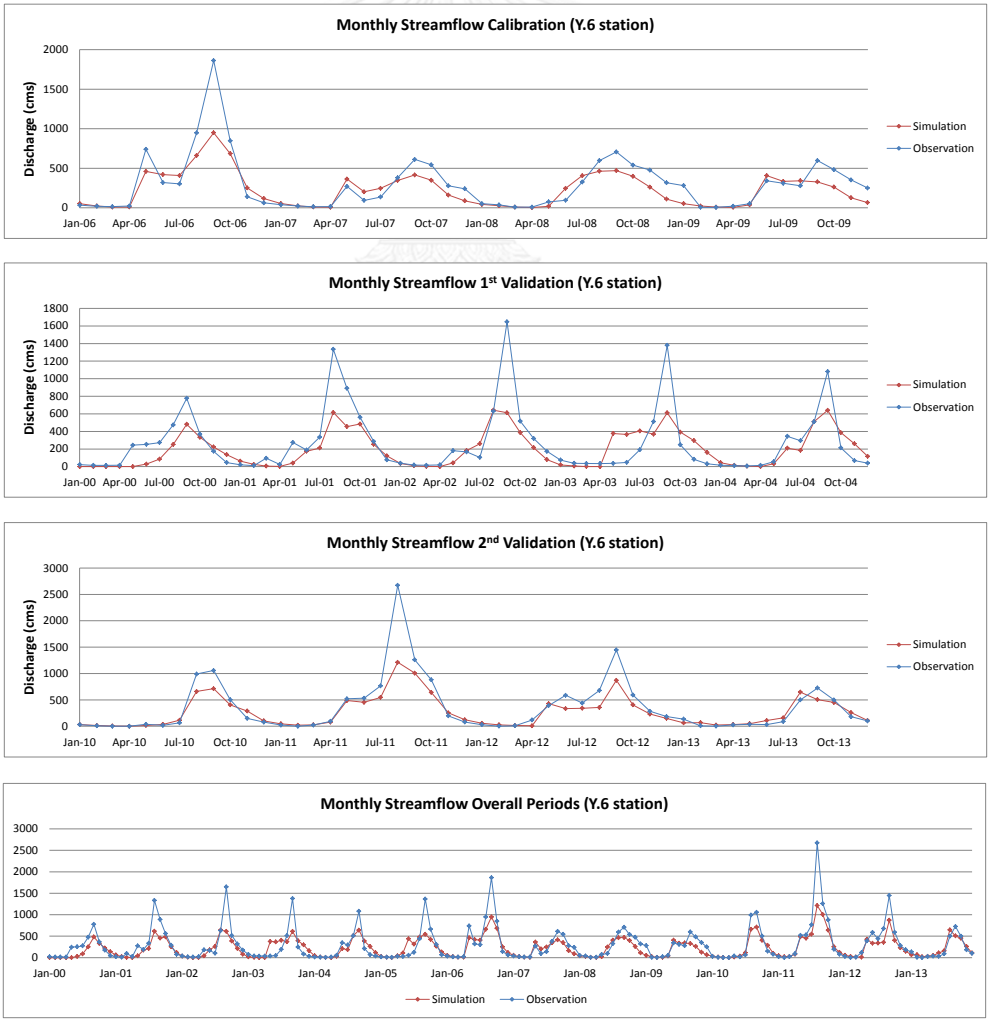

Figure 4.8 Calibration and validation results represented comparison of gauging data and streamflow simulation of station Y.6 during 2000-2013

4.1.2 Baseflow calibration and verification

Output in monthly simulation results was calibrated with groundwater recharge data derived from GW_Qmm file of SWAToutput at the same period of streamflow calibration and validation by using land use data in 2009 and the meteorological data from 2006 to 2009. Then, the validation was carried out by comparing with streamflow data in 2 phases. The 1st phase used the land use data in 2003 and the meteorological data from 2000 to 2004 and the 2nd phase used the land use data in 2009 and the meteorological data from 2010 to 2013.

The monthly groundwater recharge results were compared with the output from the Baseflow Filter Program, which was calculated from observed stremflow data as well. The result of calculation by mathematical baseflow separation equations in BFLOW has three categories, including 1) the perennial streams with porous aquifers (Type 1), 2) the ephemeral streams with porous aquifers (Type 2), and 3) the perennial streams with hard rock aquifers (Type 3). Each categories of calculation were based on the ratio of BFLOW/SFLOW or Baseflow index (BFI). (Arnold and Allen 1999), (Zhang, Srinivasan et al. 2011) and (Luo, Arnold et al. 2012)

1) *Y.36 station*

BFLOW separation results, which used streamflow data at Y.36 as an input, presented the baseflow in 3 categories of baseflow index (BFI), which were 0.72, 0.59, and 0.50 for the perennial streams with porous aquifers (Type 1), the ephemeral streams with porous aquifers (Type 2), the perennial streams with hard rock aquifers (Type 3), respectively. The results of groundwater recharge derived from calibration and validation processes of SWAT model at Y.36 were compared to those (BFLOW) from the Baseflow Filter program. For monthly baseflow calibration, results showed a similar pattern, but the peak of baseflow from SWAT is less than those calculated from the Baseflow Filter program with R^2 of 0.793, 0.761, and 0.808 for the aquifer type 1, type 2 and type 3, respectively, as shown in **Figure 4.9**.

For 2 phases of the monthly validation results, results of 1st phase showed a well fit with those from the Baseflow Filter program with R^2 of 0.581, 0.561, and

0.656 for the aquifers type 1, type 2 and type 3, respectively. The results of 2nd phase showed a similar pattern, but the peak of baseflow from SWAT in the rainy season of 2011 is less than those from the Baseflow Filter program. The 2nd validation has R^2 of 0.447, 0.385, and 0.429 for the aquifer type 1, type 2 and type as shown in **Figure 4.9**.

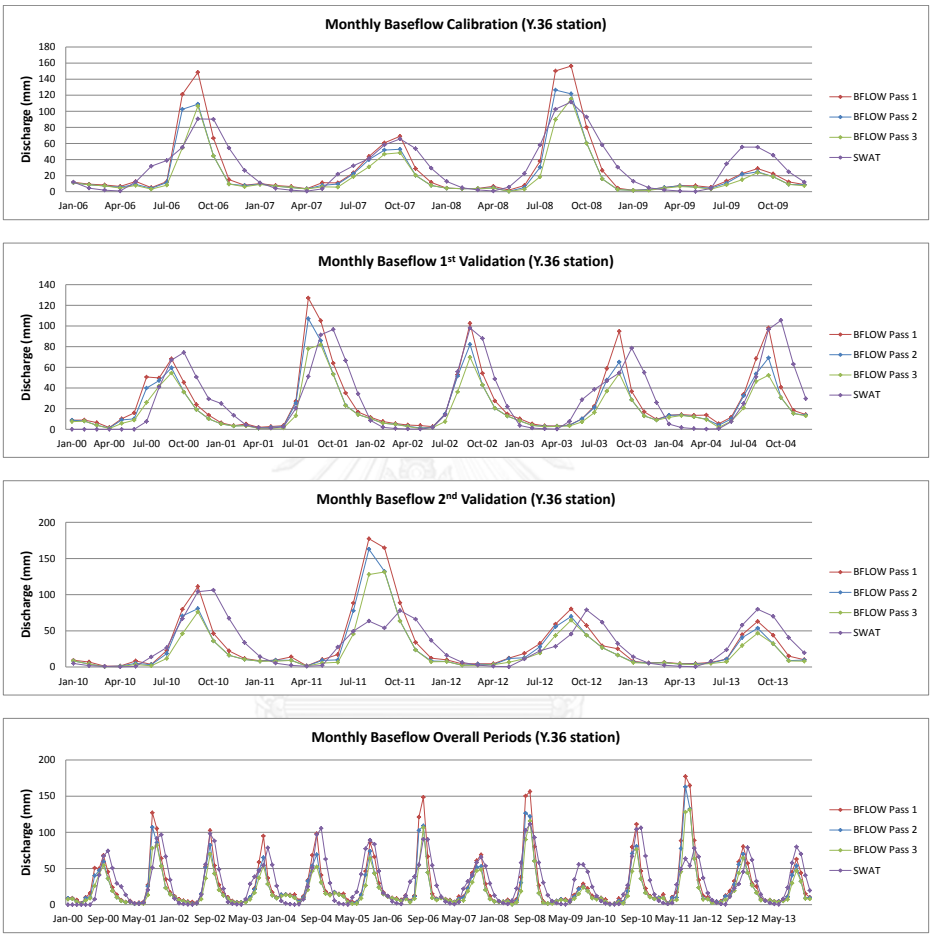

Figure 4.9 Calibration and validation results represented comparison of BFLOW output from the Baseflow Filter program and SWAT baseflow of station Y.36 during 2000-2013

2) *Y.24 station*

BFLOW separation results, which used streamflow data at Y.24 as an input, presented the baseflow in 3 categories of baseflow index (BFI), which were 0.57, 0.42, and 0.34 for aquifers type 1, type 2 and type 3, respectively. The results of groundwater recharge derived from calibration and validation processes of SWAT model at Y.24 were compared to those (BFLOW) from the Baseflow Filter program. For monthly baseflow calibration, results showed a similar pattern, but the peak of baseflow from SWAT is less than those calculated from the Baseflow Filter program

with R^2 of 0.541, 0.486, and 0.538 for the aquifers type 1, type 2 and type 3, respectively, as shown in **Figure 4.10**.

For 2 phases of the monthly validation results, results of 1st phase showed similar pattern, but the peak of baseflow from SWAT in the rainy season of 2011 is less than those from the Baseflow Filter program with R^2 of 0.438, 0.453, and 0.531 for the aquifers type 1, type 2 and type 3, respectively. The results of 2nd phase showed a similar pattern, including the peak of baseflow from SWAT and those from the Baseflow Filter program. The 2nd validation has a higher R^2 of 0.676, 0.644, and 0.752 for the aquifer type 1, type 2 and type as shown in **Figure 4.10**.

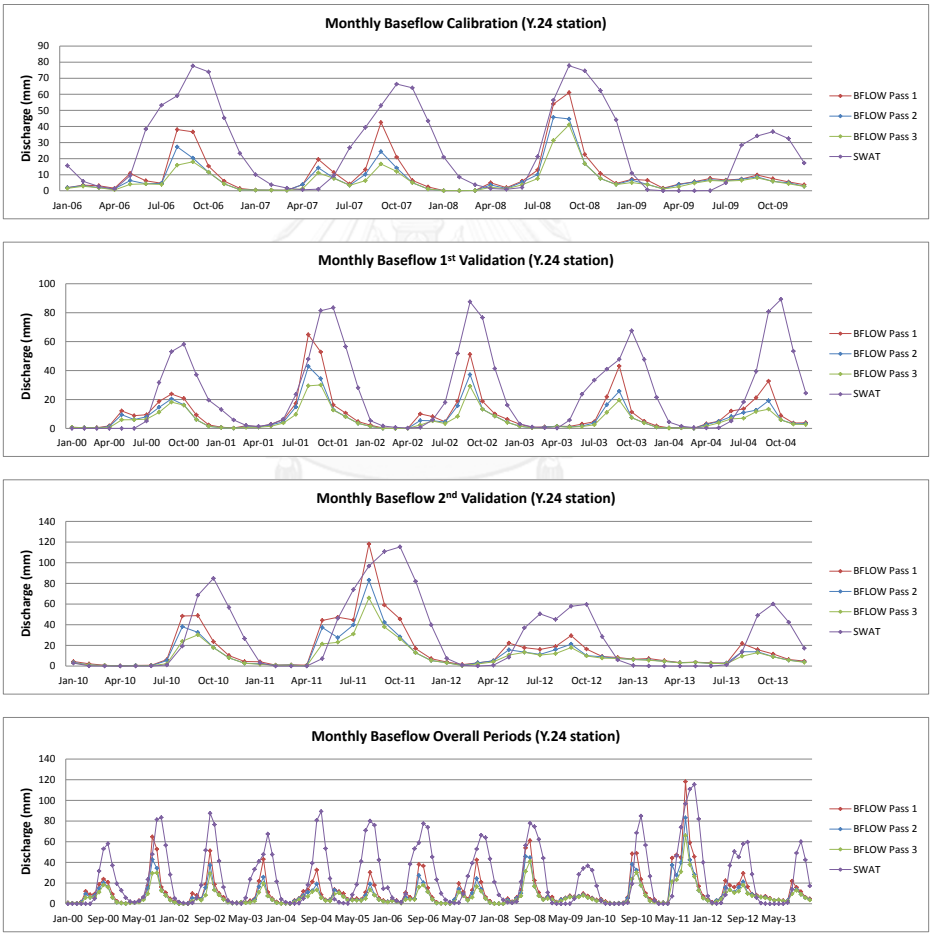

Figure 4.10 Calibration and validation results represented comparison of BFLOW output from the Baseflow Filter program and SWAT baseflow of station Y.24 during 2000-2013

3) *Y.20 station*

BFLOW separation results, which used streamflow data at Y.20 as an input, presented the baseflow in 3 categories of baseflow index (BFI), which were 0.64, 0.50, and 0.42 for aquifers type 1, type 2 and type 3, respectively. The results of groundwater recharge derived from calibration and validation processes of SWAT model at Y.20 were compared to those (BFLOW) from the Baseflow Filter program. For monthly baseflow calibration, results showed a similar pattern, but the peak of baseflow from SWAT is less than those calculated from the Baseflow Filter program with R^2 about 0.500, 0.453, and 0.550 for the aquifers type 1, type 2 and type 3, respectively, as shown in **Figure 4.11**.

For 2 phases of the monthly validation results, results of 1st phase showed a similar pattern, but the peak of baseflow from SWAT in the rainy season during 2000-2004 is less than those from the Baseflow Filter program with R^2 about 0.539, 0.528, and 0.580 for the aquifers type 1, type 2 and type 3, respectively. Similarly, the results of 2nd phase showed a similar pattern, but the peak of baseflow from SWAT in the rainy season during 2010-2013 is less than those from the Baseflow Filter program, but the 2nd validation has a higher R^2 of 0.586, 0.542, and 0.602 for the aquifer type 1, type 2 and type as shown in **Figure 4.11**.

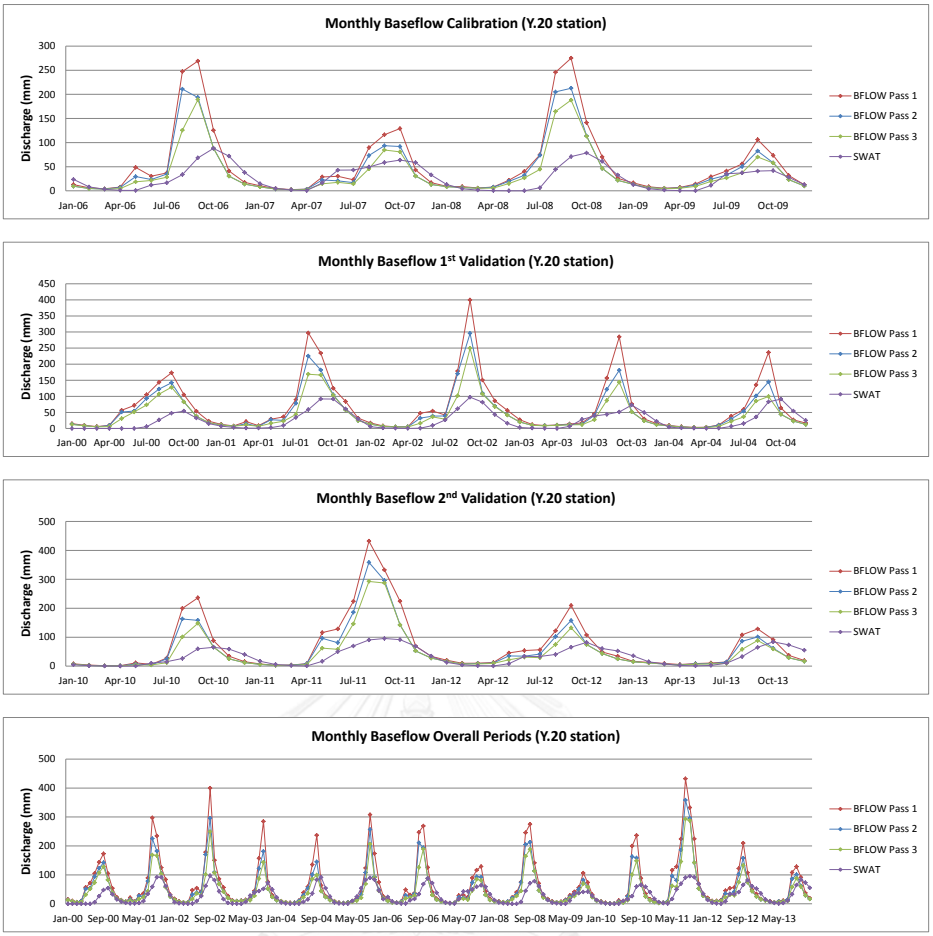

Figure 4.11 Calibration and validation results represented comparison of BFLOW output from the Baseflow Filter program and SWAT baseflow of station Y.20 during 2000-2013

4) *Y.38 station*

BFLOW separation results, which used streamflow data at Y.38 as an input, presented the baseflow in 3 categories of baseflow index (BFI), which were 0.66, 0.52, and 0.44 for aquifers type 1, type 2 and type 3, respectively. The results of groundwater recharge derived from calibration and validation processes of SWAT model at Y.38 were compared to those (BFLOW) from the Baseflow Filter program. For monthly baseflow calibration, results showed a similar pattern, but the peak of baseflow from SWAT is higher than those calculated from the Baseflow Filter program with R^2 about 0.690, 0.637, and 0.684 for the aquifers type 1, type 2 and type 3, respectively, as shown in **Figure 4.12**.

For 2 phases of the monthly validation results, results of 1st and 2nd phase showed a similar pattern, but the peak of baseflow from SWAT is higher than those

calculated from the Baseflow Filter program with R^2 of 0.528, 0.581, and 0.645 for the aquifers type 1, type 2 and type 3, respectively, for the 1st validation phase, as well as with R^2 of 0.584, 0.557, and 0.605 for the aquifers type 1, type 2 and type 3, respectively, for the 2nd validation phase as shown in **Figure 4.12**.

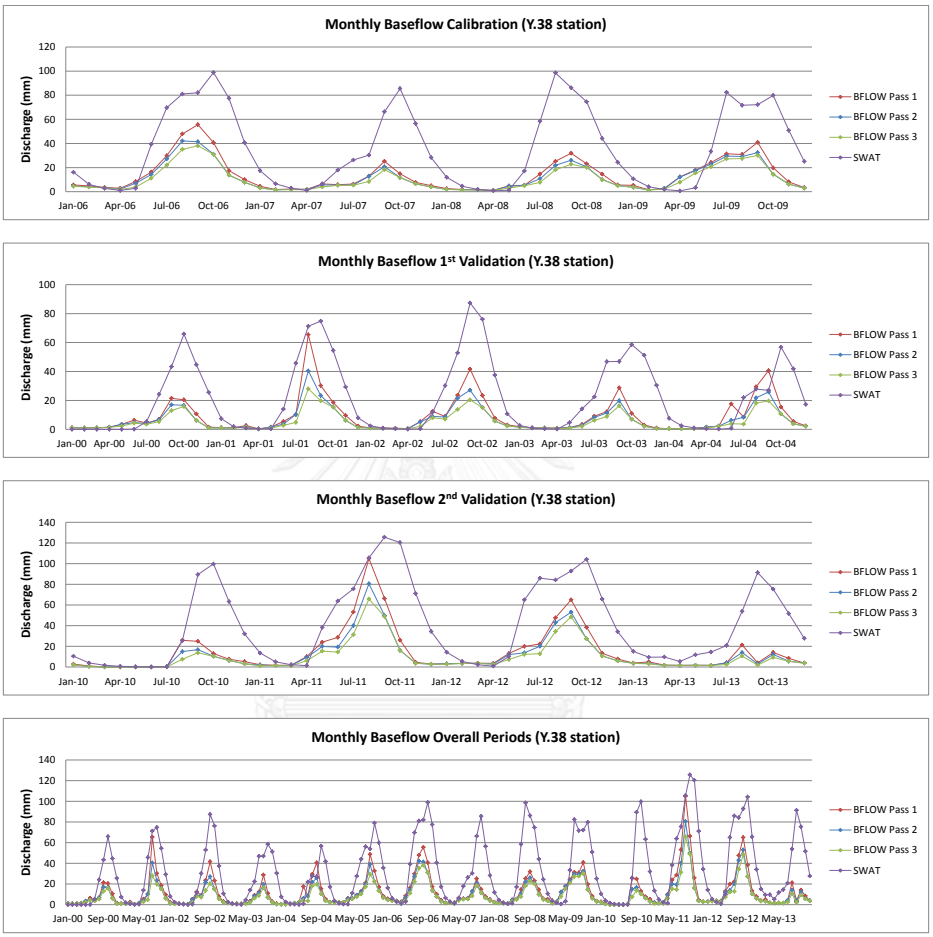

Figure 4.12 Calibration and validation results represented comparison of BFLOW output from the Baseflow Filter program and SWAT baseflow of station Y.38 during 2000-2013

5) *Y.1C station*

BFLOW separation results, which used streamflow data at Y.1C as an input, presented the baseflow in 3 categories of baseflow index (BFI), which were 0.62, 0.47, and 0.38 for aquifers type 1, type 2 and type 3, respectively. The results of groundwater recharge derived from calibration and validation processes of SWAT model at Y.38 were compared to those (BFLOW) from the Baseflow Filter program. For monthly baseflow calibration, results showed a similar pattern, but the peak of baseflow from SWAT is less than those calculated from the Baseflow Filter program

with R^2 about 0.578, 0.562, and 0.600 for the aquifers type 1, type 2 and type 3, respectively, as shown in **Figure 4.13**.

For 2 phases of the monthly validation results, results of 1st and 2nd phase showed a similar pattern, but peak from SWAT showed extremely less than those calculated from the Baseflow Filter program with R^2 of 0.513, 0.517, and 0.578 for the aquifers type 1, type 2 and type 3, respectively, for the 1st validation phase, as well as with R^2 of 0.664, 0.602, and 0.662 for the aquifers type 1, type 2 and type 3, respectively, for the 2nd validation phase as shown in **Figure 4.13**.

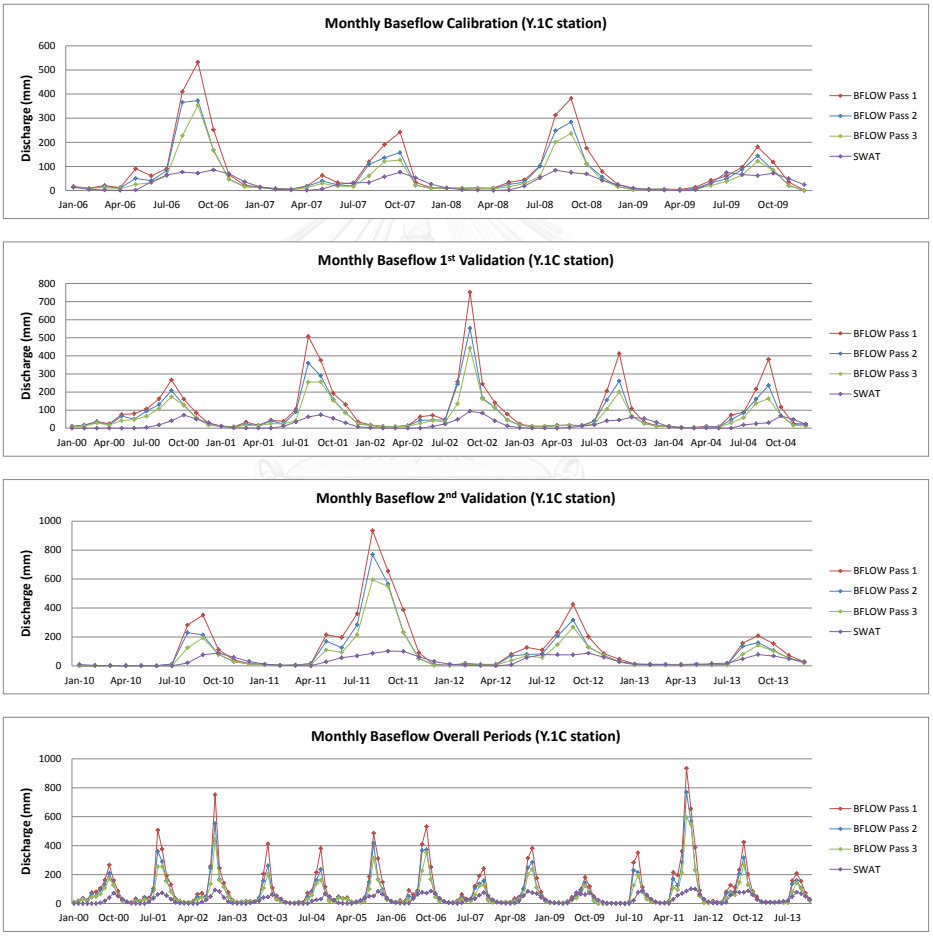

Figure 4.13 Calibration and validation results represented comparison of BFLOW output from the Baseflow Filter program and SWAT baseflow of station Y.1C during 2000-2013

6) *Y.14 station*

BFLOW separation results, which used streamflow data at Y.14 as an input, presented the baseflow in 3 categories of baseflow index (BFI), which were 0.65, 0.50, and 0.41 for aquifers type 1, type 2 and type 3, respectively. The results of groundwater recharge derived from calibration and validation processes of SWAT model at Y.14 were compared to those (BFLOW) from the Baseflow Filter program. For monthly baseflow calibration, results showed a similar pattern, but the peak of baseflow from SWAT is extremely less than those calculated from the Baseflow Filter program with R^2 about 0.493, 0.455, and 0.499 for the aquifers type 1, type 2 and type 3, respectively, as shown in **Figure 4.14**.

For 2 phases of the monthly validation results, results of 1st and 2nd phase showed a similar pattern, but peak from SWAT showed extremely less than those calculated from the Baseflow Filter program with R^2 of 0.444, 0.455, and 0.486 for the aquifers type 1, type 2 and type 3, respectively, for the 1st validation phase, as well as with R^2 of 0.574, 0.499, and 0.582 for the aquifers type 1, type 2 and type 3, respectively, for the 2nd validation phase as shown in **Figure 4.14**.

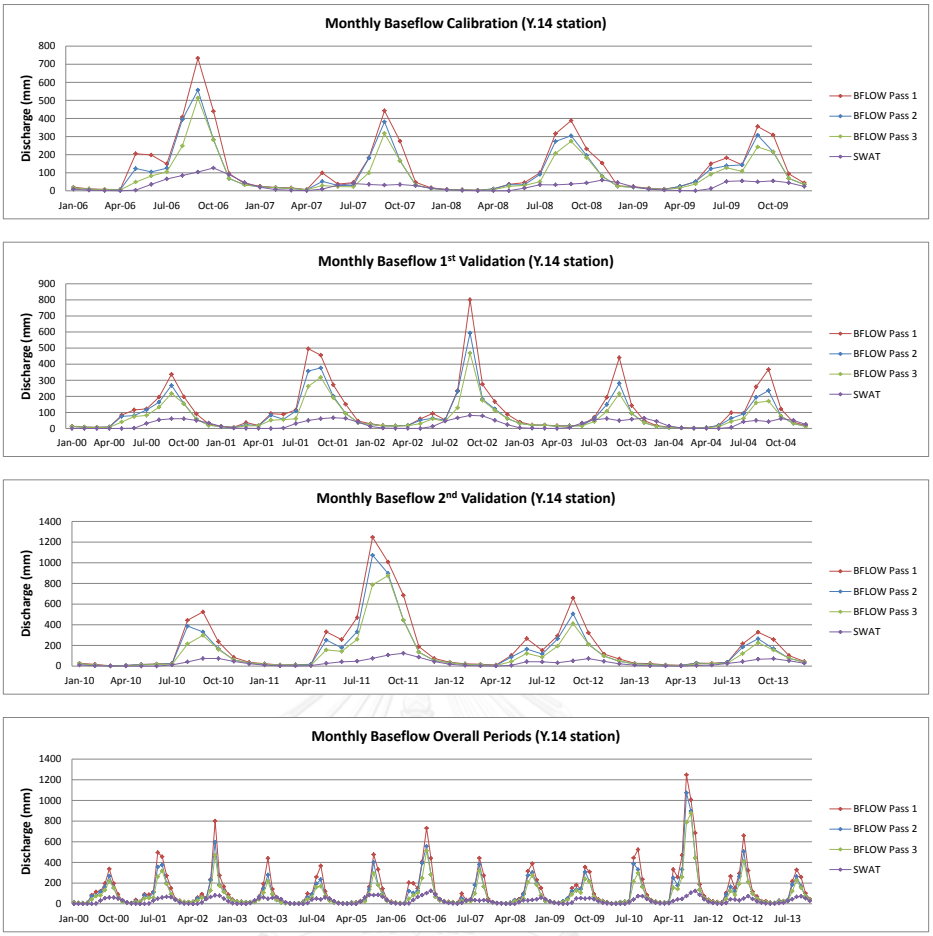

Figure 4.14 Calibration and validation results represented comparison of BFLOW output from the Baseflow Filter program and SWAT baseflow of station Y.14 during 2000-2013

7) *Y.6 station*

BFLOW separation results, which used streamflow data at Y.6 as an input, presented the baseflow in 3 categories of baseflow index (BFI), which were 0.65, 0.50, and 0.42 for aquifers type 1, type 2 and type 3, respectively. The results of groundwater recharge derived from calibration and validation processes of SWAT model at Y.6 were compared to those (BFLOW) from the Baseflow Filter program. For monthly baseflow calibration, results showed a similar pattern, but the peak of baseflow from SWAT is extremely less than those calculated from the Baseflow Filter program with R^2 about 0.549, 0.520, and 0.537 for the aquifers type 1, type 2 and type 3, respectively, as shown in **Figure 4.15**.

For 2 phases of the monthly validation results, results of 1st and 2nd phase showed a similar pattern, but peak from SWAT showed extremely less than those

calculated from the Baseflow Filter program with R^2 of 0.348, 0.327, and 0.377 for the aquifers type 1, type 2 and type 3, respectively, for the 1st validation phase, as well as with R^2 of 0.569, 0.508, and 0.608 for the aquifers type 1, type 2 and type 3, respectively, for the 2nd validation phase as shown in **Figure 4.15**.

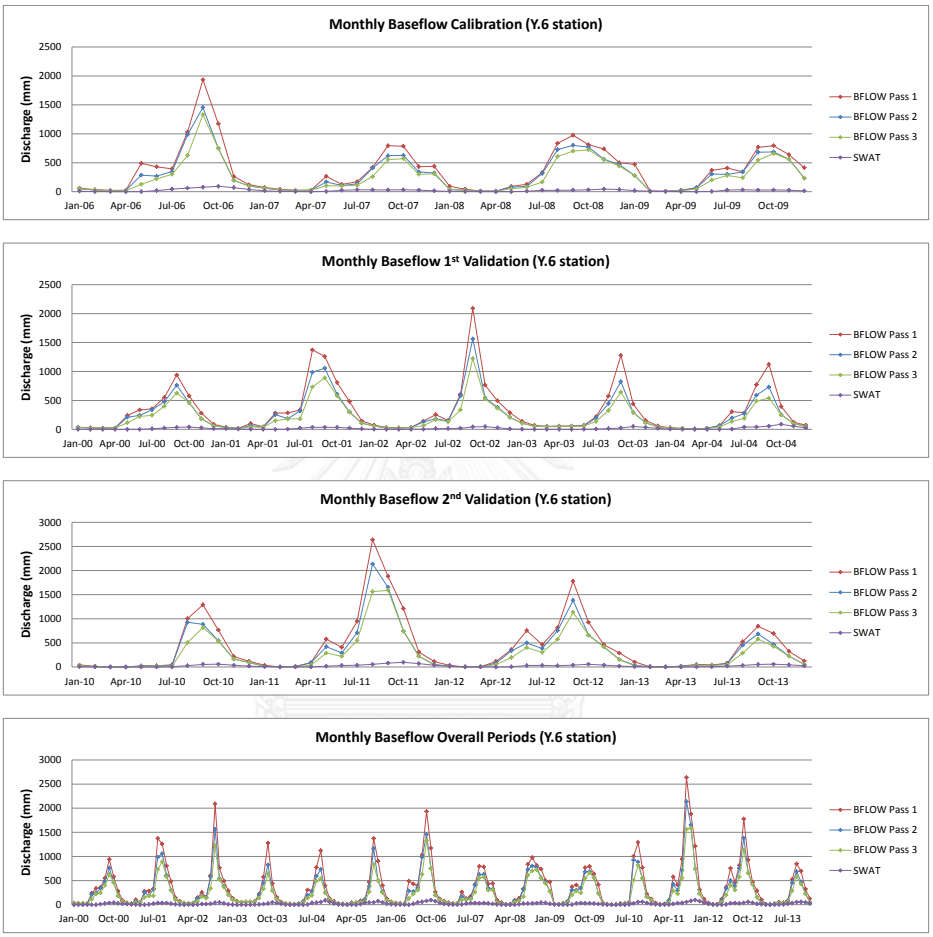

Figure 4.15 Calibration and validation results represented comparison of BFLOW output from the Baseflow Filter program and SWAT baseflow of station Y.36 during 2000-2013

4.1.3 Effects of landuse change on streamflow and groundwater recharge in the Yom river basin

1) Y.36 station

As comparing the results of SWAT simulation due to land use change from 2003 to 2009 with the same precipitation data of year 2005, the monthly streamflow appeared to be clearly increased in the rainy season (from July to October), while it seemed to be a similar discharge during January to July as presented in **Figure 4.16(a)**. The average streamflow results calculated by using landuse in 2003 and 2009 were 16.00 cms. and 42.42 cms., respectively. Due to land use change from 2003 to 2009, it would conclude that the average streamflow has increased 62.27%.

For groundwater recharge, by using landuse data from year 2003 and 2009, results of baseflow from SWAT model showed that the highest groundwater recharge was appeared in September and October, respectively. However, the groundwater recharge hydrograph in 2003 came a bit earlier than that in 2009. It occurred groundwater recharge (using landuse 2003) and gradually increase from May, while groundwater recharge started from June when using landuse 2009. Moreover, groundwater recharge per the annual precipitation in 2005 has decreased 5.12% because impact of landuse change from 2003 (~31.38%) to 2009 (~26.2%) as shown in **Figure 4.16(b)**.

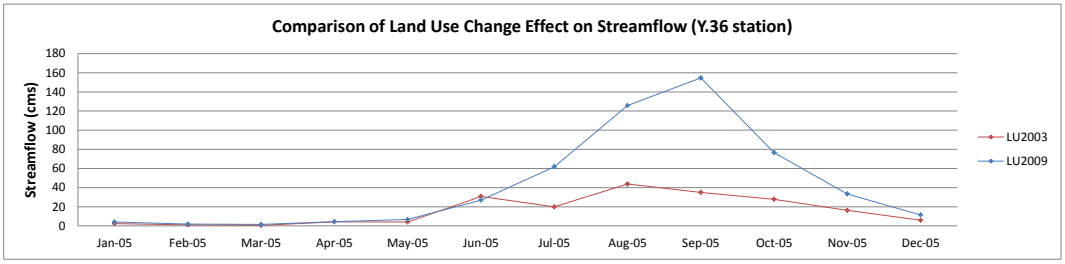

(a)

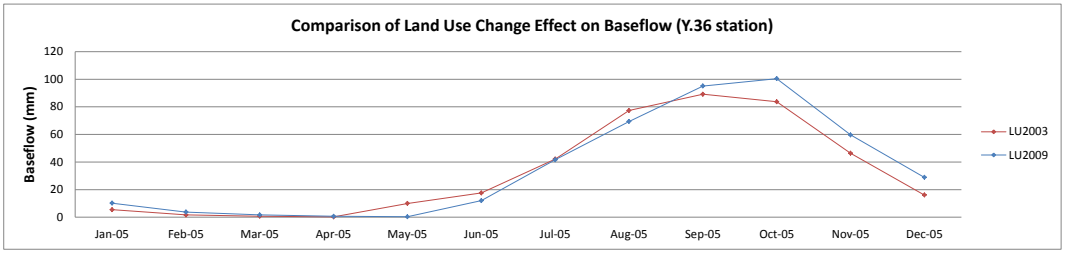

(b)

Figure 4.16 Effects of landuse change from 2003 to 2009 of station Y.36
(a) Comparison of simulated stream data and **(b)** comparison of groundwater recharge hydrographs

2) Y.24 station

As comparing the results of SWAT simulation due to land use change from 2003 to 2009 with the same precipitation data of year 2005, the monthly streamflow appeared to be clearly increased in the rainy season (from July to October), while it seemed to be a similar discharge during January to June as presented in **Figure 4.17(a)**. The average streamflow results calculated by using landuse in 2003 and 2009 were 13.59 cms. and 60.79 cms., respectively. Due to land use change from 2003 to 2009, it would conclude that the average streamflow has increased 77.64%.

For groundwater recharge, by using landuse data from year 2003 and 2009, results of baseflow from SWAT model showed that the highest groundwater recharge was appeared in September and October, respectively. However, the groundwater recharge hydrograph in 2003 came earlier than that in 2009. It occurred groundwater recharge (using landuse 2003) and gradually increase from May, while groundwater recharge started from June when using landuse 2009. Moreover, groundwater recharge per the annual precipitation in 2005 has decreased 2.07% because impact of landuse change from 2003 (~28.89%) to 2009 (~26.81%) as shown in **Figure 4.17(b)**.

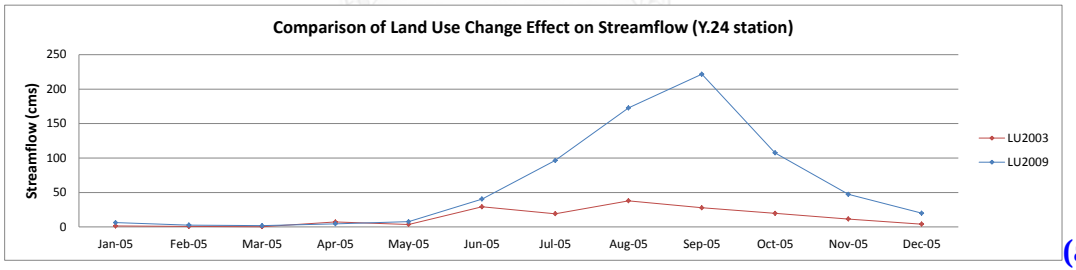

(a)

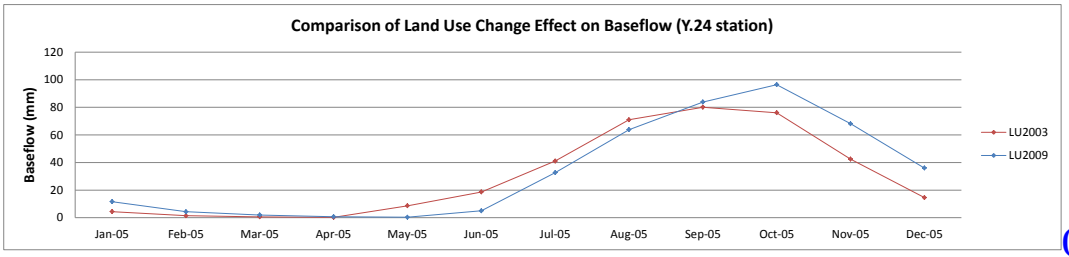

(b)

Figure 4.17 Effects of landuse change from 2003 to 2009 of station Y.24
(a) Comparison of simulated stream data and **(b)** comparison of groundwater recharge hydrographs

3) Y.20 station

As comparing the results of SWAT simulation due to land use change from 2003 to 2009 with the same precipitation data of year 2005, the monthly streamflow appeared to be clearly increased in the rainy season (from August to November), while it seemed to be a similar discharge during January to June as presented in **Figure 4.18(a)**. The average streamflow results calculated by using landuse in 2003 and 2009 were 77.55 cms. and 91.30 cms., respectively. Due to land use change from 2003 to 2009, it would conclude that the average streamflow has increased 21.63%.

For groundwater recharge, by using landuse data from year 2003 and 2009, results of baseflow from SWAT model showed that the highest groundwater recharge was appeared in September and October, respectively. However, the groundwater recharge hydrograph in 2003 came earlier than that in 2009. It occurred groundwater recharge (using landuse 2003) and gradually increase from May, while groundwater recharge started from June when using landuse 2009. Moreover, groundwater recharge per the annual precipitation in 2005 has decreased 3.41% because impact of landuse change from 2003 (~33.17%) to 2009 (~29.76%) as shown in **Figure 4.18(b)**.

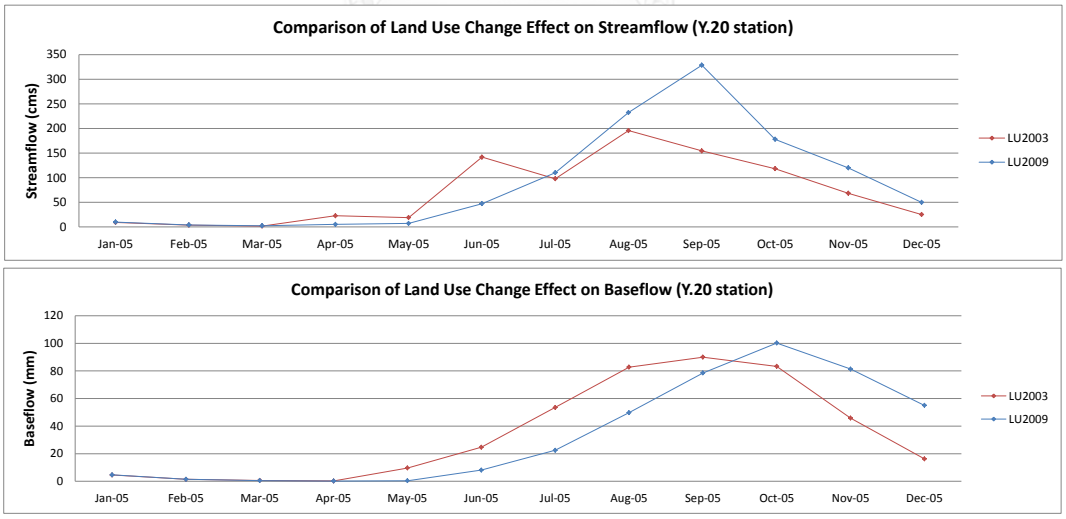

Figure 4.18 Effects of landuse change from 2003 to 2009 of station Y.20
(a) Comparison of simulated stream data and **(b)** comparison of groundwater recharge hydrographs

4) Y.38 station

As comparing the results of SWAT simulation due to land use change from 2003 to 2009 with the same precipitation data of year 2005, the monthly streamflow appeared to be clearly increased in the late rainy season (from September to November), while it the streamflow simulated by using landuse of year 2003 as compared to those streamflow estimated by using the landuse data of year 2009, found to be higher from May to July as presented in **Figure 4.19(a)**. The average streamflow results calculated by using landuse in 2003 and 2009 were 10.06 cms. and 10.58 cms., respectively. Due to land use change from 2003 to 2009, it would conclude that the average streamflow has increased 4.94%.

For groundwater recharge, by using landuse data from year 2003 and 2009, results of baseflow from SWAT model showed that the highest groundwater recharge was appeared in the same month in October, respectively. However, the groundwater recharge hydrograph in 2003 came earlier than that in 2009. It occurred groundwater recharge (using landuse 2003) and gradually increase from May, while groundwater recharge started from July when using landuse 2009. The late of occurrence of groundwater recharge may be caused from the influence of land use change. Moreover, groundwater recharge per the annual precipitation in 2005 has decreased 2.14% because impact of landuse change from 2003 (~33.49%) to 2009 (~31.35%) as shown in **Figure 4.19(b)**.

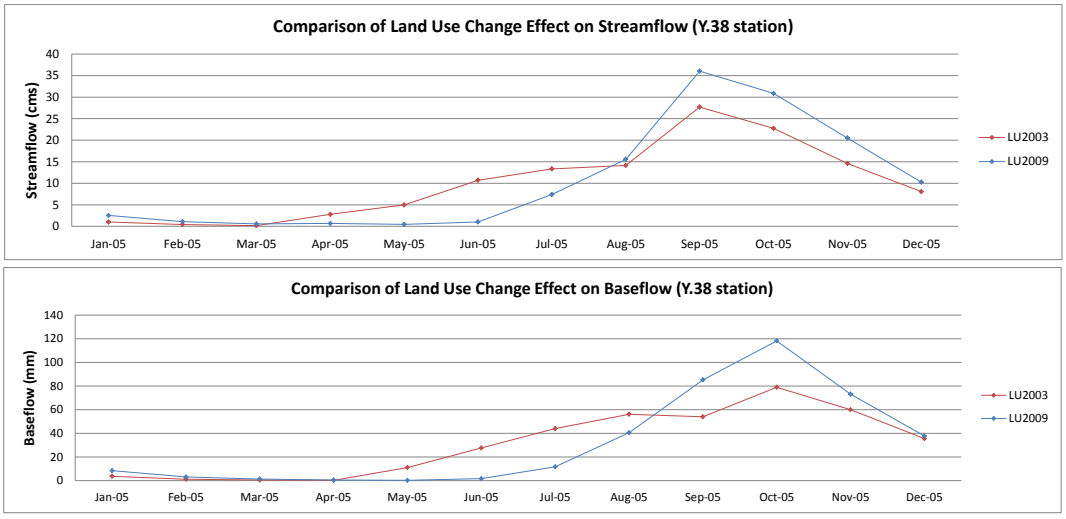

Figure 4.19 Effects of landuse change from 2003 to 2009 of station Y.38
(a) Comparison of simulated stream data and **(b)** comparison of groundwater recharge hydrographs

5) Y.1C station

As comparing the results of SWAT simulation due to land use change from 2003 to 2009 with the same precipitation data of year 2005, the monthly streamflow appeared to be clearly increased in the late rainy season (from September to November), while it the streamflow simulated by using landuse of year 2003 as compared to those streamflow estimated by using the landuse data of year 2009, found to be higher from May to July as presented in **Figure 4.20(a)**. The average streamflow results calculated by using landuse in 2003 and 2009 were 131.92 cms. and 165.59 cms., respectively. Due to land use change from 2003 to 2009, it would conclude that the average streamflow has increased 20.34%.

For groundwater recharge, by using landuse data from year 2003 and 2009, results of baseflow from SWAT model showed that the highest groundwater recharge was appeared in the same month in October, respectively. However, the groundwater recharge hydrograph in 2003 came earlier than that in 2009. It occurred groundwater recharge (using landuse 2003) and gradually increase from May, while groundwater recharge started from July when using landuse 2009. The late of occurrence of groundwater recharge may be caused from the influence of land use change. Moreover, groundwater recharge per the annual precipitation in 2005 has decreased 4.97% because impact of landuse change from 2003 (~32.49% to 2009 (~27.53%) as shown in **Figure 4.16(b)**.

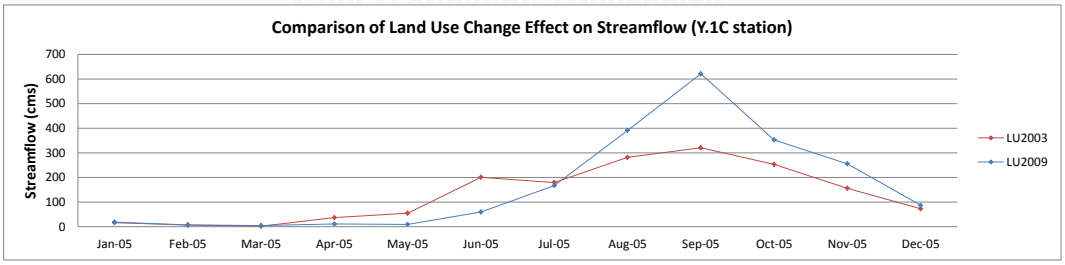

(a)

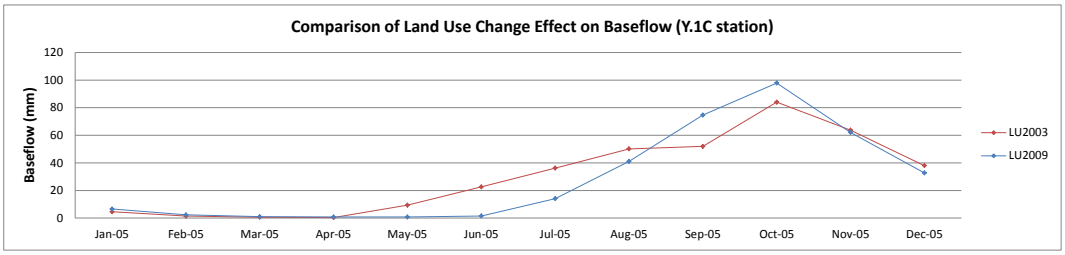

(b)

Figure 4.20 Effects of landuse change from 2003 to 2009 of station Y.1C **(a)** Comparison of simulated stream data and **(b)** comparison of groundwater recharge hydrographs

6) Y.14 station

As comparing the results of SWAT simulation due to land use change from 2003 to 2009 with the same precipitation data of year 2005, the monthly streamflow appeared to be clearly increased in the late rainy season (from September to November), while it the streamflow simulated by using landuse of year 2003 as compared to those streamflow estimated by using the landuse data of year 2009, found to be higher from May to July as presented in **Figure 4.21(a)**. The average streamflow results calculated by using landuse in 2003 and 2009 were 178.45 cms. and 234.87 cms., respectively. Due to land use change from 2003 to 2009, it would conclude that the average streamflow has increased 24.02%.

For groundwater recharge, by using landuse data from year 2003 and 2009, results of baseflow from SWAT model showed that the highest groundwater recharge was appeared in the same month in October, respectively. However, the groundwater recharge hydrograph in 2003 and 2009 showed a similar pattern and started from June, but the groundwater recharge hydrograph in 2009 was higher than those in 2003 from June to December, suggesting the influence of land use change. Moreover, groundwater recharge per the annual precipitation in 2005 has decreased 3.42% because impact of landuse change from 2003 (~28.10%) to 2009 (~24.68%) as shown in **Figure 4.21(b)**.

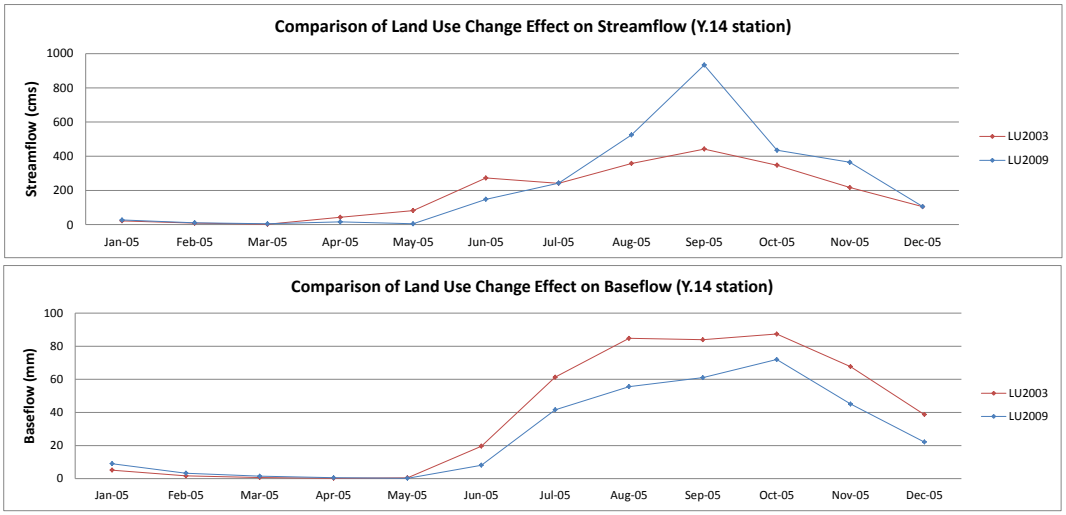

Figure 4.21 Effects of landuse change from 2003 to 2009 of station Y.14
(a) Comparison of simulated stream data and **(b)** comparison of groundwater recharge hydrographs

7) Y.6 station

As comparing the results of SWAT simulation due to land use change from 2003 to 2009 with the same precipitation data of year 2005, the monthly streamflow appeared to be clearly increased in the late rainy season (from September to November), while it the streamflow simulated by using landuse of year 2003 as compared to those streamflow estimated by using the landuse data of year 2009, found to be higher from May to July as presented in **Figure 4.22(a)**. The average streamflow results calculated by using landuse in 2003 and 2009 were 232.47 cms. and 245.37 cms., respectively. Due to land use change from 2003 to 2009, it would conclude that the average streamflow has increased 5.26%.

For groundwater recharge, by using landuse data from year 2003 and 2009, results of baseflow from SWAT model showed that the highest groundwater recharge was appeared in the same month in October, respectively. However, the groundwater recharge hydrograph in 2003 and 2009 showed a similar pattern and started from June, but the groundwater recharge hydrograph in 2009 showed a bit higher than those in 2003. It seemed not be shown a significant difference of groundwater recharge, suggesting that this station is located in the discharge areas and the change of landuse has not been changed much during 2003-2009. Moreover, groundwater recharge per the annual precipitation in 2005 has decreased 0.26% because impact of landuse change from 2003 (~21.84%) to 2009 (~21.58%) as shown in **Figure 4.22(b)**.

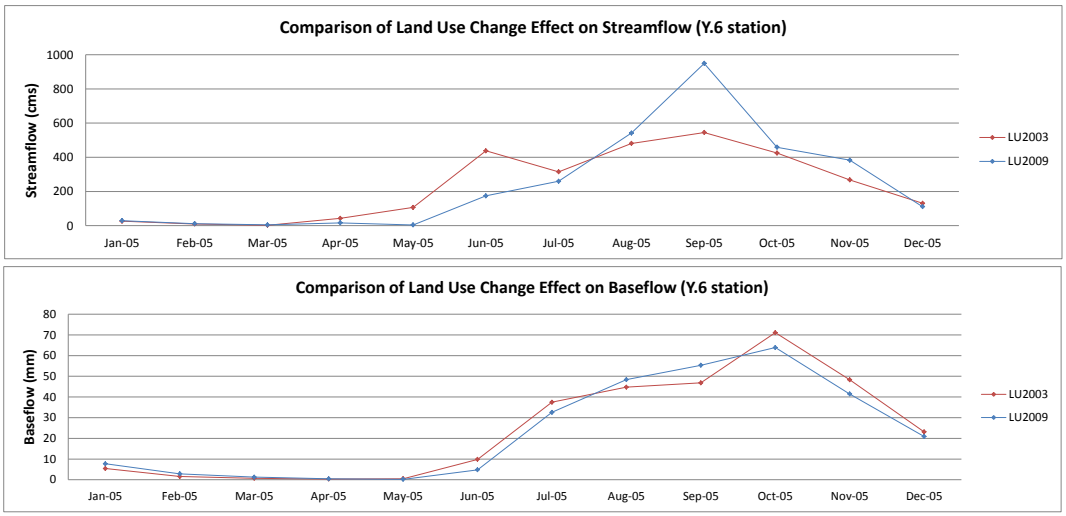

Figure 4.22 Effects of landuse change from 2003 to 2009 of station Y.14
(a) Comparison of simulated stream data and **(b)** comparison of groundwater recharge hydrographs

4.1.4 Runoff coefficient

Annual runoff significantly increased in the central part of Yom basin with the rate of 10.0 mm per year and Huay Mae Sin subbasin which is in the south part of Yom basin but adjacent to the central part with the rate of 6.7 mm/yr. while others area show the rate of change of not more than 6 mm/yr. The area with the significant increasing in annual runoff coincided with the area with the increasing in rainfall, so the increasing in rainfall could cause the increasing in runoff in the area, as show in **Figure 4.23(a)**.

In order to exclude the effect of rainfall on runoff, trends of runoff coefficient were determined. The result showed a significant increasing in runoff coefficient in the central part of the basin with the rate of 0.006 per year. Mae Mok subbasin, the mountainous subbasin southern part of yom basin, also has a non-significant but considerable high increasing trend with the amount of 0.004 per year while others subbasin did not show an increasing trend for more than 0.003 per year. It could be inferred that the change in rainfall in the central part of the basin was not only the cause of the increasing in runoff. Another main cause of that increasing could be a landuse change. In Mae Mok subbasin, even though the runoff was increasing, there was no significant change in the runoff coefficient, so the main cause of the increasing of the runoff could be the increasing in rainfall. However, Mae Mok subbasin was possibly another subbasin which a landuse change caused the runoff coefficient to increase, as show in **Figure 4.23(b)**. When compared runoff coefficient effect from landuse change, that represent homologous to SWAT runoff simulation.

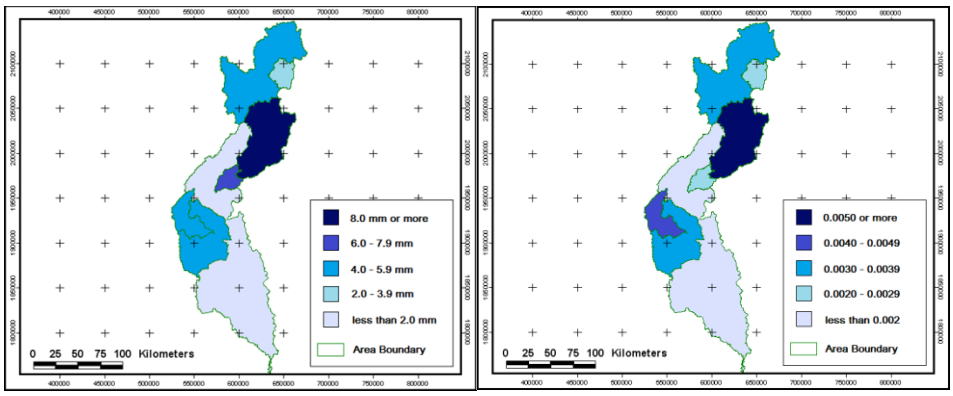

Figure 4.23 Effects of landuse change to runoff coefficient in Yom River Basin **(a)** Increased runoff and **(b)** increased runoff coefficient in each subbasin

4.1.5 Groundwater recharge results

1) *Groundwater recharge output from SWAT model*

Due to the limitations of exported groundwater recharge output data in HRUs cells, we necessary to use the GW_Qmm output at each delineate subwatersheds instead. When comparing the duration of groundwater recharge simulation by SWAT model, selected GW_Qmm data from SWAT simulation period for use as the input data, groundwater recharge (mm/month), for MODFLOW model. Groundwater recharge from SWAT output simulation in 2013 was shown in **Table 4.4**, and monthly groundwater recharge maps in 2013 were shown in **Figure 4.24**.

Table 4.4 Groundwater recharge from SWAT output simulation in 2013

Subbasin	Jan-13	Feb-13	Mar-13	Apr-13	May-13	Jun-13	Jul-13	Aug-13	Sep-13	Oct-13	Nov-13	Dec-13	Mean (mm/mth)	Total (mm/yr)
1	3.243	2.644	2.604	2.243	2.038	1.737	1.629	1.693	2.217	2.927	3.193	3.355	2.460	29.523
2	13.994	5.315	2.464	0.935	0.389	7.965	23.816	57.849	79.845	70.108	40.692	19.572	26.912	322.944
3	0.248	0.152	0.002	0.000	0.000	0.088	3.621	48.988	81.407	76.699	43.580	12.375	22.263	267.160
4	6.822	4.898	3.964	2.532	1.756	1.266	1.281	2.153	4.501	6.648	7.162	6.964	4.162	49.947
5	8.720	6.092	5.198	3.646	2.693	2.182	2.673	4.985	8.444	10.732	10.552	9.808	6.310	75.725
6	16.189	10.922	11.699	6.488	15.037	18.459	26.965	62.419	97.333	81.069	56.710	30.573	36.155	433.863
7	15.159	9.480	9.708	5.354	11.854	14.474	20.876	53.814	91.347	75.361	51.660	27.733	32.235	386.820
8	13.115	7.410	9.230	5.230	9.348	15.721	19.313	48.195	78.487	68.259	50.003	28.293	29.384	352.604
9	4.923	3.757	3.299	2.188	1.286	0.852	1.103	2.344	4.023	5.195	5.192	4.976	3.262	39.138
10	5.405	4.274	3.944	2.802	1.769	1.175	1.332	2.521	4.191	5.433	5.508	5.390	3.645	43.744
11	4.873	3.721	3.365	2.325	1.392	0.904	1.004	1.950	3.467	4.790	5.000	4.881	3.139	37.672
12	2.217	1.142	0.713	0.378	0.326	0.676	0.590	0.673	1.857	3.232	3.417	2.761	1.499	17.982
13	1.966	1.226	0.970	0.636	0.399	0.265	0.351	0.655	1.358	2.207	2.413	2.177	1.219	14.623
14	1.200	0.542	0.303	0.157	0.421	0.873	1.674	2.667	3.932	4.820	4.303	3.325	2.018	24.217
15	1.464	0.801	0.570	0.378	0.474	0.628	1.059	1.705	2.837	3.798	3.556	2.756	1.669	20.026

Figure 4.24 Monthly groundwater recharge maps from SWAT output in 2013

January *February* *March*

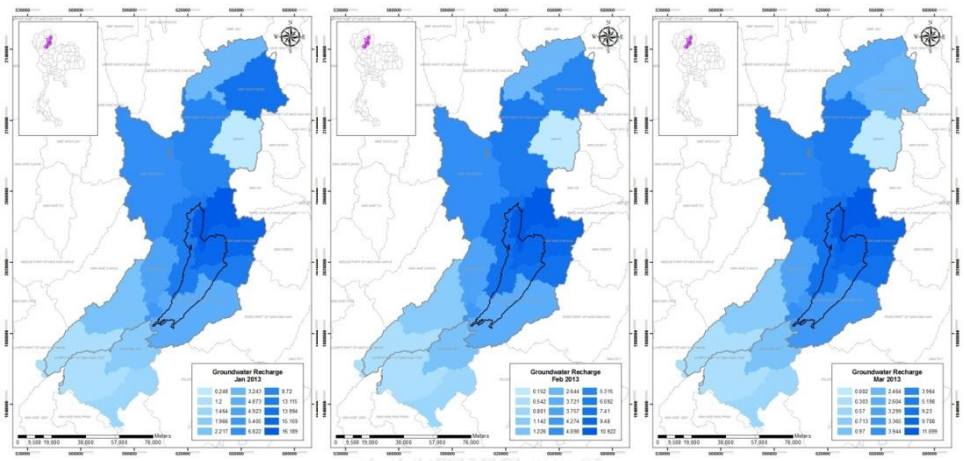

Aprill *May* *June*

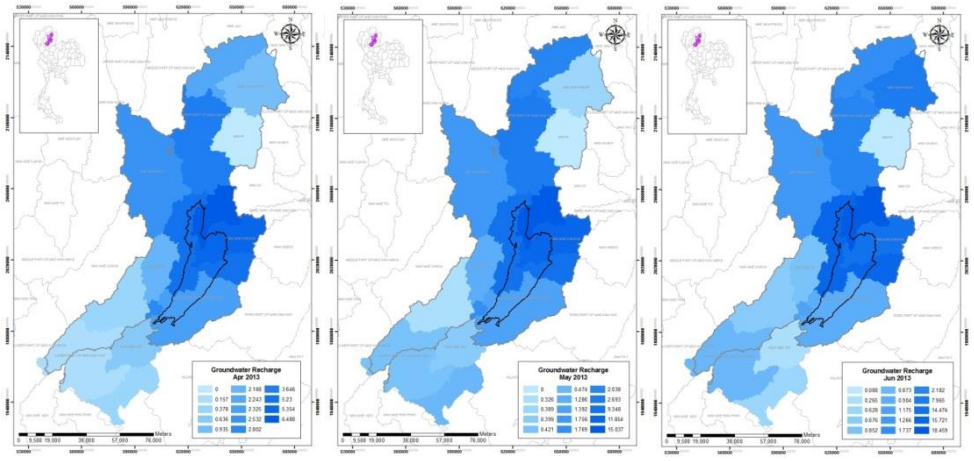

Figure 4.24 Monthly groundwater recharge maps from SWAT output in 2013 (continue)

July *August* *September*

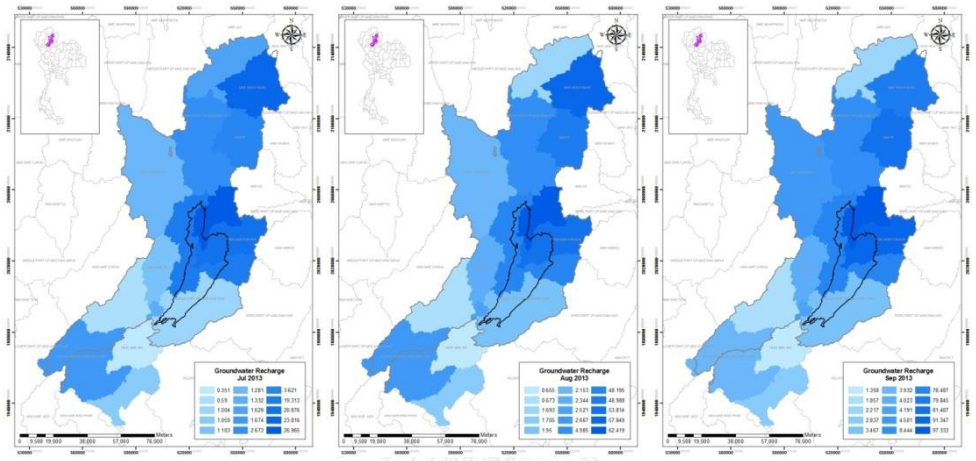

October *November* *December*

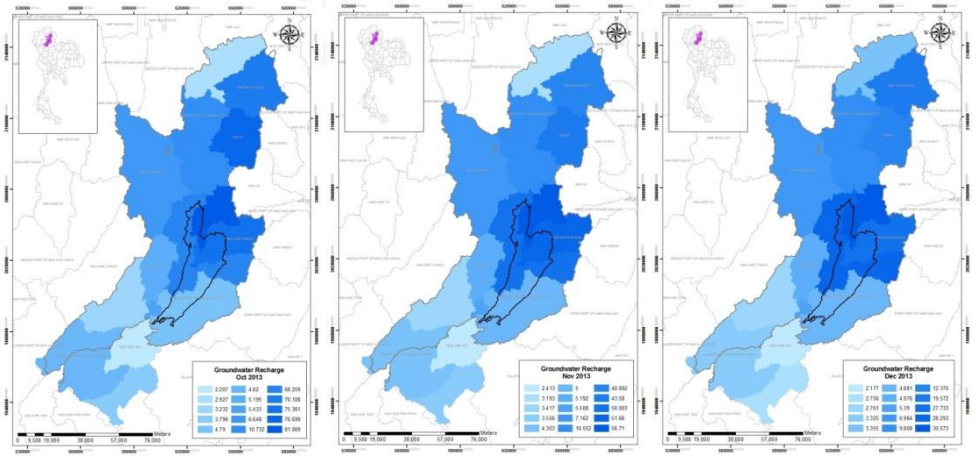

2) *Groundwater recharge as a input of MODFLOW model*

Groundwater recharge output from the SWAT model in subbasin nos. 6, 7, 8 and 11 (**Figure 4.25**) is considered as a groundwater recharge input to MODFLOW, which needed to be estimated as monthly groundwater recharge maps within the hydrogeological boundary of the Quaternary unconsolidated sedimentary aquifers, based on the assumption of a uniformly distributed recharge over each subbasin. The groundwater recharge, delineated by the boundary of the Quaternary unconsolidated sedimentary aquifers, was used as input to MODFLOW as shown in **Table 4.5**. Estimation of monthly groundwater recharge results as the input of transient state to MODFLOW are shown in **Table 4.6**.

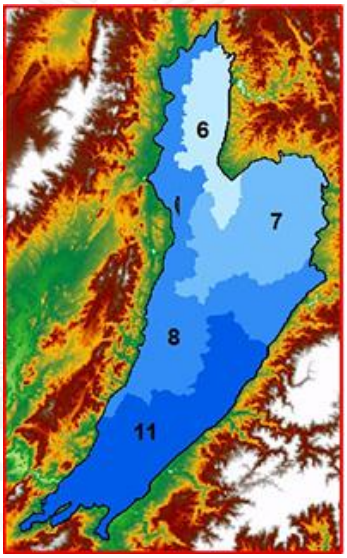

Figure 4.25 Groundwater recharge area for input to MODFLOW model.

Table 4.5 Comparison of groundwater recharge areas of each subbasin between SWAT output and MODFLOW input.

Subbasin	SWAT	MODFLOW	
	Area (km^2)	Area (km^2)	%
6	488.44	115.47	23.64
7	667.70	244.47	36.61
8	1107.90	339.87	30.68
11	1206.60	291.29	24.14

Table 4.6 Monthly groundwater recharge (m/day) for MODFLOW input preparation in 2013

Subbasin	31	59	90	120	151	181	212	243	273	304	334	362	X (m/day)
6	1.23E-04	9.22E-05	8.92E-05	5.11E-05	1.15E-04	1.45E-04	2.06E-04	4.76E-04	7.67E-04	6.18E-04	4.47E-04	2.33E-04	2.80E-04
7	1.79E-04	1.24E-04	1.15E-04	6.53E-05	1.40E-04	1.77E-04	2.47E-04	6.36E-04	1.11E-03	8.90E-04	6.30E-04	3.28E-04	3.87E-04
8	1.30E-04	8.12E-05	9.13E-05	5.35E-05	9.25E-05	1.61E-04	1.91E-04	4.77E-04	8.03E-04	6.75E-04	5.11E-04	2.80E-04	2.96E-04
11	3.79E-05	3.21E-05	2.62E-05	1.87E-05	1.08E-05	7.27E-06	7.82E-06	1.52E-05	2.79E-05	3.73E-05	4.02E-05	3.80E-05	2.50E-05

Then, groundwater recharge, which was estimated as the input to MODFOW, needed to convert a unit from mm/month to m/day. Model stress period has been designed 1 stress period per 1 month. The steady state simulation used the average groundwater recharge in 2012 and transient state simulation use the monthly average recharge in each stress period.

4.2 Groundwater model results

There are many data formats for importing to create aquifer layers in MODFLOW. This research used .grd format from Surfer program that is transformed from .xlsx format. The data collected from January 2013 (dry season) was defined as the start value for running model in the steady state with 31-day period, and the data collected from July 2013 (rainy season) was defined as the end in transient state simulation with 212-day period.

MODFLOW model was used to determine groundwater flow characteristics and groundwater balance in the study area. Groundwater level measurement data from the field in January 2013 was used for both steady state and transient state (in day 31) calibration, and the data from the field in July 2013 was used for transient state calibration (in day 212). Then, the groundwater model was run within 1 year (or until day 365) to calculate the groundwater balance in the aquifers. This research aimed to use the model to simulate the groundwater balance and safe yield in the aquifers in 2013 by integrating with various distributed groundwater recharge from SWAT model as earlier mentioned in frameworks of model calibration and verification of SWAT and MODFLOW models are shown in **Table 4.1**.

Furthermore, additional parameters were adjusted during flow calibration and validation procedures as presented in **Table 4.7.**

Table 4.7 Description, optimal values used in the MODFLOW model calibration.

Aquifer	Range	Kx and Ky (m/s)	Kz (m/s)	Effective Porosity	Total Porosity	Sy	Ss (1/m)
Floodplain deposits aquifers (Qfd)	Min	1.62E-05	1.62E-06			0.12	1.50E-05
	Max	1.41E-04	1.41E-05			0.18	1.80E-05
	Optimal	2.43E-05	2.43E-06	0.15	0.30	0.18	1.80E-05
Younger terrace deposits aquifer (Qyt)	Min	1.41E-05	1.41E-06			0.12	1.50E-05
	Max	1.24E-04	1.24E-05			0.18	1.80E-05
	Optimal	2.12E-05	2.12E-06	0.15	0.30	0.12	1.50E-05
Old terrace deposits aquifer (Qot)	Min	1.18E-05	1.18E-06			0.01	1.01E-06
	Max	1.04E-04	1.04E-05			0.18	1.80E-05
	Optimal	1.77E-05	1.77E-06	0.15	0.30	0.01	2.42E-06

4.2.1 Field investigation results and classification of aquifers

Based on hydrogeological characteristics and database of Pasutara groundwater wells of DGR, observation wells in field investigation can be classified into 3 aquifers as follows: Qfd, Qyt and Qot. In case of wells with uncompleted details, well bottom was correlated with the nearby observation wells and geological cross-sections of Department of Mineral Resources (DMR). Detail information of observation wells in 3 aquifer of Qfd, Qyt, and Qot are shown in **Tables 4.8-4.10**, respectively.

Table 4.8 Detail information of observation wells in Qfd.

ID	X	Y	Depth (m)	Elevation (msl)	Aquifer	Basin	WL01_2013 (m)	WL07_2013 (m)	Bottom (msl)	WL_Dry (msl)	WL_Wet (msl)	Change (m)
DCD13181	633813	2112614	29	291	Qfd	Pr	3.63	1.71	262	287.37	289.29	-1.92
MRO507	626225	2047140	-	204	Qfd	Pr	4.8	5.9	#VALUE!	198.1	199.2	-1.1
PW4824	630919	2028669	21	200	Qfd	Pr	5.29	6.55	179	193.45	194.71	-1.26
DCD15749	632120	2024155	54	182	Qfd	Pr	1.65	0.8	128	180.35	181.2	-0.85
DCD15937	623889	2023725	-	168	Qfd	Pr	5.1	6.25	#VALUE!	161.75	162.9	-1.15
Unknow7	621010	2020122	-	172	Qfd	Pr	10.66	3.47	#VALUE!	168.53	161.34	7.19
PW15954	627880	2015185	30	167	Qfd	Pr	20.17	22.47	137	144.53	146.83	-2.3
PW346	627913	2015162	26	173	Qfd	Pr	15.41	16.55	147	156.45	157.59	-1.14
New7	632001	2014926	-	186	Qfd	Pr	7.02	9.8	#VALUE!	176.2	178.98	-2.78
MR54	620501	2011138	33	160	Qfd	Pr	8.91	2.75	127	157.25	151.09	6.16
New14	620641	2006323	-	158	Qfd	Pr	13.71	4.5	#VALUE!	153.5	144.29	9.21
MR292	619671	2006296	27	147	Qfd	Pr	7.87	8.16	120	138.84	139.13	-0.29
Unknow2	617501	2005859	-	161	Qfd	Pr	11.59	10.25	#VALUE!	150.75	149.41	1.34
A7	599882	1994652	30	160	Qfd	Pr	5.6	2.81	130	154.4	157.19	-2.79

Table 4.9 Detail information of observation wells in Qyt.

ID	X	Y	Depth (m)	Elevation (msl)	Aquifer	Basin	WL01_2013 (m)	WL07_2013 (m)	Bottom (msl)	WL_Dry (msl)	WL_Wet (msl)	Change (m)
MR433	630484	2015248	51	185	Qyt	Pr	8.24	8.04	134	176.96	176.76	0.2
NEW13	618764	2006245	-	155	Qyt	Pr	7.21	7.55	#VALUE!	147.45	147.79	-0.34
New12	619834	2005748	-	152	Qyt	Pr	8.57	10.68	#VALUE!	141.32	143.43	-2.11
New4	589664	2000524	-	158	Qyt	Pr	13.22	14.08	#VALUE!	143.92	144.78	-0.86
DCD15827	589579	2000451	-	118	Qyt	Pr	0.52	0.45	#VALUE!	147.55	147.48	0.07
DCD16633	589410	1998871	-	133	Qyt	Pr	2.47	1.7	#VALUE!	131.3	130.53	0.77
ก1270	587047	1997779	-	141	Qyt	Pr	3.49	2.46	#VALUE!	138.54	137.51	1.03
MR573	590390	1989807	24	148	Qyt	Pr	2.94	2.98	124	145.02	145.06	-0.04
ก2824	578985	1987136	-	132	Qyt	Pr	4.89	2.7	#VALUE!	129.3	127.11	2.19
MR465	563854	1984063	26	132	Qyt	Pr	5.87	4.93	106	127.07	126.13	0.94
New2	562831	1978485	-	121	Qyt	Pr	7.69	6.5	#VALUE!	114.5	113.31	1.19
New1	562800	1978442	-	120	Qyt	Pr	8.1	6.41	#VALUE!	113.59	111.9	1.69
MR458	609448	1991291	48	149	Qfd	Pr	6.73	4.88	101	142.27	144.12	-1.85

Table 4.10 Detail information of observation wells in Qot.

ID	X	Y	Depth (m)	Elevation (msl)	Aquifer	Basin	WL01_2013 (m)	WL07_2013 (m)	Bottom (msl)	WL_Dry (msl)	WL_Wet (msl)	Change (m)
MR580	627694	2045770	114	195	Qot	Pr	2.1	2.15	81	192.85	192.9	-0.05
PR184(NT54/2)	624906	2035500	90	172	Qot	Pr	-0.6	-0.7	82	172.6	172.7	-0.1
PR183(NT54/1)	624907	2035499	90	172	Qot	Pr	-0.7	-0.75	82	172.7	172.75	-0.05
DCD1570	631132	2028698	-	203	Qot	Pr	8.09	8.84	#VALUE!	194.16	194.91	-0.75
NEW11	636165	2024208	-	195	Qot	Pr	2.34	2.94	#VALUE!	192.06	192.66	-0.6
ก1642	634883	2022887	-	196	Qot	Pr	2.53	2.06	#VALUE!	193.94	193.47	0.47
New8	634835	2022883	110	199	Qot	Pr	2.68	3.51	89	195.49	196.32	-0.83
DOH11990	629625	2017806	-	171	Qot	Pr	2.2	2.88	#VALUE!	168.12	168.8	-0.68
MR612	623596	2009575	114	161	Qot	Pr	26.51	13.9	47	147.1	134.49	12.61
DOH2007	628358	2004832	-	187	Qot	Pr	24.31	21.9	#VALUE!	165.1	162.69	2.41
MR40	620244	2001812	72	158	Qot	Pr	17.88	18.8	86	139.2	140.12	-0.92
Unknow6	623374	1999326	-	170	Qot	Pr	7.78	6.22	#VALUE!	163.78	162.22	1.56
MR190	589080	1998871	24	126	Qot	Pr	2.2	106	102	124.94	123.8	1.14
MR574	584769	1997801	90	126	Qot	Pr	2.2	2.05	36	123.8	123.95	-0.15
MB24	614274	1995457	60	120	Qot	Pr	9.26	9.42	60	110.58	110.74	-0.16
MR458	609447	1991291	48	145	Qot	Pr	7.71	8.1	97	136.9	137.29	-0.39
PR140	574097	1990310	92	146	Qot	Pr	4.26	4.38	54	141.62	141.74	-0.12
MR278	615382	1990009	-	167	Qot	Pr	7.03	6.5	#VALUE!	160.5	159.97	0.53
MR666	612357	1988553	63	154	Qot	Pr	5.13	4.63	91	149.37	148.87	0.5

4.2.2 Groundwater contour and flow direction

After aquifers classification process, the observation wells data was imported to the Surfer program in order to define elevation of each aquifers, aquifer thickness. Moreover, groundwater contour in each aquifer can be used for specifying boundary condition of groundwater model, i.e., constant head and general head of each aquifer. Importing aquifers bottom layers and groundwater head of observation wells to Visual MODFLOW can use many formats, but this research used data in .grd (Surfer Grid) format from databases in .xlsx (Microsoft Excel). Groundwater contour and flow direction in dry and rainy seasons of Qfd, Qyt, and Qot were shown in **Figures 4.26-4.28**.

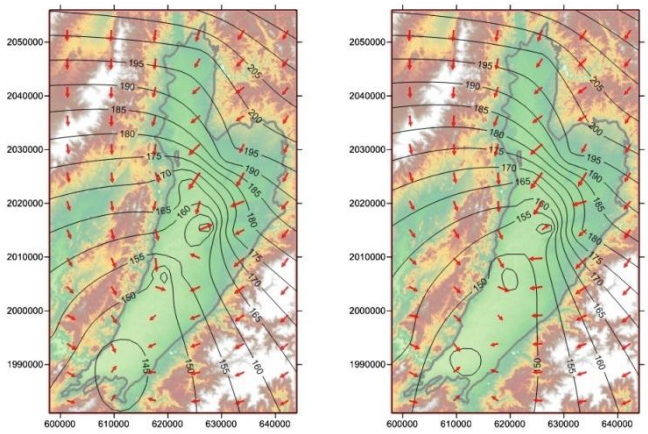

(a) **(b)**

Figure 4.26 Groundwater head contour and flow direction in the Qfd aquifer in **(a)** dry season and **(b)** rainy season

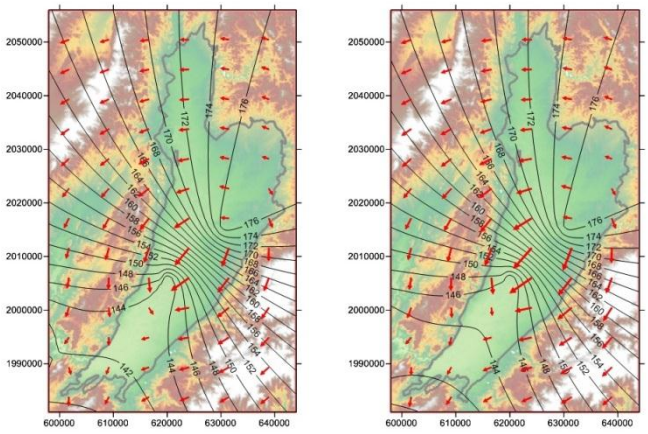

(a) **(b)**

Figure 4.27 Groundwater head contour and flow direction in the Qyt aquifer in **(a)** dry season and **(b)** rainy season

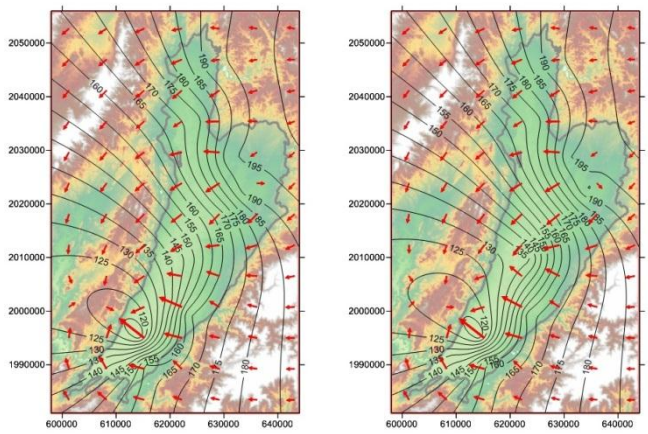

(a) **(b)**

Figure 4.28 Groundwater head contour and flow direction in the Qot aquifer in **(a)** dry season and **(b)** rainy season

4.2.3 Groundwater calibration: the steady state condition

The simulation of groundwater flow under the steady state condition was calibrated with observed groundwater level in January of 2013 with the stress period of 31 day. **Figure 4.29** shows the results of the simulate results compared with the observed groundwater level data in January, 2013. Comparison between the results from the statistical calculation and those measured in all 27 observed groundwater wells, 12 wells in Qfd aquifer, 4 wells in Qyt aquifer, and 11 wells in Qot aquifer shows the calibrated results that are summarized in **Table 4.11**.

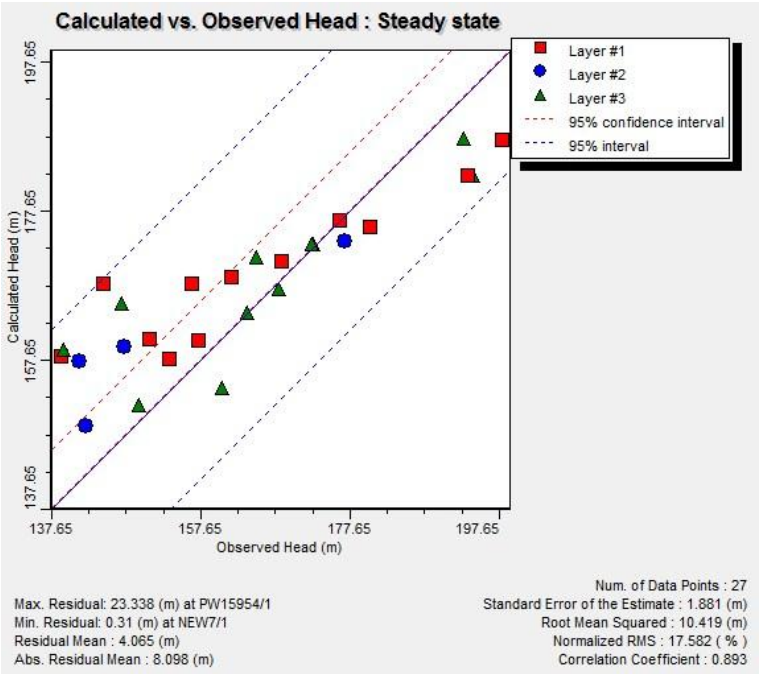

Figure 4.29 Model calibration in the steady state condition with a stress period of 31 days

Table 4.11 Model statistical results in the steady state condition with stress period of 31 days

	Qfd	Qyt	Qot	All
Residual Mean (m)	5.995	-2.076	4.441	4.156
Absolute Residual Mean (m)	10.562	8.511	14.651	11.819
Standard Error of the Estimate (m)	4.876	8.511	8.052	3.801
Root Mean Squared (m)	12.443	8.76	16.706	13.806
Normalized RMS (%)	22.785	25.253	29.679	24.371
Correlation Coefficient	0.942	1	0.599	0.737

4.2.1 Groundwater calibration: the transient state condition

The simulation of groundwater flow under the steady state condition was calibrated with observed groundwater level in January of 2013 with the stress period of 31 day. **Figure 4.30** shows the results of the simulate results compared with the observed groundwater level data in January, 2013. The simulation of groundwater flow under the transient state condition was calibrated with observed groundwater level in January and July of 2013 with stress period of 31 and of 212 days. Then, model was continually run to the end period 365 days to assess groundwater balance of 1 year. The prediction of water balance was simulated continuously in the same stress period with river stage, recharge, and pumping wells. **Figure 4.31** shows the simulated results compared with the observed groundwater level data in the transient state of 212 days. Comparison between the results from the statistical calculation with those measured in all 27 observed groundwater wells in Qfd (12 wells), Qyt (4 wells), and Qot (11 wells) aquifers shows the calibrated results that are summarized in **Table 4.12** and **Table 4.13**.

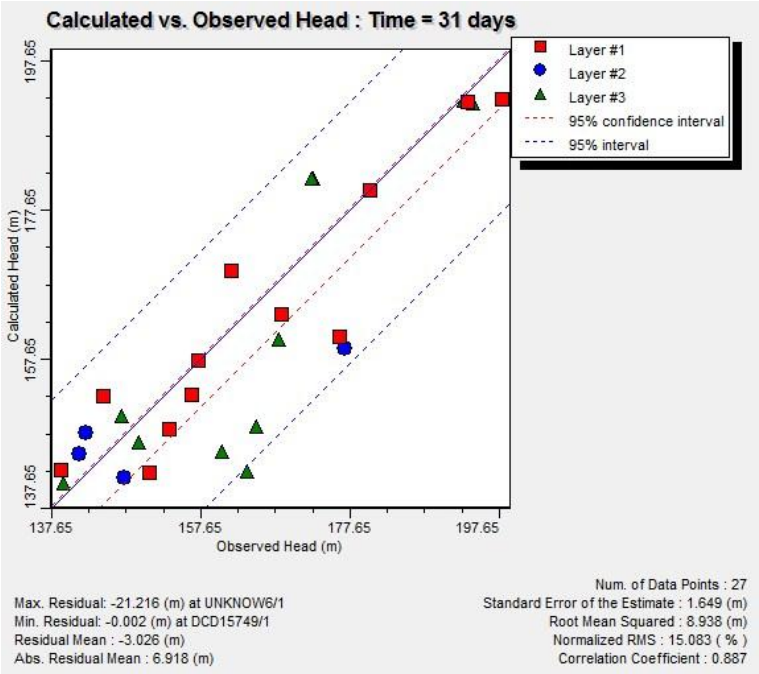

Figure 4.30 Model calibration in the transient state condition with a stress period of 31 day.

Table 4.12 Model statistical results in the transient state condition with stress period of 31 days

	Qfd	Qyt	Qot	All
Residual Mean (m)	9.239	0.364	5.046	6.261
Absolute Residual Mean (m)	9.971	6.166	13.793	10.855
Standard Error of the Estimate (m)	4.05	6.166	7.371	3.383
Root Mean Squared (m)	12.937	6.177	15.581	13.285
Normalized RMS (%)	23.69	17.806	27.681	23.451
Correlation Coefficient	0.936	1	0.67	0.801

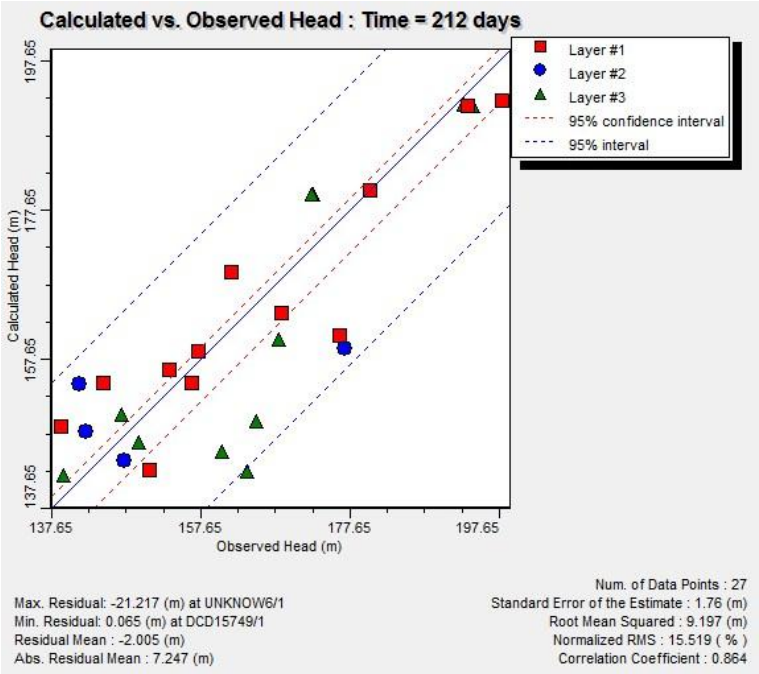

Figure 4.31 Model calibration in the transient state condition with a stress period of 212 day.

Table 4.13 Model statistical results in the transient state condition with stress period of 31 days

	Qfd	Qyt	Qot	All
Residual Mean (m)	12.344	3.393	5.576	8.364
Absolute Residual Mean (m)	13.742	9.282	14.257	13.254
Standard Error of the Estimate (m)	4.976	9.282	7.604	3.802
Root Mean Squared (m)	16.619	9.882	16.198	15.601
Normalized RMS (%)	29.901	30.277	28.822	27.28
Correlation Coefficient	0.969	1	0.644	0.756

4.2.2 Groundwater balance in steady state condition

The simulation of groundwater flow in steady state condition uses data in January, 2013. The simulation results show that in the study area the total recharge from rainfall is 113270.9 m^3/mth, leakage from rivers is +1301.6 m^3/mth, and leakage into rivers is -119220 m^3/day. The total groundwater abstraction from groundwater wells in the study area is +113270.9 m^3/mth. The groundwater balance of steady state is +69.317 m^3/mth. Describe of each aquifer steady state simulation as show in **Table 4.14**, **Table 4.15**, **Table 4.16** and total summation of all aquifers as show in **Table 4.17**.

Table 4.14 Groundwater balance in steady state condition in Qfd aquifer.

Stress period		**IN**		**OUT**
(day)		(flow m^3/mth)		(flow m^3/mth)
Total	Qfd			
31	Constant Head	710420	Constant Head	36146
	Well	0	Well	2384.3
	River Leakage	1301.6	River Leakage	119220
	Head Depth Boundary	21475	Head Depth Boundary	0
	Recharge	105400	Recharge	0
	Qyt to Qfd	106900	Qfd to Qyt	787760
	Total	945496.6	Total	945510.3
	Summary:			
	IN - OUT	-13.7		

Table 4.15 Groundwater balance in steady state condition in Qyt aquifer.

Stress period		**IN**		**OUT**
(day)		(flow m^3/mth)		(flow m^3/mth)
Total	Qyt			
31	Constant Head	0	Constant Head	0
	Well	0	Well	1776.6
	River Leakage	0	River Leakage	0
	Head Depth Boundary	0	Head Depth Boundary	294.86
	Recharge	7795.1	Recharge	0
	Qfd to Qyt	787760	Qyt to Qfd	106900
	Qot to Qyt	81458	Qyt to Qot	767960
	Total	877013.1	Total	876931.46
	Summary:			
	IN - OUT	81.64		

Table 4.16 Groundwater balance in steady state condition in Qot aquifer.

Stress period		**IN**		**OUT**
(day)		(flow m^3/mth)		(flow m^3/mth)
Total	Qot			
31	Constant Head	50848	Constant Head	736400
	Well	0	Well	1024.2
	River Leakage	0	River Leakage	0
	Head Depth Boundary	0	Head Depth Boundary	0.22349
	Recharge	75.8	Recharge	0
	Qyt to Qot	767960	Qot to Qyt	81458
	Total	818883.8	Total	818882.4235
	Summary:			
	IN - OUT	1.37651		

Table 4.17 Total groundwater balance in steady state condition of all aquifers.

Stress period		**IN**		**OUT**
(day)		(flow m^3/mth)		(flow m^3/mth)
Total	Qfd+Qyt+Qot			
31	Constant Head	761268	Constant Head	772546
	Well	0	Well	5185.1
	River Leakage	1301.6	River Leakage	119220
	Head Depth Boundary	21475	Head Depth Boundary	295.08349
	Recharge	113270.9	Recharge	0
	Qyt to Qfd	106900	Qfd to Qyt	787760
	Qfd to Qyt	787760	Qyt to Qfd	106900
	Qot to Qyt	81458	Qyt to Qot	767960
	Qyt to Qot	767960	Qot to Qyt	81458
	Total	2641393.5	Total	2641324.183
	Summary:			
	IN - OUT	69.31651		

4.2.3 Groundwater balance in transient state condition

The simulation of groundwater flow in transient state condition uses data in January and July, 2013. The simulation results show that in the study area the total recharge from rainfall, leakage from rivers, and leakage into rivers, total groundwater abstraction from groundwater wells. Show total amount of groundwater balance of transient state is +665.685 m^3/yr. Describe of each aquifer transient state simulation as show in **Table 4.18**, **Table 4.19**, **Table 4.20** and total summation of all aquifers as show in **Table 4.21**.

Table 4.18 Groundwater balance in transient state condition in Qfd aquifer.

Stress period (day)		**IN** (flow m^3/mth)		**OUT** (flow m^3/mth)
31	Constant Head	735670	Constant Head	42662
	Well	0	Well	2410.9
	River Leakage	1798000	River Leakage	1635500
	Head Depth Boundary	22509	Head Depth Boundary	0
	Recharge	108750	Recharge	0
	Storage	2583400	Storage	2013400
	Qyt to Qfd	342100	Qfd to Qyt	1896600
	Total	5590429	Total	5590572.9
	Summary:			
	IN - OUT	-143.9		
59	Constant Head	706420	Constant Head	41841
	Well	0	Well	2410.9
	River Leakage	472590	River Leakage	253130
	Head Depth Boundary	22191	Head Depth Boundary	0
	Recharge	74773	Recharge	0
	Storage	747010	Storage	566990
	Qyt to Qfd	291270	Qfd to Qyt	1450000
	Total	2314254	Total	2314371.9
	Summary:			
	IN - OUT	-117.9		
90	Constant Head	706530	Constant Head	41312
	Well	0	Well	2410.9
	River Leakage	197140	River Leakage	168820
	Head Depth Boundary	21953	Head Depth Boundary	0
	Recharge	73908	Recharge	0
	Storage	528350	Storage	290370
	Qyt to Qfd	287690	Qfd to Qyt	1312800
	Total	1815571	Total	1815712.9
	Summary:			
	IN - OUT	-141.9		

Table 4.18 Groundwater balance in transient state condition in Qfd aquifer (continue).

Stress period (day)		**IN** (flow m^3/mth)		**OUT** (flow m^3/mth)
120	Constant Head	706620	Constant Head	40899
	Well	0	Well	2410.9
	River Leakage	150080	River Leakage	159960
	Head Depth Boundary	21801	Head Depth Boundary	0
	Recharge	43487	Recharge	0
	Storage	446510	Storage	218580
	Qyt to Qfd	276910	Qfd to Qyt	1223700
	Total	1645408	Total	1645549.9
	Summary:			
	IN - OUT	-141.9		
151	Constant Head	706710	Constant Head	40547
	Well	0	Well	2410.9
	River Leakage	139660	River Leakage	156540
	Head Depth Boundary	21690	Head Depth Boundary	0
	Recharge	79581	Recharge	0
	Storage	360450	Storage	215790
	Qyt to Qfd	268110	Qfd to Qyt	1161000
	Total	1576201	Total	1576287.9
	Summary:			
	IN - OUT	-86.9		
181	Constant Head	706770	Constant Head	40260
	Well	0	Well	2410.9
	River Leakage	126730	River Leakage	162480
	Head Depth Boundary	21615	Head Depth Boundary	0
	Recharge	112860	Recharge	0
	Storage	308120	Storage	216650
	Qyt to Qfd	260200	Qfd to Qyt	1114600
	Total	1536295	Total	1536400.9
	Summary:			
	IN - OUT	-105.9		
212	Constant Head	706820	Constant Head	40016
	Well	0	Well	2410.9
	River Leakage	124310	River Leakage	155560
	Head Depth Boundary	21558	Head Depth Boundary	0
	Recharge	146720	Recharge	0
	Storage	250230	Storage	225250
	Qyt to Qfd	252640	Qfd to Qyt	1079200
	Total	1502278	Total	1502436.9
	Summary:			
	IN - OUT	-158.9		

Table 4.18 Groundwater balance in transient state condition in Qfd aquifer (continue).

Stress period (day)		**IN** (flow m^3/mth)		**OUT** (flow m^3/mth)
243	Constant Head	706580	Constant Head	39849
	Well	0	Well	2410.9
	River Leakage	150950	River Leakage	137990
	Head Depth Boundary	21483	Head Depth Boundary	0
	Recharge	365860	Recharge	0
	Storage	154050	Storage	405010
	Qyt to Qfd	260410	Qfd to Qyt	1074100
	Total	1659333	Total	1659359.9
	Summary:			
	IN - OUT	-26.9		
273	Constant Head	706310	Constant Head	39710
	Well	0	Well	2410.9
	River Leakage	121800	River Leakage	208700
	Head Depth Boundary	21396	Head Depth Boundary	0
	Recharge	622500	Recharge	0
	Storage	98246	Storage	510130
	Qyt to Qfd	273430	Qfd to Qyt	1082900
	Total	1843682	Total	1843850.9
	Summary:			
	IN - OUT	-168.9		
304	Constant Head	706320	Constant Head	39572
	Well	0	Well	2410.9
	River Leakage	95692	River Leakage	227130
	Head Depth Boundary	21352	Head Depth Boundary	0
	Recharge	512970	Recharge	0
	Storage	127420	Storage	397600
	Qyt to Qfd	260460	Qfd to Qyt	1057700
	Total	1724214	Total	1724412.9
	Summary:			
	IN - OUT	-198.9		
334	Constant Head	706410	Constant Head	39428
	Well	0	Well	2410.9
	River Leakage	82665	River Leakage	218380
	Head Depth Boundary	21345	Head Depth Boundary	0
	Recharge	378050	Recharge	0
	Storage	160520	Storage	302250
	Qyt to Qfd	244580	Qfd to Qyt	1031200
	Total	1593570	Total	1593668.9
	Summary:			
	IN - OUT	-98.9		

Table 4.18 Groundwater balance in transient state condition in Qfd aquifer (continue).

Stress period (day)		**IN** (flow m^3/mth)		**OUT** (flow m^3/mth)
365	Constant Head	706570	Constant Head	39275
	Well	0	Well	2410.9
	River Leakage	83989	River Leakage	181310
	Head Depth Boundary	21367	Head Depth Boundary	0
	Recharge	205490	Recharge	0
	Storage	186970	Storage	206650
	Qyt to Qfd	227490	Qfd to Qyt	1002300
	Total	1431876	Total	1431945.9
	Summary:			
	IN - OUT	-69.9		

Table 4.19 Groundwater balance in transient state condition in Qyt aquifer.

Stress period		**IN**		**OUT**
(day)		(flow m^3/mth)		(flow m^3/mth)
31	Constant Head	0	Constant Head	0
	Well	0	Well	1776.6
	River Leakage	0	River Leakage	0
	Head Depth Boundary	0	Head Depth Boundary	305.95
	Recharge	4478.1	Recharge	0
	Storage	122750	Storage	803740
	Qfd to Qyt	1896600	Qyt to Qfd	342100
	Qot to Qyt	439850	Qyt to Qot	1315600
	Total	2463678.1	Total	2463522.55
	Summary:			
	IN - OUT	155.55		
59	Constant Head	0	Constant Head	0
	Well	0	Well	1776.6
	River Leakage	0	River Leakage	0
	Head Depth Boundary	0	Head Depth Boundary	296.04
	Recharge	3177.7	Recharge	0
	Storage	38168	Storage	210650
	Qfd to Qyt	1450000	Qyt to Qfd	291270
	Qot to Qyt	305270	Qyt to Qot	1292300
	Total	1796615.7	Total	1796292.64
	Summary:			
	IN - OUT	323.06		
90	Constant Head	0	Constant Head	0
	Well	0	Well	1776.6
	River Leakage	0	River Leakage	0
	Head Depth Boundary	0	Head Depth Boundary	296.54
	Recharge	3099.4	Recharge	0
	Storage	37367	Storage	101570
	Qfd to Qyt	1312800	Qyt to Qfd	287690
	Qot to Qyt	242190	Qyt to Qot	1204000
	Total	1595456.4	Total	1595333.14
	Summary:			
	IN - OUT	123.26		

Table 4.19 Groundwater balance in transient state condition in Qyt aquifer (continue).

Stress period (day)		**IN** (flow m^3/mth)		**OUT** (flow m^3/mth)
120	Constant Head	0	Constant Head	0
	Well	0	Well	1776.6
	River Leakage	0	River Leakage	0
	Head Depth Boundary	0	Head Depth Boundary	294.87
	Recharge	1939.3	Recharge	0
	Storage	35041	Storage	58161
	Qfd to Qyt	1223700	Qyt to Qfd	276910
	Qot to Qyt	210680	Qyt to Qot	1134100
	Total	1471360.3	Total	1471242.47
	Summary:			
	IN - OUT	117.83		
151	Constant Head	0	Constant Head	0
	Well	0	Well	1776.6
	River Leakage	0	River Leakage	0
	Head Depth Boundary	0	Head Depth Boundary	293.86
	Recharge	2621.2	Recharge	0
	Storage	31775	Storage	38555
	Qfd to Qyt	1161000	Qyt to Qfd	268110
	Qot to Qyt	192320	Qyt to Qot	1079000
	Total	1387716.2	Total	1387735.46
	Summary:			
	IN - OUT	-19.26		
181	Constant Head	0	Constant Head	0
	Well	0	Well	1776.6
	River Leakage	0	River Leakage	0
	Head Depth Boundary	0	Head Depth Boundary	291.12
	Recharge	3857.5	Recharge	0
	Storage	29542	Storage	27813
	Qfd to Qyt	1114600	Qyt to Qfd	260200
	Qot to Qyt	179840	Qyt to Qot	1037800
	Total	1327839.5	Total	1327880.72
	Summary:			
	IN - OUT	-41.22		

Table 4.19 Groundwater balance in transient state condition in Qyt aquifer (continue).

Stress period (day)		**IN** (flow m^3/mth)		**OUT** (flow m^3/mth)
212	Constant Head	0	Constant Head	0
	Well	0	Well	1776.6
	River Leakage	0	River Leakage	0
	Head Depth Boundary	0	Head Depth Boundary	290.17
	Recharge	4690	Recharge	0
	Storage	26614	Storage	21114
	Qfd to Qyt	1079200	Qyt to Qfd	252640
	Qot to Qyt	170380	Qyt to Qot	1005000
	Total	1280884	Total	1280820.77
	Summary:			
	IN - OUT	63.23		
Prediction				
243	Constant Head	0	Constant Head	0
	Well	0	Well	1776.6
	River Leakage	0	River Leakage	0
	Head Depth Boundary	0	Head Depth Boundary	310.63
	Recharge	11563	Recharge	0
	Storage	20681	Storage	21510
	Qfd to Qyt	1074100	Qyt to Qfd	260410
	Qot to Qyt	171250	Qyt to Qot	993620
	Total	1277594	Total	1277627.23
	Summary:			
	IN - OUT	-33.23		
273	Constant Head	0	Constant Head	0
	Well	0	Well	1776.6
	River Leakage	0	River Leakage	0
	Head Depth Boundary	0	Head Depth Boundary	316.89
	Recharge	19639	Recharge	0
	Storage	16566	Storage	24933
	Qfd to Qyt	1082900	Qyt to Qfd	273430
	Qot to Qyt	177710	Qyt to Qot	996290
	Total	1296815	Total	1296746.49
	Summary:			
	IN - OUT	68.51		

Table 4.19 Groundwater balance in transient state condition in Qyt aquifer (continue).

Stress period (day)		**IN** (flow m^3/mth)		**OUT** (flow m^3/mth)
304	Constant Head	0	Constant Head	0
	Well	0	Well	1776.6
	River Leakage	0	River Leakage	0
	Head Depth Boundary	0	Head Depth Boundary	305.55
	Recharge	16893	Recharge	0
	Storage	16249	Storage	17117
	Qfd to Qyt	1057700	Qyt to Qfd	260460
	Qot to Qyt	169320	Qyt to Qot	980400
	Total	1260162	Total	1260059.15
	Summary:			
	IN - OUT	102.85		
334	Constant Head	0	Constant Head	0
	Well	0	Well	1776.6
	River Leakage	0	River Leakage	0
	Head Depth Boundary	0	Head Depth Boundary	294.58
	Recharge	13103	Recharge	0
	Storage	17223	Storage	12537
	Qfd to Qyt	1031200	Qyt to Qfd	244580
	Qot to Qyt	159510	Qyt to Qot	961790
	Total	1221036	Total	1220978.18
	Summary:			
	IN - OUT	57.82		
365	Constant Head	0	Constant Head	0
	Well	0	Well	1776.6
	River Leakage	0	River Leakage	0
	Head Depth Boundary	0	Head Depth Boundary	288.12
	Recharge	7739	Recharge	0
	Storage	19949	Storage	9112.4
	Qfd to Qyt	1002300	Qyt to Qfd	227490
	Qot to Qyt	149160	Qyt to Qot	940500
	Total	1179148	Total	1179167.12
	Summary:			
	IN - OUT	-19.12		

Table 4.20 Groundwater balance in transient state condition in Qot aquifer.

Stress period		**IN**		**OUT**
(day)		(flow m^3/mth)		(flow m^3/mth)
31	Constant Head	297630	Constant Head	1182900
	Well	0	Well	1024.2
	River Leakage	0	River Leakage	0
	Head Depth Boundary	0	Head Depth Boundary	0.21664
	Recharge	37.9	Recharge	0
	Storage	21440	Storage	11025
	Qyt to Qot	1315600	Qot to Qyt	439850
	Total	1634707.9	Total	1634799.417
	Summary:			
	IN - OUT	-91.51664		
59	Constant Head	157000	Constant Head	1143100
	Well	0	Well	1024.2
	River Leakage	0	River Leakage	0
	Head Depth Boundary	0	Head Depth Boundary	0.21475
	Recharge	32.1	Recharge	0
	Storage	543.51	Storage	470.34
	Qyt to Qot	1292300	Qot to Qyt	305270
	Total	1449875.61	Total	1449864.755
	Summary:			
	IN - OUT	10.85525		
90	Constant Head	96944	Constant Head	1057900
	Well	0	Well	1024.2
	River Leakage	0	River Leakage	0
	Head Depth Boundary	0	Head Depth Boundary	0.21478
	Recharge	26.2	Recharge	0
	Storage	336.7	Storage	247.76
	Qyt to Qot	1204000	Qot to Qyt	242190
	Total	1301306.9	Total	1301362.175
	Summary:			
	IN - OUT	-55.27478		
120	Constant Head	72148	Constant Head	994740
	Well	0	Well	1024.2
	River Leakage	0	River Leakage	0
	Head Depth Boundary	0	Head Depth Boundary	0.21441
	Recharge	18.7	Recharge	0
	Storage	317.73	Storage	175.46
	Qyt to Qot	1134100	Qot to Qyt	210680
	Total	1206584.43	Total	1206619.874
	Summary:			
	IN - OUT	-35.44441		

Table 4.20 Groundwater balance in transient state condition in Qot aquifer (continue).

Stress period (day)		**IN** (flow m^3/mth)		**OUT** (flow m^3/mth)
151	Constant Head	59186	Constant Head	944850
	Well	0	Well	1024.2
	River Leakage	0	River Leakage	0
	Head Depth Boundary	0	Head Depth Boundary	0.21417
	Recharge	10.8	Recharge	0
	Storage	242.23	Storage	219.96
	Qyt to Qot	1079000	Qot to Qyt	192320
	Total	1138439.03	Total	1138414.374
	Summary:			
	IN - OUT	24.65583		
181	Constant Head	51710	Constant Head	908640
	Well	0	Well	1024.2
	River Leakage	0	River Leakage	0
	Head Depth Boundary	0	Head Depth Boundary	0.2136
	Recharge	7.27	Recharge	0
	Storage	227.73	Storage	217.36
	Qyt to Qot	1037800	Qot to Qyt	179840
	Total	1089745	Total	1089721.774
	Summary:			
	IN - OUT	23.2264		
212	Constant Head	46914	Constant Head	880450
	Well	0	Well	1024.2
	River Leakage	0	River Leakage	0
	Head Depth Boundary	0	Head Depth Boundary	0.2134
	Recharge	7.82	Recharge	0
	Storage	196.78	Storage	248.72
	Qyt to Qot	1005000	Qot to Qyt	170380
	Total	1052118.6	Total	1052103.133
	Summary:			
	IN - OUT	15.4666		
243	Constant Head	42520	Constant Head	863280
	Well	0	Well	1024.2
	River Leakage	0	River Leakage	0
	Head Depth Boundary	0	Head Depth Boundary	0.21743
	Recharge	15.2	Recharge	0
	Storage	113.02	Storage	709.71
	Qyt to Qot	993620	Qot to Qyt	171250
	Total	1036268.22	Total	1036264.127
	Summary:			
	IN - OUT	4.09257		

Table 4.20 Groundwater balance in transient state condition in Qot aquifer (continue).

Stress period		**IN**		**OUT**
(day)		(flow m^3/mth)		(flow m^3/mth)
273	Constant Head	41224	Constant Head	857750
	Well	0	Well	1024.2
	River Leakage	0	River Leakage	0
	Head Depth Boundary	0	Head Depth Boundary	0.21868
	Recharge	27.9	Recharge	0
	Storage	76.657	Storage	1135.1
	Qyt to Qot	996290	Qot to Qyt	177710
	Total	1037618.557	Total	1037619.519
	Summary:			
	IN - OUT	-0.96168		
304	Constant Head	40870	Constant Head	850780
	Well	0	Well	1024.2
	River Leakage	0	River Leakage	0
	Head Depth Boundary	0	Head Depth Boundary	0.21649
	Recharge	37.3	Recharge	0
	Storage	173.39	Storage	358.42
	Qyt to Qot	980400	Qot to Qyt	169320
	Total	1021480.69	Total	1021482.836
	Summary:			
	IN - OUT	-2.14649		
334	Constant Head	40954	Constant Head	842360
	Well	0	Well	1024.2
	River Leakage	0	River Leakage	0
	Head Depth Boundary	0	Head Depth Boundary	0.2144
	Recharge	40.2	Recharge	0
	Storage	381.77	Storage	271.55
	Qyt to Qot	961790	Qot to Qyt	159510
	Total	1003165.97	Total	1003165.964
	Summary:			
	IN - OUT	0.0056		
365	Constant Head	41142	Constant Head	831770
	Well	0	Well	1024.2
	River Leakage	0	River Leakage	0
	Head Depth Boundary	0	Head Depth Boundary	0.21319
	Recharge	38	Recharge	0
	Storage	465.82	Storage	189.07
	Qyt to Qot	940500	Qot to Qyt	149160
	Total	982145.82	Total	9.82E+05
	Summary:			
	IN - OUT	2.33681		

Table 4.21 Total groundwater balance in transient state condition of all aquifers.

Stress period		**IN**		**OUT**
(day)		(flow m^3/mth)		(flow m^3/mth)
Total	Qfd			
Year	Constant Head	8507730	Constant Head	485371
	Well	0	Well	28930.8
	River Leakage	3543606	River Leakage	3665500
	Head Depth Boundary	260260	Head Depth Boundary	0
	Recharge	2724949	Recharge	0
	Storage	5951276	Storage	5568670
	Qyt to Qfd	3245290	Qfd to Qyt	14486100
	Total	24233111	Total	24234571.8
	Summary:			
	IN - OUT	-1460.8		
Total	Qyt			
Year	Constant Head	0	Constant Head	0
	Well	0	Well	21319.2
	River Leakage	0	River Leakage	0
	Head Depth Boundary	0	Head Depth Boundary	3584.32
	Recharge	92800.2	Recharge	0
	Storage	411925	Storage	1346812.4
	Qfd to Qyt	14486100	Qyt to Qfd	3245290
	Qot to Qyt	2567480	Qyt to Qot	12940400
	Total	30189997.93	Total	30187766.74
	Summary:			
	IN - OUT	2231.19		
Total	Qot			
Year	Constant Head	988242	Constant Head	11358520
	Well	0	Well	12290.4
	River Leakage	0	River Leakage	0
	Head Depth Boundary	0	Head Depth Boundary	2.58194
	Recharge	299.39	Recharge	0
	Storage	24515.337	Storage	15268.45
	Qyt to Qot	12940400	Qot to Qyt	2567480
	Total	13953456.73	Total	13953561.43
	Summary:			
	IN - OUT	-104.70494		

Table 4.21 Total groundwater balance in transient state condition of all aquifers (continue).

Stress period		**IN**		**OUT**
(day)		(flow m^3/mth)		(flow m^3/mth)
Total	Qfd+Qyt+Qot			
	Constant Head	9495972	Constant Head	11843891
	Well	0	Well	62540.4
	River Leakage	3543606	River Leakage	3665500
	Head Depth Boundary	260260	Head Depth Boundary	3586.90194
	Recharge	2818048.59	Recharge	0
	Storage	6387716.337	Storage	6930750.85
	Qyt to Qfd	3245290	Qfd to Qyt	14486100
	Qfd to Qyt	14486100	Qyt to Qfd	3245290
	Qot to Qyt	2567480	Qyt to Qot	12940400
	Qyt to Qot	12940400	Qot to Qyt	2567480
	Total	68376565.66	Total	68375899.97
	Summary:			
	IN - OUT	665.68506		

4.2.4 Groundwater safe yield

This section are show in term of fixed constant head and assuming the groundwater recharge and any parameters are used same to original transient state except only one parameter is pumping rate for prove the effect to groundwater balance. Volume of pumping wells increased as the rate 25%, 50% and 100% along 1 year same to transient period. The results can show the changing of groundwater level of three cases. In case of increased pumping rate 25% total groundwater balance equal to +237.08 m^3/yr, and 50% equal to -1043.34 m^3/yr, and 100% equal to -1617.17 m^3/yr. Describe of each aquifer safe yield simulation incase 25%, 50% and 100% as show in **Table 4.2**2, **Table 4.2**3, and **Table 4.24**, respectively.

Table 4.22 Groundwater safe yield when increased pumping rate 25% condition of all aquifers.

Stress period (day)		**IN** (flow m^3/yr)		**OUT** (flow m^3/yr)
Total	Qfd			
1 Year	Constant Head	8507730	Constant Head	485371
	Well	0	Well	5607.96
	River Leakage	3535203	River Leakage	3671510
	Head Depth Boundary	260260	Head Depth Boundary	0
	Recharge	2724949	Recharge	0
	Storage	5941959	Storage	5592340
	Qyt to Qfd	3257950	Qfd to Qyt	14474500
	Total	24228051	Total	24229328.96
	Summary:			
	IN - OUT	-1277.96		
Total	Qyt			
1 Year	Constant Head	0	Constant Head	0
	Well	0	Well	4972.8
	River Leakage	0	River Leakage	0
	Head Depth Boundary	0	Head Depth Boundary	3584.96
	Recharge	92800.2	Recharge	0
	Storage	411158	Storage	1346905.2
	Qfd to Qyt	14474500	Qyt to Qfd	3257950
	Qot to Qyt	2572510	Qyt to Qot	12936630
	Total	17550968.2	Total	17550042.96
	Summary:			
	IN - OUT	925.24		
Total	Qot			
1 Year	Constant Head	988242	Constant Head	11358520
	Well	0	Well	2761.68
	River Leakage	0	River Leakage	0
	Head Depth Boundary	0	Head Depth Boundary	2.58214
	Recharge	299.39	Recharge	0
	Storage	24499.122	Storage	15286.45
	Qyt to Qot	12936630	Qot to Qyt	2572510
	Total	13949670.51	Total	13949080.71
	Summary:			
	IN - OUT	589.79986		

Table 4.22 Groundwater safe yield when increased pumping rate 25% condition of all aquifers (continue).

Stress period (day)		**IN** (flow m^3/yr)		**OUT** (flow m^3/yr)
Total	Qfd+Qyt+Qot			
1 Year	Constant Head	9495972	Constant Head	11843891
	Well	0	Well	13342.44
	River Leakage	3535203	River Leakage	3671510
	Head Depth Boundary	260260	Head Depth Boundary	3587.54214
	Recharge	2818048.59	Recharge	0
	Storage	6377616.122	Storage	6954531.65
	Qyt to Qfd	3257950	Qfd to Qyt	14474500
	Qfd to Qyt	14474500	Qyt to Qfd	3257950
	Qot to Qyt	2572510	Qyt to Qot	12936630
	Qyt to Qot	12936630	Qot to Qyt	2572510
	Total	55728689.71	Total	55728452.63
	Summary:			
	IN - OUT	237.07986		

Table 4.23 Groundwater safe yield when increased pumping rate 50% condition of all aquifers.

Stress period (day)		**IN** (flow m^3/yr)		**OUT** (flow m^3/yr)
Total	Qfd			
1 Year	Constant Head	8507730	Constant Head	485371
	Well	0	Well	43395.6
	River Leakage	3549785	River Leakage	3661840
	Head Depth Boundary	260261	Head Depth Boundary	0
	Recharge	2724949	Recharge	0
	Storage	5957252	Storage	5554150
	Qyt to Qfd	3237970	Qfd to Qyt	14494700
	Total	24237947	Total	24239456.6
	Summary:			
	IN - OUT	-1509.6		
Total	Qyt			
1 Year	Constant Head	0	Constant Head	0
	Well	0	Well	31980
	River Leakage	0	River Leakage	0
	Head Depth Boundary	0	Head Depth Boundary	3583.92
	Recharge	92800.2	Recharge	0
	Storage	412399	Storage	1346749.7
	Qfd to Qyt	14494700	Qyt to Qfd	3237970
	Qot to Qyt	2564820	Qyt to Qot	12943570
	Total	17564719.2	Total	17563853.62
	Summary:			
	IN - OUT	865.58		
Total	Qot			
1 Year	Constant Head	988242	Constant Head	11358520
	Well	0	Well	18435.6
	River Leakage	0	River Leakage	0
	Head Depth Boundary	0	Head Depth Boundary	2.58183
	Recharge	299.39	Recharge	0
	Storage	24527.702	Storage	15260.23
	Qyt to Qot	12943570	Qot to Qyt	2564820
	Total	13956639.09	Total	13957038.41
	Summary:			
	IN - OUT	-399.31983		

Table 4.23 Groundwater safe yield when increased pumping rate 50% condition of all aquifers (continue).

Stress period (day)		**IN** (flow m^3/yr)		**OUT** (flow m^3/yr)
Total	Qfd+Qyt+Qot			
1 Year	Constant Head	9495972	Constant Head	11843891
	Well	0	Well	93811.2
	River Leakage	3549785	River Leakage	3661840
	Head Depth Boundary	260261	Head Depth Boundary	3586.50183
	Recharge	2818048.59	Recharge	0
	Storage	6394178.702	Storage	6916159.93
	Qyt to Qfd	3237970	Qfd to Qyt	14494700
	Qfd to Qyt	14494700	Qyt to Qfd	3237970
	Qot to Qyt	2564820	Qyt to Qot	12943570
	Qyt to Qot	12943570	Qot to Qyt	2564820
	Total	55759305.29	Total	55760348.63
	Summary:			
	IN - OUT	-1043.33983		

Table 4.24 Groundwater safe yield when increased pumping rate 100% condition of all aquifers.

Stress period (day)		**IN** (flow m^3/yr)		**OUT** (flow m^3/yr)
Total	Qfd			
1 Year	Constant Head	8507730	Constant Head	485371
	Well	0	Well	57861.6
	River Leakage	3555976	River Leakage	3658350
	Head Depth Boundary	260262	Head Depth Boundary	0
	Recharge	2724949	Recharge	0
	Storage	5963523	Storage	5539950
	Qyt to Qfd	3230890	Qfd to Qyt	14503400
	Total	24243330	Total	24244932.6
	Summary:			
	IN - OUT	-1602.6		
Total	Qyt			
1 Year	Constant Head	0	Constant Head	0
	Well	0	Well	42639.6
	River Leakage	0	River Leakage	0
	Head Depth Boundary	0	Head Depth Boundary	3583.46
	Recharge	92800.2	Recharge	0
	Storage	412911	Storage	1346744.4
	Qfd to Qyt	14503400	Qyt to Qfd	3230890
	Qot to Qyt	2562360	Qyt to Qot	12946710
	Total	17571471.2	Total	17570567.46
	Summary:			
	IN - OUT	903.74		
Total	Qot			
1 Year	Constant Head	988242	Constant Head	11358520
	Well	0	Well	24582
	River Leakage	0	River Leakage	0
	Head Depth Boundary	0	Head Depth Boundary	2.58169
	Recharge	299.39	Recharge	0
	Storage	24535.453	Storage	15240.57
	Qyt to Qot	12946710	Qot to Qyt	2562360
	Total	13959786.84	Total	13960705.15
	Summary:			
	IN - OUT	-918.30869		

Table 4.24 Groundwater safe yield when increased pumping rate 100% condition of all aquifers (continue)

Stress period (day)		**IN** (flow m^3/yr)		**OUT** (flow m^3/yr)
Total	Qfd+Qyt+Qot			
1 Year	Constant Head	9495972	Constant Head	11843891
	Well	0	Well	125083.2
	River Leakage	3555976	River Leakage	3658350
	Head Depth Boundary	260262	Head Depth Boundary	3586.04169
	Recharge	2818048.59	Recharge	0
	Storage	6400969.453	Storage	6901934.97
	Qyt to Qfd	3230890	Qfd to Qyt	14503400
	Qfd to Qyt	14503400	Qyt to Qfd	3230890
	Qot to Qyt	2562360	Qyt to Qot	12946710
	Qyt to Qot	12946710	Qot to Qyt	2562360
	Total	55774588.04	Total	55776205.21
	Summary:			
	IN - OUT	-1617.16869		

Chapter V

Disscusstions and Conclusions

5.1 Calibration and verification of streamflow in the Yom river basin

The calibration and verification processes from 2000 to 2013 in this part can be used to explain effects of land use change (in 2003 and 2009) onto streamflow and assess spatio-temporal monthly groundwater recharge. The results can be summarized in Table 5.1. the maximum root mean square (R^2) was found at station Y.20, the representative of Upper Part of Mae Nam Yom subbasin and minimum root mean square (R^2) was found at station Y.24 representative of Nam Pi subbasin. However, root mean square errors (R^2) of a calibration period were in a range from 0.721 to 0.833, which is more than 0.60 for acceptable correlation. Most stations have R^2 of validation processes were higher than 0.60, especially in the 2nd validation period, except for stations 20, 24 and 36 only in the 1st validation period, which may be error from the rainfall data. Statistical evaluation of calibration and validation of monthly streamflow in each station were summarized in **Table 5.1**.

Table 5.1 Statistical evaluation of calibration **(a)**, 1st validation **(b)** and 2nd validation **(c)** of monthly streamflow in each station

(a) Calibration statistical evaluation in 2006-2009

Station	Standard error (m^3/s)		% Error	Calibration	
	Observation	Simulation		R^2	NSE
Y.36	7.201	5.081	0.294	0.833	0.788
Y.24	2.570	6.891	-1.681	0.721	-5.719
Y.20	22.156	9.118	0.588	0.886	0.492
Y.38	1.979	1.512	0.236	0.745	0.730
Y.1C	32.276	17.902	0.445	0.835	0.689
Y.14	49.751	29.579	0.405	0.844	0.717
Y.6	49.197	31.303	0.364	0.803	0.691

(b) 1st Validation statistical evaluation in 2000-2004

Station	Standard error (m^3/s)		% Error	1st Validation	
	Observation	Simulation		R^2	NSE
Y.36	4.906	2.160	0.560	0.560	0.253
Y.24	2.398	1.777	0.259	0.433	0.422
Y.20	23.408	9.165	0.608	0.528	0.225
Y.38	2.125	1.328	0.375	0.703	0.642
Y.1C	33.310	16.372	0.509	0.673	0.502
Y.14	43.024	22.175	0.485	0.672	0.519
Y.6	46.678	26.101	0.441	0.641	0.546

(c) 2nd Validation statistical evaluation in 2010-2013

Station	Standard error (m^3/s)		% Error	2nd Validation	
	Observation	Simulation		R^2	NSE
Y.36	7.067	5.455	0.228	0.594	0.591
Y.24	4.119	8.794	-1.135	0.648	-2.731
Y.20	29.576	11.490	0.611	0.833	0.434
Y.38	3.346	1.888	0.436	0.686	0.608
Y.1C	48.956	22.791	0.534	0.789	0.581
Y.14	81.632	39.702	0.514	0.896	0.631
Y.6	72.419	42.013	0.420	0.887	0.727

5.2 Baseflow calibration and verification

The baseflow calibration and verification processes from 2000 to 2013 in this part can be used to assess spatio-temporal monthly groundwater recharge. The results can be summarized in Table 5.2. The maximum root mean square (R^2) was found at station Y.36 representative of Mae Nam Khuan subbasin and minimum root mean square (R^2) was found at station Y.6 representative of Lower Part of Mae Nam Yom subbasin. However, root mean square errors (R^2) of a calibration period were in a range from 0.367 – 0.709 and R^2 of validation periods were in a range from 0.327 – 0.581. Most stations have R^2 of calibration and validation processes were lower than 0.60, which is the acceptable level. Statistical evaluation of calibration and validation of monthly streamflow in each station were summarized in **Table 5.2**.

In this section, we found that the results of baseflow from Baseflow Filter Program was not reached the acceptable level, although all 3 types of aquifers were used. It can be explained that the Baseflow Filter Program was not created based on the concept of hydrological system but baseflow separation equation was developed

based on the electrical signal. That is the reason why it cannot represent the real baseflow or groundwater recharge in the study. Therefore, researcher needed to focus onto the baseflow results from SWAT program instead. Then, researcher was believed in groundwater recharge results from SWAT model rather than BFLOW from the Baseflow Filter Program. In conclusions, results of groundwater recharge from SWAT model would be used in groundwater modeling with MODFLOW in the next section.

Table 5.2 Statistical evaluation of calibration and validation of monthly groundwater recharge in each station

Station	BFLOW Types	Calibration R^2	1st Validation R^2	2nd Validation R^2
Y.36	Pass 1	0.709	0.575	0.459
	Pass 2	0.678	0.555	0.407
	Pass 3	0.722	0.649	0.442
Y.24	Pass 1	0.403	0.438	0.474
	Pass 2	0.367	0.453	0.449
	Pass 3	0.426	0.531	0.573
Y.20	Pass 1	0.422	0.539	0.510
	Pass 2	0.379	0.528	0.471
	Pass 3	0.474	0.580	0.539
Y.38	Pass 1	0.659	0.528	0.507
	Pass 2	0.627	0.581	0.485
	Pass 3	0.665	0.645	0.520
Y.1C	Pass 1	0.533	0.513	0.517
	Pass 2	0.527	0.517	0.458
	Pass 3	0.545	0.578	0.514
Y.14	Pass 1	0.493	0.436	0.574
	Pass 2	0.455	0.440	0.499
	Pass 3	0.499	0.480	0.582
Y.6	Pass 1	0.551	0.348	0.527
	Pass 2	0.530	0.327	0.467
	Pass 3	0.548	0.377	0.566

5.3 Land use change effect

As comparing the results of SWAT simulation due to land use change from 2003 to 2009 with the same precipitation data of year 2005, the monthly streamflow appeared to be clearly increased in the rainy season (from July to October), while it seemed to be a similar discharge during January to July. Based on effects of land use change effect onto streamflow, we realized that the percentage changes in the maximum streamflow at station Y.24, Nam Pi subbasin and the percentage changes in the minimum streamflow at station Y.38, Nam Mae Kham Mi subbasin. In summary, percentage changes of streamflow were in a range from 4.94% to 77.64% as shown in Table 5.3.

For groundwater recharge, by using landuse data from year 2003 and 2009, results of baseflow from SWAT model showed that the highest groundwater recharge was appeared in September and October, respectively. The percentage changes in the maximum of groundwater recharge found at station Y.36, Mae Nam Khuan subbasin and the minimum of groundwater recharge found at station Y.6, Lower Part of Mae Nam Yom subbasin. In summary, percentage changes of streamflow were in a range from 0.26% to 5.12% as shown in **Table 5.3**.

Table 5.3 Land use change effect to runoff and groundwater recharge.

Station	Annual average runoff (m^3/s)			% Groundwater recharge / Precipitation		
	LU 2003	LU 2009	% Change	LU 2003	LU 2009	% Change
Y.36	16.00	42.42	62.27%	31.38%	26.26%	5.12%
Y.24	13.59	60.79	77.64%	28.89%	26.81%	2.07%
Y.20	71.55	91.30	21.63%	33.17%	29.76%	3.41%
Y.38	10.06	10.58	4.94%	33.49%	31.35%	2.14%
Y.1C	131.92	165.59	20.34%	32.49%	27.53%	4.97%
Y.14	178.45	234.87	24.02%	28.10%	24.68%	3.42%
Y.6	232.47	245.37	5.26%	21.84%	21.58%	0.26%

5.4 Groundwater recharge

The monthly groundwater recharge estimation from SWAT model in 2013 varies from 0 to 97.33 mm/month. Simulation results from SWAT has a maximum value of an average monthly groundwater recharge found at subbasin 6,thea Middle Part of Mae Nam Yom subbasin and a minimum value of an average monthly groundwater recharge found at subbasin 13 , the Lower Part of Mae Nam Yom subbasin. Annual groundwater recharge was in a range from 14.62 to 433.86 mm/yr. Moreover, based on hydrogeological boundary, groundwater recharge used as an input for MODFLOW recalculated in subbasin nos. 6, 7, 8, and 11 of of 2.80×10^{-4}, 3.87×10^{-4}, 2.96×10^{-4}, and 2.50×10^{-4} m/day, respectively.

5.5 Groundwater balance and safe yield

The groundwater balance of steady state was +69.317 m^3/month with the stress period of 31 days. Next, groundwater balance of transient state is +665.685 m^3/yr with the stress period of 365 days. The suitable safe yield in the aquifers should not increase the pumping rate exceeding over 50%.

REFERENCES

Abbaspour, K. C., et al. (2015). "A continental-scale hydrology and water quality model for Europe: Calibration and uncertainty of a high-resolution large-scale SWAT model." Journal of Hydrology **524**: 733-752.

Abraham, L. Z., et al. (2007). Calibration and Validation of SWAT Hydrologic Model for Meki Watershed, Ethiopia. Conference on International Agricultural Research for Development.

Arnold, J. G. and P. M. Allen (1999). "AUTOMATED METHODS FOR ESTIMATING BASEFLOW AND GROUND WATER RECHARGE FROM STREAMFLOW RECORDS." Journal of the American Water Resources Association **35**(2): 411-424.

Arnold, J. G., et al. (1995). "Automated Base Flow Separation and Recession Analysis Techniques." Ground Water **33**(6): 1010-1018.

Arnold, J. G., et al. (2000). "Regional estimation of base flow and groundwater recharge in the Upper Mississippi river basin." Journal of Hydrology **227**: 21-40.

Bejranonda, W. (2006). COUPLING SURFACE WATER AND GROUNDWATER MODELS FOR WATER BALANCE ANALYSIS WITH AN APPLICATION TO THE UPPER CENTRAL GROUNDWATER BASIN. Department of Water Resources Engineering, Chulalongkorn University. **Master of Engineering Program in Water Resources Engineering:** 255.

Boonkaewwan, S. (2013). AN ASSESSMENT OF NITRATE AND PHOSPHATE IN LOWER YOM RIVER USING SWAT. (Interdisciplinary Program) Graduate School, Chulalongkorn University. **Master of Science Program in Environmental Science:** 186.

Chaisayun, P. and B. Kwanyuen (2004). "Groundwater Modeling for Sukhothai Groundwater Project using MODFLOW Program." Kamphaengsaen Acad. J. **2**(1): 61-71.

Chotpantarat, S., et al. (2011). Water Potential and Demand Research for Sustainable Water Resources Management in Yom River Basin Using Conjunctive Use Application and for Land Use Planning in The Future.

Chung, I.-M., et al. (2010). "Assessing distributed groundwater recharge rate using integrated surface water-groundwater modelling: application to Mihocheon watershed, South Korea." Hydrogeology Journal **18**(5): 1253-1264.

Guzman, J. A., et al. (2012). An Integrated Hydrologic Modeling Framework For Coupling SWAT With MODFLOW. International SWAT Conference & Workshops New Delphi, INDIA, TEXAS A&M University.

Kim, N. W., et al. (2008). "Development and application of the integrated SWAT–MODFLOW model." Journal of Hydrology **356**(1-2): 1-16.

Kornkul, J. (2013). GROUNDWATER BALANCE OF PHRAE BASIN USINGE MODFLOW AND GIS IN CHANGWAT PHRAE. Department of Geology, Chulalongkorn University. **Master of Science Program in Earth Sciences:** 218.

Luo, Y., et al. (2012). "Baseflow simulation using SWAT model in an inland river basin in Tianshan Mountains, Northwest China." Hydrology and Earth System Sciences **16**(4): 1259-1267.

Petchprayoon, P., et al. (2010). "Hydrological impacts of land use/land cover change in a large river basin in central-northern Thailand." International Journal of Climatology **30**(13): 1917-1930.

Pitaksaithong, W. (2004). Water Balance in Yom Basin. Department of Water Resources Engineering, Chulalongkorn University. **Degree of Master of Engineering in Water Resources Engineering:** 233.

Sawatpru, K. and S. Konyai "The Estimation of Base Flow Index in Yom River basin by using Program MATLAB." 1-12.

Silva, M. A. M., et al. (2015). "Spatial and Temporal variation of Dissolved Inorganic Nutrients, and Chlorophyll-a in a Tropical Estuary in Northeastern Brazil: Dynamics of Nutrient Removal." Brazilian Journal of Oceanography **63**(1): 1-15.

Vesurai, O. (2005). THE IMPACTS OF LAND USE CHANGES ON RUNOFF IN THE UPPER NAN BASIN USING SWAT HYDROLOGIC MODEL. Department of Water Resources Engineering, Chulalongkorn University. **Master of Engineering Program in Water Resources Engineering:** 210.

Wang, Z., et al. (2013). "Watershed Modeling of Surface Water-Groundwater Interaction under Projected Climate Change and Water Management in the Haihe River Basin, China." British Journal of Environmental & Climate Change **3**(3): 421-443.

Zhang, X., et al. (2011). "Simultaneous calibration of surface flow and baseflow simulations: a revisit of the SWAT model calibration framework." HYDROLOGICAL PROCESSES **25**: 2313-2320.

APPENDIX

VITA

Mr. Karun Taraka was born in Bangkok, Thailand on February 1, 1987. In 2009 he received a Bachelor of Science degree in Geography with second class honors from Department of Geoinformatic, Faculty of Humanities and Social Sciences, Burapha University. After then he entered the Earth Sciences program, Department of Geology, Faculty of Science, Chulalongkorn University for a Master of Science degree study.

Mr. Karun Taraka graduated high school from Singburi School in 2003. Thereafter, he graduated Bachelor's Degree (B.Sc.) at Physics program, Department of Physics, Faculty of Science, Chulalongkorn University in 2011. After then he entered to study in Master of Science's Degree at Earth Sciences program, Department of Geology, Faculty of Science, Chulalongkorn University in 2012.